

**Pavement Marking Retroreflectivity: Exploring Degradation Factors and Relationship  
with Road Safety**

By

Md Mahmud Hossain

A dissertation submitted to the Graduate Faculty of  
Auburn University  
in partial fulfillment of the  
requirements for the Degree of  
Doctor of Philosophy

Auburn, Alabama  
December 14, 2024

Keywords: Pavement Marking Retroreflectivity, Retroreflectivity Degradation Factors,  
Regression Models, Crash Data Analysis, Curve Segments

Copyright 2024 by Md Mahmud Hossain

Approved by

Huaguo Zhou, Chair, Elton Z. and Lois G. Huff Professor of Civil and Environmental  
Engineering

Rod E Turochy, James Madison Hunnicutt Professor of Traffic Engineering

Jeffrey LaMondia, Professor of Civil and Environmental Engineering

Jingyi Zheng, Associate Professor of Mathematics and Statistics

Luyu Liu, Assistant Professor of Geosciences

## Abstract

The evaluation of pavement marking materials is primarily based on their retroreflectivity (RL), which refers to how well they reflect vehicle headlights back toward the driver. This study focuses on rural roadways and thermoplastic markings to i) identify key factors contributing to RL degradation, ii) understand the relationship between subjective ratings and measured RL by marking line types, iii) develop RL prediction models without initial RL and marking age information as inputs, and iv) explore the statistical relationship between RL and road crashes. Two years of RL data (2020 and 2021) were collected from ALDOT for the Montgomery area. The associated traffic flow, road, location, and crash information were extracted from six different data sources. Beta regression, multiple linear regression, and binary logit models were employed to uncover statistically significant relationships. The results showed that the effects of factors contributing to RL degradation vary by marking line type. For example, yellow centerlines in residential, business, and mixed-use areas exhibited statistically significant RL degradation. RL degradation for white right edgeline (WREL) was significantly higher on curve segments compared to adjacent straight segments. In addition, the analyses found evidence supporting the hypothesis that officers may struggle to assign accurate subjective ratings, particularly for yellow markings. Moreover, this research demonstrated an effective approach for examining the statistical relationship between RL and road crashes by increasing the sample size through developed RL prediction models. The safety analyses identified that lower RL levels of WREL (below 250 mcd/m<sup>2</sup>/lux) statistically increase the likelihood of single-vehicle run-off-road (ROR) crashes on curve segments and in dark conditions. The findings can help ALDOT's pavement management system in identifying locations with high RL degradation, enabling more targeted restriping at these specific segments. Moreover, the developed RL prediction models offer local transportation

agencies a useful tool for forecasting RL with only one year RL measurement and associated traffic flow information. The results from crash data analyses highlight the importance of maintaining adequate RL levels for highway safety. Overall, the findings of this research align with one of the core principles of the Safe System Approach: 'Making Our Roads Safer'.

## Acknowledgments

This dissertation was generously funded by the Alabama Department of Transportation. Throughout my Ph.D. journey, a number of individuals have provided invaluable assistance and encouragement, and without their guidance and collaboration, this work would not have been possible.

First, I wish to express my deepest gratitude to my advisor and mentor, Dr. Huaguo Zhou. His profound knowledge, unwavering support, and exceptional guidance have been pivotal to my success. Dr. Zhou's patience, enthusiasm, and insightful feedback continuously inspired me to strive for excellence. I would also like to extend my sincere thanks to my dissertation committee members, Dr. Turochy, Dr. LaMondia, and Dr. Zheng. Their constructive feedback, insightful questions, and thoughtful suggestions greatly enriched this research. Moreover, I want to thank Dr. Liu for reviewing my dissertation and providing valuable feedback.

I want to express my heartfelt appreciation to my parents, who have supported me unconditionally throughout my life. Their unwavering belief in my abilities and their constant encouragement have been the foundation of my journey. I am especially grateful to my mother, to whom I dedicate this dissertation. Her love, prayers, and sacrifices have been a constant source of strength for me. Finally, to my loving wife, Lamia Nushrat Nadia, I extend my deepest gratitude. Thank you for standing by my side through every challenge, for your patience and understanding. Your care, love, and unwavering belief in me have been my greatest support system.

## Table of Contents

Abstract.....	ii
Acknowledgments.....	iv
Table of Contents .....	iv
List of Tables.....	ix
List of Figures.....	xii
List of Abbreviations.....	xv
Chapter 1    Introduction.....	1
1.1    Background.....	1
1.2    Research Objectives.....	7
Chapter 2    Literature Review.....	9
2.1    RL Degradation Modeling .....	9
2.2    Subjective Assessment of Pavement Marking .....	16
2.3    Relationship Between RL and Road Safety .....	17
2.4    Existing Research Gaps .....	21
Chapter 3    Study Data.....	23
3.1    RL Data.....	23
3.2    Crash Data.....	25
3.3    Traffic Flow and Road Inventory Data .....	26
Chapter 4    Contributing Factors of RL Degradation .....	30

4.1	Data Preprocessing.....	30
4.2	Descriptive Statistics.....	34
4.3	Methodology.....	42
4.3.1	Beta Regression .....	42
4.3.2	Paired t-test .....	43
4.3.2	Wilcoxon Signed-Rank Test .....	44
4.4	Results & Discussions.....	45
4.4.1	RL Degradation Factors by Marking Line Type.....	45
4.4.2	Contributing Factors of RL Degradation on Curve Segments.....	50
4.4.3	RL Degradation by Horizontal Alignment.....	50
4.4.4	Additional Factors Contributing to RL Degradation of WREL.....	51
4.5	Key findings.....	56
Chapter 5	Relationship between Subjective Rating and Measured RL.....	58
5.1	Data Preprocessing.....	58
5.2	Descriptive Analysis .....	59
5.3	Methodology.....	65
5.3.1	Pooled t-test .....	65
5.3.2	Welch's t-test .....	66
5.4	Analysis & Discussions .....	67
5.5	Key Findings.....	69

Chapter 6	RL Prediction Model.....	71
6.1	Descriptive Analysis .....	71
6.2	Methodology.....	72
6.3	Results and Discussions.....	73
6.3.1	RL Prediction Model for YCL .....	74
6.3.2	RL Prediction Model for WREL (Rural Two-lane) .....	75
6.3.3	RL Prediction Model for WREL (Rural Multilane).....	76
6.3.4	Prediction Models Limitations.....	78
6.4	Key Findings.....	85
Chapter 7	Statistical Relationship between RL and Road Safety.....	86
7.1	Data Preprocessing.....	86
7.2	Descriptive Analysis .....	91
7.3	Methodology.....	100
7.3.1	Binary Logit Regression .....	100
7.3.2	Negative Binomial (NB) Regression .....	101
7.4	Analysis & Discussions .....	103
7.4.1	Regression Results for Rural Two-Lane Segments.....	104
7.4.2	Regression Results for Rural Multilane Segments .....	107
7.4.3	Regression Results for Curve Segments.....	110
7.5	Key Findings.....	111

Chapter 8	Conclusions.....	113
8.1	Research Contributions.....	113
8.2	Recommendations.....	116
8.3	Study Limitations and Future Scope.....	119
	References.....	120
	Appendix.....	132



## List of Tables

Table 1.1 RL states of thermoplastic markings (Ortiz-García et al., 2006; Porrás-Alvarado et al., 2014; Chimba et al. 2018).....	3
Table 1.2 Vehicle safety features associated with ADAS to minimize lane departure incidents ....	4
Table 1.3 Minimum RL values in 2009 MUTCD revisions.....	7
Table 2.1 Regression equations for RL prediction in Alabama .....	11
Table 2.2 A summary of studies in the U.S. on RL degradation modeling.....	13
Table 2.3 Overview of studies investigating the association between target crashes and RL .....	19
Table 4.1 Observation counts in final datasets for regression analysis.....	35
Table 4.2 Overview of variables used in degradation proportion modeling by marking line type	37
Table 4.3 Overview of variables used to model RL degradation proportion of WREL for curved sections.....	39
Table 4.4 Overview of datasets to compare degradation proportion by horizontal alignment .....	41
Table 4.5 Summary of beta regression model for marking line types of rural two-lane (YCL and WREL).....	47
Table 4.6 Summary of beta regression model for WREL of rural multilane .....	48
Table 4.7 Summary of beta regression model for YLEL and WLL of rural multilane .....	49
Table 4.8 Summary of beta regression model for WREL on curve segments .....	50
Table 4.9 Summary of paired tests between curve and corresponding straight road segments....	51
Table 5.1 Overview of measured RL (mcd/m <sup>2</sup> /lux) for YCL by subjective rating .....	60
Table 5.2 Overview of measured RL (mcd/m <sup>2</sup> /lux) for YLEL by subjective rating.....	60
Table 5.3 Overview of measured RL (mcd/m <sup>2</sup> /lux) for WLL by subjective rating .....	61
Table 5.4 Overview of measured RL (mcd/m <sup>2</sup> /lux) for WREL by subjective rating.....	61

Table 6.1 Distribution of datasets by $RL_{2020}$ .....	71
Table 6.2 Linear regression results for YCL using the previous RL prediction model .....	74
Table 6.3 MNL results for YCL .....	75
Table 6.4 Linear regression results for WREL (rural two-lane) using the earlier RL prediction model.....	75
Table 6.5 MNL results for WREL (rural two-lane).....	76
Table 6.6 Linear regression results for WREL (rural multilane) using the previous RL prediction model.....	77
Table 6.7 MNL results for WREL (rural multilane) .....	77
Table 7.1 Summary of 0.5-mile segments for safety analyses in relation to WREL .....	88
Table 7.2 Summary of crash datasets on rural two-lane segments .....	94
Table 7.3 Summary of crash datasets on rural multilane segments .....	95
Table 7.4 Summary of crash datasets on curve segments and at dark no streetlighting conditions .....	96
Table 7.5 Summary of regression results for single-vehicle ROR crashes on rural two-lane segments.....	105
Table 7.6 Summary of regression results for single-vehicle ROR crashes on rural two-lane segments at dark, dusk, and dawn conditions .....	105
Table 7.7 Summary of regression results for single-vehicle ROR crashes on rural two-lane segments at dark not-lighted conditions .....	105
Table 7.8 Summary of regression results for crashes on rural two-lane segments at dark not-lighted conditions (interaction of line type as a covariate).....	106

Table 7.9 Summary of regression results for crashes on rural two-lane segments at dark not-lighted conditions.....	106
Table 7.10 Summary of regression results for single-vehicle ROR crashes on rural multilane segments (RL category 1).....	108
Table 7.11 Summary of regression results for single-vehicle ROR crashes on rural multilane segments (RL category 2).....	108
Table 7.12 Summary of regression results for single-vehicle ROR crashes on rural multilane segments at dark, dusk, and dawn conditions (RL category 1).....	109
Table 7.13 Summary of regression results for single-vehicle ROR crashes on rural multilane segments at dark, dusk, and dawn conditions (RL category 2).....	109
Table 7.14 Summary of regression results for single-vehicle ROR crashes on rural multilane segments at dark not-lighted conditions (RL category 1).....	109
Table 7.15 Summary of regression results for single-vehicle ROR crashes on rural multilane segments at dark not-lighted conditions (RL category 2).....	110
Table 7.16 Summary of regression results for single-vehicle ROR crashes on curve segments.....	111

## List of Figures

Figure 1.1 Pavement marking line type by lane configurations .....	2
Figure 1.2 Pavement markings with different RL levels at nighttime (FHWA, 2017) .....	3
Figure 3.1 A sample of original RL datasets collected from ALDOT .....	24
Figure 3.2 Rural locations of RL measurement in Montgomery .....	25
Figure 3.3 A sample of the original traffic flow datasets .....	26
Figure 3.4 ‘COGO’ package of ArcGIS for obtaining horizontal curve attributes .....	27
Figure 3.5 Extracted variables from different data sources .....	29
Figure 4.1 Segmentations between curved and adjacent straight road segments .....	34
Figure 4.2 Distribution of $RL_{2020}$ by marking line type .....	38
Figure 4.3 Distribution of RL degradation proportion by marking line type .....	38
Figure 4.4 Distribution of $RL_{2020}$ for curve segments .....	40
Figure 4.5 Distribution of RL degradation proportion for curve segments .....	40
Figure 4.6 Analytical framework to explore the relationship between curve and adjacent straight road segments in terms of RL degradation proportion .....	45
Figure 4.7 Additional right-turn lane as potential contributor of RL degradation .....	53
Figure 4.8 U-turn and left-turn movement as potential contributor of RL degradation .....	53
Figure 4.9 Bridge as potential contributor of RL degradation .....	54
Figure 4.10 Presence of ramp as potential contributor of RL degradation .....	55
Figure 4.11 Shoulder presence as potential contributor of RL degradation .....	55
Figure 4.12 Residential driveway as potential contributor of RL degradation .....	56
Figure 5.1 Key descriptive statistics parameters of measured RL (mcd/m <sup>2</sup> /lux) for YCL by subjective rating .....	63

Figure 5.2 Key descriptive statistics parameters of measured RL (mcd/m <sup>2</sup> /lux) for YLEL by subjective rating .....	63
Figure 5.3 Key descriptive statistics parameters of measured RL (mcd/m <sup>2</sup> /lux) for WLL by subjective rating .....	64
Figure 5.4 Key descriptive statistics parameters of measured RL (mcd/m <sup>2</sup> /lux) for WREL by subjective rating .....	64
Figure 5.5 Analytical framework of exploring relationship between subjective ratings and marking line type in context of the measured RL values.....	66
Figure 5.6 Statistical relationship between subjective ratings with respect to marking positions in terms of measured RL values.....	68
Figure 5.7 Statistical relationship between marking line types by subjective ratings in terms of measured RL values .....	69
Figure 6.1 QQ and Residual plots for YCL model (rural two-lane).....	79
Figure 6.2 QQ and Residual plots for WREL model (rural two-lane).....	80
Figure 6.3 QQ and Residual plots for WREL model (rural multilane).....	80
Figure 6.4 Predicted RL of YCL by month ( $RL_t = 300$ mcd/m <sup>2</sup> /lux and AADT = 10,000 vpd) ..	82
Figure 6.5 Predicted RL of YCL by month ( $RL_t = 300$ mcd/m <sup>2</sup> /lux and AADT = 546 vpd) .....	82
Figure 6.6 Predicted RL of WREL (rural two-lane) by month ( $RL_t = 450$ mcd/m <sup>2</sup> /lux and AADT = 10,000 vpd).....	83
Figure 6.7 Predicted RL of WREL (rural two-lane) by month ( $RL_t = 450$ mcd/m <sup>2</sup> /lux and AADT = 546 vpd).....	83
Figure 6.8 Predicted RL of WREL (rural multilane) by month ( $RL_t = 450$ mcd/m <sup>2</sup> /lux and AADT = 20,000 vpd).....	84

Figure 6.9 Predicted RL of WREL (rural multilane) by month ( $RL_t = 450 \text{ mcd/m}^2/\text{lux}$ and AADT = 3,610 vpd).....	84
Figure 7.1 Distribution of 0.5-mile segments by RL of WREL.....	89
Figure 7.2 Potential complexities of including intersection crashes.....	90
Figure 7.3 Distribution of 0.5-mile segments with at least one single vehicle ROR crash .....	98
Figure 7.4 Distribution of 0.5-mile segments with at least one single vehicle ROR crash at dark, dusk, and dawn.....	98
Figure 7.5 Distribution of 0.5-mile segments with at least one single vehicle ROR crash at dark no streetlighting .....	99
Figure 7.6 Distribution of 0.5-mile segments with at least one crashes at dark no streetlighting (rural two-lane only) .....	99
Figure 7.7 Distribution of 0.1-mile segments with at least one crashes on curve segments .....	100

## List of Abbreviations

AADT	Annual Average Daily Traffic
AASHTO	American Association of State Highway and Transportation Officials
ADAS	Advanced Driver Assistance Systems
Adj AADT	Adjusted Annual Average Daily Traffic
ADS	Automated Driving Systems
ADT	Average Daily Traffic
AIC	Akaike Information Criterion
ALDOT	Alabama Department of Transportation
ANN	Artificial Neural Network
AV	Autonomous Vehicle
CAPS	Center for Advanced Public Safety
CARE	Critical Analysis Reporting Environment
CTP	Cumulative Traffic Passage
DOT	Departments of Transportation
DT	Decision Tree
FHWA	Federal Highway Administration
HPMS	Highway Performance Monitoring System
LCA	Lane Centering Assistance
LDW	Lane Departure Warning
LDWS	Lane Departure Warning Systems
LKA	Lane Keeping Assistance

MNL	Multiple Linear Regression
MUTCD	Manual on Uniform Traffic Control Devices
MV	Machine Vision
NB	Negative Binomial Regression
NHTSA	National Highway Traffic Safety Administration
NTPEP	National Transportation Product Evaluation Program
RL	Retroreflectivity
ROR	Run-Off-Road
TIGER	Topologically Integrated Geographic Encoding and Referencing
WLL	White Laneline
WREL	White Right Edgeline
YCL	Yellow Centerline
YLEL	Yellow Left Edgeline
ZINB	Zero-inflated Negative Binomial



## Chapter 1 Introduction

This section offers a comprehensive overview of the retroreflective properties of pavement markings and the current practices outlined in the Manual on Uniform Traffic Control Devices (MUTCD) regarding minimum retroreflectivity (RL) requirements. This section discusses the specific RL thresholds that have been followed when restriping or installing new markings in Alabama. This section also emphasizes the importance of maintaining adequate RL levels in context of road safety and in-vehicle technologies, particularly for nighttime driving and under adverse weather conditions. Additionally, this section introduces the primary objectives of the research and outlines the key topics that will be explored in the subsequent chapters of the dissertation.

### 1.1 Background

Longitudinal pavement markings serve as crucial sources of conveying regulations, guidance, or warnings to motorists, offering insight into road geometry (Rasdorf et al., 2009). They delineate boundaries between lanes to assist drivers in choosing the correct travel path and keeping their vehicles within the designated lane (Fu and Wilmot, 2013). There is no doubt that pavement markings enhance visibility for driving both during day and night by improving the driver's ability to make informed decisions (Hussein et al., 2020; Zwahlen and Schnell, 1997). The specifics of longitudinal pavement markings can differ depending on the number of lanes on highways. For instance, on two-lane roads, as viewed from the direction of travel, they encompass a yellow centerline (YCL) and white right edgeline (WREL), while on multilane roads, they include a yellow left edgeline (YLEL), white laneline(s) (WLL), and WREL (**Figure 1.1**). The service life of pavement markings is significantly influenced by the materials used. Across the nation, the

predominant materials for longitudinal striping include thermoplastics, solvent-borne paints, and water-based paints (Idris et al., 2024). Typically, agencies regard restriping intervals ranging from 6 to 12 months for paints and 2 to 6 years for thermoplastics (Thomas and Schloz, 2001). In low traffic flow conditions, thermoplastic pavement markings can last up to 8 years. The higher durability of thermoplastics compared to paints is primarily attributed to their greater thickness and highly adhesive coating, resulting in stronger thermal bond with the pavement surface, making the markings more resistant to wear and tear (Abboud and Bowman, 2002).

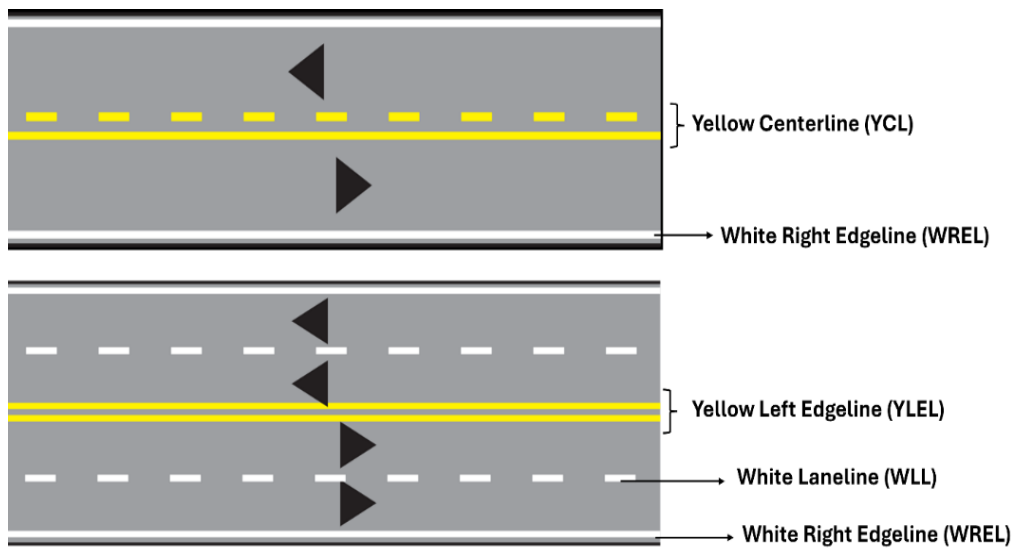


**Figure 1.1 Pavement marking line type by lane configurations**

Deciding when the pavement marking material needs to be restriped can be challenging. The evaluation of pavement marking materials primarily relies on their retroreflectivity (RL), which refers to how well they bounce light from vehicle headlights back toward the driver (Thomas and Schloz, 2001). This reflective quality is what makes the markings appear bright at night and serves as an indicator of their visibility in darkness (Abboud and Bowman, 2002). RL is usually measured in units of millicandelas per square meter per lux ( $\text{mcd}/\text{m}^2/\text{lux}$ ). Quicker identification of pavement markings is linked to their RL levels, which vary in brightness (Aktan and Schnell, 2004). For example, markings with RL of  $228 \text{ mcd}/\text{m}^2/\text{lux}$  have a longer detection distance

compared to those with RL of 118 mcd/m<sup>2</sup>/lux (**Figure 1.2**). Therefore, ensuring that markings maintain their RL is perceived to improve road safety. Maintaining an adequate level of RL could play a significant role in reducing nighttime crashes and fatalities in dark and adverse weather conditions (Hussein et al., 2020). Particularly, enhancing safety on rural roads is the primary incentive for exploring the connection between RL and crashes. Lower RL values may increase the likelihood of single-vehicle run-off-road (ROR) crashes, which are more frequent in rural areas (Smadi et al., 2008). Based on RL data experiments, the qualitative states of thermoplastic marking can be characterized from prior studies (Ortiz-García et al., 2006; Porrás-Alvarado et al., 2014), as depicted in **Table 1.1**. Assuming a failure threshold of 100 mcd/m<sup>2</sup>/lux for yellow markings, these studies observed that a similar degradation nature appeared in white markings at 150 mcd/m<sup>2</sup>/lux. The qualitative states were determined by analyzing the patterns of RL degradations using a transition probability matrix.

**Table 1.1 RL states of thermoplastic markings (Ortiz-García et al., 2006; Porrás-Alvarado et al., 2014; Chimba et al. 2018)**

Qualitative state	RL interval (mcd/m <sup>2</sup> /lux)	
	White thermoplastic	Yellow thermoplastic
Excellent	≥ 450	≥ 400
Good	350-449	300-399
Fair	250-349	200-299
Poor	150-249	100-199
Failure	≤ 150	≤ 100

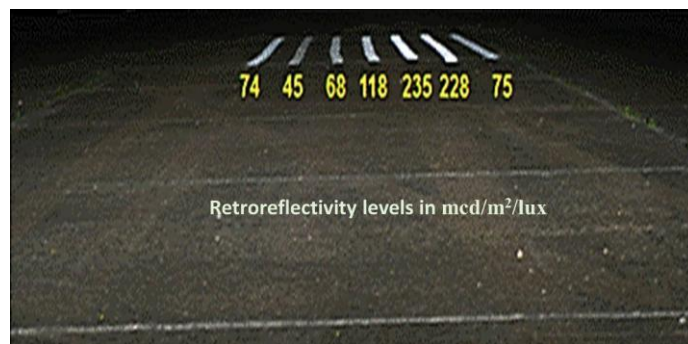


**Figure 1.2 Pavement markings with different RL levels at nighttime (FHWA, 2017)**

In recent years, pavement marking RL has been documented as a crucial characteristic for enhancing infrastructure compatibility with advanced driver assistance systems (ADAS) and automated driving systems (ADS) (Pike et al., 2018). Autonomous vehicle (AV) systems are equipped with a variety of safety features designed to prevent crashes; however, the availability and functionality of these features largely depend on the level of automation of vehicle. Advanced safety systems become more prominent where partial driving automation is introduced. Despite the potential safety benefits, many of these features are not widely utilized by the public, as vehicles equipped with ADAS are more expensive. **Table 1.2** provides an overview of a few technologies associated with ADAS contributing to crash prevention, focusing on systems specifically designed to reduce the risk of lane departure incidents.

**Table 1.2 Vehicle safety features associated with ADAS to minimize lane departure incidents**

<b>Technology</b>	<b>Functions</b>
Lane Departure Warning (LDW)	<ul style="list-style-type: none"> <li>Alerts drivers when they are drifting or have drifted out of their lane or off the roadway.</li> </ul>
Lane Keeping Assistance (LKA)	<ul style="list-style-type: none"> <li>Applies steering torque or brake pressure to prevent an impending lane departure.</li> </ul>
Lane Centering Assistance (LCA)	<ul style="list-style-type: none"> <li>Keeps the vehicle centered in the lane, assisting the driver with steering.</li> </ul>

It is well established that RL is a critical parameter for pavement marking recognition by machine vision (MV) systems in AVs equipped with driver assistance technologies (Burghardt et al., 2021; Matowicki et al., 2016). Adequate RL is essential for all vision-based MV systems to ensure proper nighttime guidance. A research from Croatia found that the minimum RL required for optimal detection quality should be above 88 mcd/m<sup>2</sup>/lx (Babić et al., 2022). However, the study was conducted in dry conditions, and detection quality highly depends on the sensors used. Furthermore, the related studies specifically focused on digital image sensors designed for camera applications, capable of capturing high-quality images even in low-light conditions (Burghardt et

al., 2021; Matowicki et al., 2016; Babić et al., 2022). Therefore, there is an opportunity to investigate how AVs equipped with combined camera, LiDAR, and radar systems perform in recognizing pavement markings with lower RL in dark conditions. Each of these sensor type offers unique capabilities that enhance pavement marking detection in different ways (Sauter et al., 2021):

- *Camera*: High-resolution imaging allows to recognize pavement marking colors, shapes, and textures, specifically in good lighting conditions.
- *LiDAR*: Precise 3D maps can identify raised or textured pavement markings and assess their position and orientation relative to the vehicle, particularly in low-visibility scenarios where camera may be less effective.
- *Radar*: Can confirm the presence of lane boundaries and detect any obstacles on or near markings, improving the vehicle's understanding of the road layout in adverse weather and low lighting conditions.

In terms of emerging technologies associated with ADAS, the performance of LDW systems improves as RL increases (Hadi and Sinha, 2011). Specifically, lower RL significantly reduces LDW performance under medium and high rainfall conditions. In dry and light rain at night, LDW performed well even at low RL levels, such as 100 mcd/m<sup>2</sup>/lx. Beyond RL, MV performance also depends on the color of pavement markings, as color contrast enhances detection (Davies, 2017). White markings are generally easier to detect than yellow ones (Davies, 2017), and glare can significantly affect the performance MV systems that rely on low-resolution monochrome cameras (Pike et al., 2018). Some studies have noted that contrast may be an even more important factor than RL in some instances (Cafiso and Pappalardo, 2020; Pike et al., 2018). Despite ongoing advancements, current MV technologies still struggle to handle road surface

irregularities obvious to human drivers, such as potholes, cracks, repair marks, excessive wheel ruts, and partially concealed or irregular markings. There has been limited research on how the material characteristics of pavement markings influence the performance of MV systems, with most studies focusing on paint, plastic, and tape markings rather than thermoplastic markings.

The degradation rate of RL, a crucial factor determining the service life of pavement markings, can be influenced by various factors, including type of material, traffic volume, geographic location, percentage of heavy vehicles, climate conditions, road surface type, material thickness, type and quality of glass beads or other reflective elements used, and the initial value of installation (Idris et al., 2024). Transportation agencies such as American Association of State Highway and Transportation Officials (AASHTO), Federal Highway Administration (FHWA), and State Departments of Transportation (DOTs) have made significant efforts to prepare comprehensive standard specifications, manuals, and procedures to ensure the appropriate application and maintenance of pavement markings (Sasidharan et al., 2009). In this perspective, FHWA aims to enhance safety by setting minimum RL levels in the Manual on Uniform Traffic Control Devices (MUTCD), thereby meeting the nighttime visibility requirements of drivers on public roadways. On August 5, 2022, FHWA published a new regulation establishing national standards for minimum RL levels of longitudinal marking lines on all roads, varying according to posted speed limits (2009 MUTCD Revision 3) (FHWA, 2022). This regulation mandates that all state agencies establish a method by 2027 to maintain the designated minimum RL level and integrate RL considerations into future restriping endeavors. As per the regulation, roads with posted speed limits equal to or greater than 35 mph need to maintain a minimum RL of 50 mcd/m<sup>2</sup>/lux, while no minimum threshold is set for speed limits below 35 mph. Furthermore, it is recommended to maintain a minimum RL of 100 mcd/m<sup>2</sup>/lux for freeways with posted speed limits

of 70 mph and above. These regulations and guidelines apply under dry conditions and exclude conditions such as ambient lighting, roads with less than 6000 annual average daily traffic (ADT), dashed extension lines, curb markings, parking spaces, and shared-use paths. The changes regarding RL in the 2009 MUTCD revisions are exhibited in **Table 1.3**. It is noteworthy that in the latest 11th Edition of the MUTCD effective in December 2023, the minimum RL requirements have remained consistent with the previous version, 2009 MUTCD Revision 3. In recent years, Alabama Department of Transportation (ALDOT) has hired a consulting firm to gather RL data on Alabama highways. According to the Standard Specifications for Highway Construction Special Provisions 2022, the initial RL of standard thermoplastic should be at least 450 mcd/m<sup>2</sup>/lux for white markings and 300 mcd/m<sup>2</sup>/lux for yellow markings (ALDOT, 2022).

**Table 1.3 Minimum RL values in 2009 MUTCD revisions**

	Revision 3 (Effective September 6, 2022)		Revision 1 & 2 (Effective June 13, 2012)				
	Standard		Guidance	Two-lane with centerline only		All other roads	
<b>Speed limit (mph)</b>	< 35	≥ 35	≥ 70	35-50	≥ 55	35-50	≥ 55
<b>RL (mcd/m<sup>2</sup>/lux)</b>	n/a	50	100	100	250	50	100

## 1.2 Research Objectives

The primary objectives of this research are follows:

- To identify the key factors contributing to the degradation of RL based on marking line type
- To understand the relationship between subjective RL ratings and measured RL in relation to marking line type
- To develop regression models to predict RL specific to WREL and YCL without initial RL and marking age information

- To explore the statistical relationship between RL and targeted road crashes

The rest of the chapter of this dissertation is organized as follows:

- Chapter 2: Comprehensive literature review to i) synthesize existing RL prediction model, ii) understand how earlier studies explained subjective RL rating with measured RL, and iii) explore the established correlations between RL and road safety.
- Chapter 3: An overview of the datasets collected from multiple sources and the variables extracted for analyses, featuring RL, traffic flow, road, and crash characteristics.
- Chapter 4: Identify the factors contributing to the degradation of RL, including traffic volume, road geometry, and pavement marking characteristics.
- Chapter 5: Explore how the distribution of measured RL varies with subjective RL rating, considering different pavement marking line types.
- Chapter 6: Employ multiple regression models to develop RL prediction models for WREL and YCL, considering lane configurations.
- Chapter 7: Analyze crash data to establish statistical correlations between RL and targeted crash frequency, with a particular focus on dark lighting conditions and single-vehicle ROR collisions.
- Chapter 8: Highlight the research contributions, discuss the key findings and recommendations, address the study limitations, and outline potential areas for future research.



## Chapter 2 Literature Review

This section provides a comprehensive review of earlier studies, synthesizing their findings to understand the diverse methodologies used to develop RL predictive models. The discussion covers a range of factors, including road conditions, traffic patterns, and pavement characteristics, that contribute to RL degradation. In addition, a thorough examination of existing literature highlights the correlation between RL levels and road crashes. The section also reviews studies that explain the relationship between measured RL and subjective RL ratings. Overall, this literature review serves two primary purposes: i) identifying potential variables essential for developing regression models to predict RL degradation, and ii) facilitating the selection of relevant crash types to explore the statistical relationship between crash frequency and RL levels.

### 2.1 RL Degradation Modeling

During the late 1990s and early 2000s, the prevalent approach to predicting RL relied on simplistic linear and nonlinear regression models centered on a single variable, such as marking age or traffic volume (Abboud and Bowman, 2002; Andrady et al., 1997; Lee et al., 1999; Migletz et al., 2001). However, the low goodness of fit of these models in capturing the complexity of RL led to their gradual replacement with multiple linear regression models. These regression models have offered considerably higher goodness of fit by incorporating numerous variables such as initial RL (within 30 days after installation), marking age, geographic location, traffic characteristics, marking color, and position (Fu and Wilmot, 2013; Malyuta, 2015; Mull and Sitzabee, 2012; Ozelim and Turochy, 2014; Robertson et al., 2013; Sasidharan et al., 2009; Sitzabee et al., 2009; Wang et al., 2016). However, considering highly correlated variables can lead to insignificant model outcomes; for instance, cumulative traffic passage (CTP) may not be

included in the model if ADT and time are already taken into account (Zhang and Wu, 2010). Additionally, in larger datasets, increased heterogeneity can significantly diminish the model's performance by introducing greater variability that is difficult to account for (Zuur et al., 2009). Among the range of material types studied, paint and thermoplastic emerged as the most commonly used. However, with growing interest in alternative durable materials like epoxy, polyurea, preformed tape, and methyl methacrylate, researchers have developed predictive models tailored to these materials (Fu and Wilmot, 2013; Idris et al., 2024; Kopf, 2004; Migletz et al., 2001; Mull and Sitzabee, 2012; Pike and Songchitruksa, 2015; Sasidharan et al., 2009; Wang et al., 2016). Regarding marking color, it is observed that yellow paint and thermoplastic generally exhibit slower RL degradation compared to white markings of the same type. However, when considering the position of markings, the influence of color on RL models is automatically regulated (with possible variations by location), as specific marking line types correspond to distinct colors: solid white for right edgeline, broken/solid yellow for centerline, broken white for laneline, and solid yellow for left edgeline. Typically, RL models are significantly associated with initial RL readings, traffic flow attributes, and marking age. It is worth noting that a few studies have revealed the non-linear degradation trend of RL, taking on an inverted parabolic shape, where readings initially rise above the initial values before gradually declining thereafter (Chimba et al., 2018; Lee, 2009; Sitzabee et al., 2009).

In Alabama, over twenty years ago, Abboud and Bowman (2002) conducted a case study aimed at determining the service life of paint and white thermoplastic markings. They utilized field data from 520 miles of longitudinal pavement markings across nine counties in Alabama, setting a minimum RL standard of 150 mcd/m<sup>2</sup>/lux for WREL. The study revealed a logarithmic relationship between RL and traffic exposure, a function of Annual Average Daily Traffic (AADT)

and marking age. Building upon this groundwork, Ozelim and Turochy (2014) embarked on a study in the last decade to assess the applicability of established RL models to Alabama's road conditions, alongside testing their newly developed models. They used four years of RL data, ensuring a comprehensive representation of road segments across the state, encompassing both two-lane and four-lane highways. While some conventional models showed promising performance on actual RL data, the service life estimates derived from the best-fitted models for thermoplastic materials seemed impractical. Consequently, the study pivoted towards developing new regression models to forecast RL for each marking color attribute. The results underscored a strong correlation between RL and factors such as marking age and AADT, with initial RL value exhibiting minimal influence on model accuracies. The unit of AADT is vehicles per day (vpd). The final regression equations from both of these Alabama studies are outlined in **Table 2.1**.

**Table 2.1 Regression equations for RL prediction in Alabama**

Reference	Equations
Abboud and Bowman (2002)	$R_L = -19.457 * \ln(VE) + 26.27 \text{ (for paint)}$ $R_L = -70.806 * \ln(VE) + 639.66 \text{ (for thermoplastic)}$ $VE = ADT_{ln} * PM_{age} * 20.4 * 10^{-3}$ <p><math>R_L</math> = retroreflectivity (mcd/m<sup>2</sup>/lux), <math>VE</math> = vehicle exposure (thousands of vehicles), <math>ADT_{ln}</math> = ADT per lane, <math>PM_{age}</math> = marking age (months).</p>
Ozelim and Turochy (2014)	$R_L = 619.4 - 5.13t - 0.00699 * AADT \text{ (for white marking)}$ $R_L = 407.3 - 4.969t - 0.00217 * AADT \text{ (for yellow marking)}$ <p><math>R_L</math> = retroreflectivity (mcd/m<sup>2</sup>/lux), <math>t</math> = marking age (months), <math>AADT</math> = Annual average daily traffic (vpd)</p>

In addition to utilizing RL data collected from specific states, numerous studies have incorporated data from the National Transportation Product Evaluation Program (NTPEP) to develop RL prediction models (Idris et al., 2024; Mousa et al., 2021; Wang et al., 2016). NTPEP selects test decks from various locations across the United States (Minnesota, Pennsylvania, Florida, and Wisconsin), encompassing diverse traffic patterns and geographical conditions, and installs marking products in a transverse direction. The degradation of RL in transverse skip lines

aligns with longitudinal pavement markings, providing a strong representation of RL degradation. RL readings are collected at 12 different time intervals (0, 1, 2, 3, 11, 12, 15, 21, 24, 27, 33, 36 months) over a period of up to three years. Consequently, there exists a substantial volume of data suitable for the implementation of comprehensive machine learning algorithms. A few researchers have taken an intriguing approach by categorizing RL levels into bins (Sitzabee et al., 2013; Xu et al., 2021). However, this method overlooks the fact that linearly deriving the thresholds is inherently limited, as RL performance has consistently demonstrated better modeling results when approached logarithmically. These researchers explore various bin intervals, ensuring that all bins maintain RL levels above previously recommended minimum thresholds. **Table 2.2** outlines a compilation of literature review in the U.S. proposing models for RL degradation.

**Table 2.2 A summary of studies in the U.S. on RL degradation modeling**

Reference	Study area	Material(s)	Input(s)	Method(s)	$R^2$
Andrady et al. (1997)	TN, KY, CO, and OH	Thermoplastics	Marking age, initial RL	Simple linear regression	0.50-0.71
Lee et al. (1999)	MI	Waterborne paint, thermoplastic, polyester, tape	Marking age	Simple linear regression	0.14-0.18
Migletz et al. (2001)	AZ, AR, CA, CO, FL, GA, IA, KS, LA, MN, MO, NH, NC, OK, UT, VI, WA, WV, WI	Waterborne paint, thermoplastics, polyurea material, epoxy paint	Traffic volume, initial RL	Linear and exponential regression	----
Abboud and Bowman (2002)	AL	Waterborne paint, thermoplastic	Marking age, traffic volume	Exponential regression	0.31-0.58
Sarasua et al. (2003)	SC	Thermoplastic, epoxy	Marking age	Simple linear regression	0.21-0.47
Thamizharasan et al. (2003)	SC	Thermoplastic and epoxy	Marking age, traffic volume	Multiple linear regression	0.21-0.78
Lindly and Wijesundera (2004)	AL	Thermoplastics and profiled	Traffic volume	Linear and exponential regression	0.53-0.67
Kopf (2004)	WA	Waterborne and solvent-borne paint	Marking color, AADT, marking age	Linear and exponential regression	0.33-0.73
Bahar et al. (2006)	AL, CA, MN, MO, PA, TX, UT, WI	Waterborne paint, thermoplastic	Marking age	Inverse polynomial model	---
Hollingsworth (2008)	NC	Waterborne paint, thermoplastic	Marking age, traffic volume,	Logarithmic	0.53
Sitzabee et al. (2009)	NC	Thermoplastic, waterborne	Marking age, initial RL,	Multiple linear regression	0.60-0.75

Reference	Study area	Material(s)	Input(s)	Method(s)	$R^2$
		paint	traffic volume, marking location, marking color		
Sasidharan et al. (2009)	PA	Epoxy and waterborne paint	Marking age, ADT, line type, Surface type	Multiple linear regression	0.27-0.44
Hummer et al. (2011)	NC	Solvent-borne paint	Initial RL, marking age	Linear mixed-effect model	0.67
Karwa and Donnell (2010)	NC	Thermoplastic	Initial RL, marking age, traffic volume, marking type, marking location	Artificial Neural Network (ANN)	---
Mull and Sitzabee (2012)	NC and OH	Solvent-borne paint	Marking age, AADT, initial RL, winter road maintenance activities	Multiple linear regression	0.76
Fu and Wilmot (2013)	LA	Thermoplastic, tape, and inverted profile thermoplastic	Marking age, traffic volume	Multiple linear regression	0.18-0.89
Robertson et al. (2013)	SC	Waterborne paint	Marking age, traffic volume, lane width, shoulder width	Multiple linear regression	0.24-0.34
Ozelim and Turochy (2014)	AL	Thermoplastic	Marking age, traffic volume, initial RL	Multiple linear regression	0.46-0.50
Malyuta (2015)	TN	Waterborne paint, thermoplastic	Marking age, traffic volume	Multiple linear regression	0.33-0.46
Pike and Songchitruksa (2015)	TX	Waterborne and epoxy paint, polyurea material, thermoplastics	Marking age, initial RL	Exponential regression	0.64-0.98
Wang et al. (2016)	FL, PA, MN	Permanent polymeric tape and methyl methacrylate	Marking age, maximum RL value, and traffic volume	Multiple linear regression	0.56-0.68
Chimba et al. (2018)	TN	Thermoplastic	Marking age	Markov Chain Model	----

<b>Reference</b>	<b>Study area</b>	<b>Material(s)</b>	<b>Input(s)</b>	<b>Method(s)</b>	<b><math>R^2</math></b>
Mohamed et al. (2019)	ID	Waterborne	Marking age	Simple linear regression	0.80-0.97
Mousa et al. (2021)	FL, PA, MN, MS	Waterborne paint	Initial RL, manufacturer, surface type, marking color, thickness, bead types, marking age, air temperature, rainfall, snowfall, traffic volume, surface age	Categorical Boosting	0.83-0.98
Idris et al. (2024)	MN, PA, FL, WI	Waterborne paint, thermoplastic, preformed thermoplastic, permanent polymeric tape, epoxy, polyurea, and methyl methacrylate	Marking age, traffic volume, snowfall, thickness, surface type, marking materials, marking color, manufacturer, bead type of the first drop, bead type of the second drop	Decision Tree (DT) and ANN	0.55-0.96

## **2.2 Subjective Assessment of Pavement Marking**

Subjective RL assessments are conducted by visually inspecting pavement markings to ensure they provide adequate visibility and presence. In Alabama, pavement marking management systems typically involve daytime visual inspections, with actual RL measurements taken on annually. However, a key limitation of visual inspections is their subjective nature, as results can vary significantly between evaluators. Additionally, the perceived brightness of pavement markings can be influenced by the contrast between the markings and the pavement. For instance, a marking on darker pavement may appear brighter than one on lighter pavement, even though both have the same RL. Consequently, multiple studies have highlighted that visual inspections are prone to human error, difficult to verify, and often produce inconsistent results (Benz et al., 2008; Satterfield et al., 2022). Despite these limitations, many districts within the ALDOT rely on subjective evaluations to determine whether pavement markings meet acceptable RL levels or require restriping. These markings are typically rated on a scale from 1 to 5, with 1 indicating poor condition and 5 indicating excellent condition. The criteria used for rating—such as color, contrast, and overall appearance—can vary from state to state, further contributing to the variability of visual inspection results.

Benz et al. (2008) conducted a comprehensive study in Texas to investigate how well subjective evaluations of RL correlated with actual measured RL. The study applied multiple trend analyses to examine how closely subjective ratings aligned with RL trends, considering factors such as marking color, line type, and pavement type. To establish consistent rating criteria, the researchers conducted a phone survey across 25 districts to gather information on current practices for assessing pavement marking RL. Based on the survey, the criteria for subjective evaluation included marking color, contrast with surrounding pavement, and overall marking condition.



Observers applied these criteria at 16 sample locations, with each location spanning between one-tenth and one-half of a mile in length. The study revealed that for RL values below 300 mcd/m<sup>2</sup>/lux, there was less variability in subjective ratings around the RL trend line, while greater variability was observed for values above 300 mcd/m<sup>2</sup>/lux. Correlation analyses between measured RL values and the subjective criteria—color, contrast, and overall quality—showed strong correlations of 0.77, 0.71, and 0.68, respectively, indicating a consistent relationship between subjective assessments and actual RL measurements, particularly for lower RL levels.

### **2.3 Relationship Between RL and Road Safety**

Because of the higher cost involved, RL data is typically collected during summers with one to three intervals per year to minimize the winter effects. This presents a challenge in accurately determining the RL levels of pavement markings at the precise time and location of each crash. Despite the availability of crash data, researchers have often had to make assumptions regarding RL levels for their analyses. Earlier, a few researchers utilized measured data to model RL for predictive purposes, while others relied on assumptions without direct measurements. Furthermore, in the majority of states, roadways with high traffic volume are restriped every 2 to 4 years with thermoplastic markings. Consequently, there are very few instances of roadways with RL levels below 50 mcd/m<sup>2</sup>/lx.

A limited number of studies have used RL measurements to assess their impact on safety and crashes. Earlier studies primarily established minimum RL thresholds based on crash rates. For instance, a study from New Zealand conducted a before-and-after comparison of crash rates to evaluate the effects of a policy implemented in 1997, setting a minimum RL of 70 mcd/m<sup>2</sup>/lx for pavement markings (Dravitzki et al., 2006). This study was performed on the assumption of increased brightness in the post-implementation period. Subsequent studies have utilized measured

RL data, available for specific road segments across various settings over multiple years. Retroreflective markings reflect the light from headlights back toward the driver, enhancing the visibility of road lanes, edges, and centerlines in low-light or dark conditions. As a result, most studies have concentrated on examining the impact of RL on nighttime crashes and crashes in dark conditions, given its critical role in improving driver guidance and safety during these conditions. However, very few have successfully established a statistical relationship between crashes and RL. One key challenge lies in the scarcity of target crashes within segments, making it difficult to select appropriate statistical techniques. Moreover, the distribution of RL is highly skewed, necessitating a logarithmic description of the data rather than a linear one. **Table 2.3** summarizes studies that have endeavored to establish the correlation between crashes and RL.

**Table 2.3 Overview of studies investigating the association between target crashes and RL**

References	Study area	Method(s)	Target crashes	Key findings
Bowman (2001)	AL	Descriptive analysis	Nighttime	Thermoplastic long lines offered a safer traffic operation compared to painted highways.
Dravitzki et al. (2006)	New Zealand	Descriptive analysis	Dark conditions, nighttime, curve, curve during dark	No significant changes observed in crash trends following the maintenance of a minimum RL of 70 mcd/m <sup>2</sup> /lx.
Masliah et al. (2007)	CA	Innovative time series analysis	Nighttime and non-intersection	Minimal effect of RL on crash modification factors.
Smadi et al. (2008)	IA	Logistic regression	Nighttime and lane departure not attributed to collision with animals or objects, vehicle-to-vehicle collisions, maneuvers to avoid collisions with other vehicles, or equipment malfunctions.	Lower RL associated with higher crash probability when segments with RL ≤ 70 mcd/m <sup>2</sup> /lx analyzed separately.
Donnell et al. (2009)	NC	ANN and generalized estimating equations with negative binomial (NB) distribution	Nighttime, sideswipe collisions, and ROR collisions involving fixed objects in non-work zones, without alcohol involvement, and in dry weather.	Increasing RL on two-lane highways may correspond to reduced frequencies of target crashes. The related outcomes for YCL showed marginal significance, whereas the results for WREL were not found to be significant.
Carlson et al. (2013)	MI	NB regression	Nighttime and single-vehicle nighttime crashes at non-intersection during the nonwinter months	The expected crash frequency decreased when RL increases; varies in datasets within the range of ≤ 150-200 mcd/m <sup>2</sup> /lx across marketing positions.
Avelar and Carlson (2014)	MI	Generalized linear mixed-effects models	Single-vehicle, sideswipe, and ROR crashes at night	Segments with higher RL were observed to have fewer crashes compared to segments with lower retroreflectivity, for both WREL and YCL

<b>References</b>	<b>Study area</b>	<b>Method(s)</b>	<b>Target crashes</b>	<b>Key findings</b>
Bektas et al. (2016)	IA	NB regression	Nighttime, ROR crashes, and nighttime ROR crashes	For 1-mile four-lane road segments, the expected number of crashes decreased significantly as the increase of RL of WREL

## 2.4 Existing Research Gaps

RL measurements require mobilizing equipment and personnel, making it challenging to conduct quarterly/monthly readings of selected road segments within the constraints of limited budgets and manpower. Therefore, agencies often prioritize restricting RL assessments to one or two readings per segment per year. Additionally, state DOTs commonly enlist private consulting firms to measure RL in specific road segments, yet without precise records indicating the timing of pavement marking installation or restriping. Thus, to expand the practice and implementation of pavement marking RL measurement as a crucial aspect of road service life and safety, it becomes imperative to develop RL models that do not rely on input regarding the marking age and initial RL readings. These regression models can help ALDOT's pavement management system in identifying locations where RL levels are projected to drop below safe thresholds in the coming years.

In previous studies examining factors influencing RL degradation or developing RL prediction models, researchers typically focused on calculating the average RL for each 1-mile road segment. While this approach provides a general view, a more effective and practical method would involve calculating the average RL for road segments with similar geometric and traffic characteristics. By grouping segments with comparable factors—such as traffic volume, posted speed limit, functional class, lane configuration, and horizontal alignment—this approach can yield more precise insights into RL degradation patterns. In addition, this method can reduce heterogeneity within the dataset, leading to more accurate and reliable predictions of RL degradation. Previous studies have predominantly emphasized marking and traffic characteristics over road geometric design factors. For example, vehicles navigating through curves may inadvertently brush against or overlap the markings, leading to more rapid wear and tear of WREL

markings. Therefore, the RL in curved segments could be degraded more rapidly compared to straight sections. Furthermore, it is crucial to consider the impact of horizontal alignment when analyzing RL data to comprehend the critical factors contributing to RL degradation. Moreover, most studies have combined WREL data for rural two-lane and multi-lane roads in their analyses, even though degradation patterns may vary depending on the number of lanes. Furthermore, RL degradation may exhibit inconsistencies within one road segment, yet no prior study has delved into the underlying reasons for this phenomenon. These analyses could assist state DOTs in restriping specific areas with higher RL degradation instead of the entire segment, thereby reducing maintenance costs. To gain a deeper understanding of the correlation between subjective RL ratings and measured RL, further research is necessary to explore how RL values are distributed across each rating category. Additionally, it is important to investigate how measured RL varies according to pavement marking line types within each rating scale and assess the statistical significance of these variations. Such analyses would provide valuable insights into the consistency and reliability of subjective evaluations and improve pavement marking management practices.

Establishing the statistical correlation between RL and road safety relies significantly on meticulous data preparation, segmentation, and practical assumptions regarding the assignment of retroreflectivity values for each segment throughout the specified analytical period. Hence, there is a need for further research to thoroughly investigate the statistical relationship between RL and crashes. This entails organizing and segmenting the dataset using multiple criteria/assumptions and adopting appropriate statistical techniques to uncover meaningful insights into this correlation. The findings can help determine the RL threshold below which the probability of crashes increases significantly.

## Chapter 3 Study Data

This section provides an overview of the datasets collected from multiple sources to extract the variables required to fulfill the research objectives. This section discusses the accessibility, limitations, and constraints associated with each data source, as such factors play a significant role in selecting the preliminary contributing factors and the choice of analytical methodologies. The primary datasets encompass RL data and crash data acquired from ALDOT, traffic flow data sourced from ALDOT's traffic data website, and road inventory data obtained from Google Earth Pro, crash data, and the Highway Performance Monitoring System (HPMS).

### 3.1 RL Data

Thermoplastic is a widely used material for pavement markings due to its moderate cost and exceptional durability, making it the predominant choice in Alabama. When reapplying thermoplastics over existing markings, there is no need to remove the old markings. For this study, RL data were collected from ALDOT for the Montgomery area in 2020 and 2021. All RL measurements were conducted under dry weather and daylight conditions. A thorough analysis of the RL data revealed that 575 miles of road segments were covered in 2020, with approximately 75% located in rural areas. In 2021, coverage increased to 1,525 miles, adding 950 miles that were measured only that year. Of these additional 950 miles, around 90% were in rural areas. Notably, the original dataset lacked area setting information, which was subsequently extracted from Topologically Integrated Geographic Encoding and Referencing (TIGER) database using latitude and longitude information. This database is created and maintained by the United States Census Bureau, offers detailed road networks (highways, local roads, and railroads) along with their classifications and area contexts. RL measurements were typically taken every 1/10th mile along

most road segments. The datasets and relevant documents did not specify which RL measurement method was used. However, previous studies have indicated that LaserLux vans were usually used to collect RL data on freeways and four-lane roads, while handheld Retroreflectometer LTL-X devices were used on other roads (Smadi et al., 2008; Ozelim and Turochy, 2014).

The original RL datasets included route identification numbers, mile markers, measured RL values, marking line types, measurement direction, date of RL measurements, geocoordinates, and subjective ratings. A sample of the original RL datasets is shown in **Figure 3.1**. In 2020, subjective ratings ranged from 1 to 4, whereas in 2021, the scale was expanded to range from 1 to 5. Within urban road segments, a majority had no RL values on WREL due to the frequent minor road interactions. Consequently, this research focuses on only the rural road segments, as they are more pertinent to the type of collisions identified in the literature to be associated with RL, such as single-vehicle ROR crashes. **Figure 3.2** illustrates the rural sites where RL data were collected for both years, as well as exclusively for 2021. In the original datasets, RL of each 0.1-mile segment was measured in September 2020 and November 2021.

ROUTE_ID	MILE_MARKER	RL	LINE	DIRECTION	DATE_COLLECTED	GPS_LAT	GPS_LONG	SUB_RATE
AL0000030000	178.6	168	LEL	NB	9/12/2020	32.32923667	-86.34622	3
AL0000030000	178.7	283	LEL	NB	9/12/2020	32.32957333	-86.34791833	3
AL0000030000	178.8	246	LEL	NB	9/12/2020	32.329905	-86.34959667	3
AL0000030000	178.9	199	LEL	NB	9/12/2020	32.33024333	-86.35122833	3
AL0000030000	179	195	LEL	NB	9/12/2020	32.330585	-86.35289	3
AL0000030000	179.1	167	LEL	NB	9/12/2020	32.33098	-86.35456167	3
AL0000030000	179.2	0	LEL	NB	9/12/2020	32.33142333	-86.35619167	3
AL0000030000	179.3	142	LEL	NB	9/12/2020	32.33195667	-86.35776833	3
AL0000030000	179.4	125	LEL	NB	9/12/2020	32.33258	-86.35931167	3
AL0000030000	179.5	128	LEL	NB	9/12/2020	32.3333833	-86.360865	3
AL0000030000	179.6	134	LEL	NB	9/12/2020	32.33411833	-86.362255	3
AL0000030000	179.7	135	LEL	NB	9/12/2020	32.335005	-86.36360833	3

**Figure 3.1 A sample of original RL datasets collected from ALDOT**



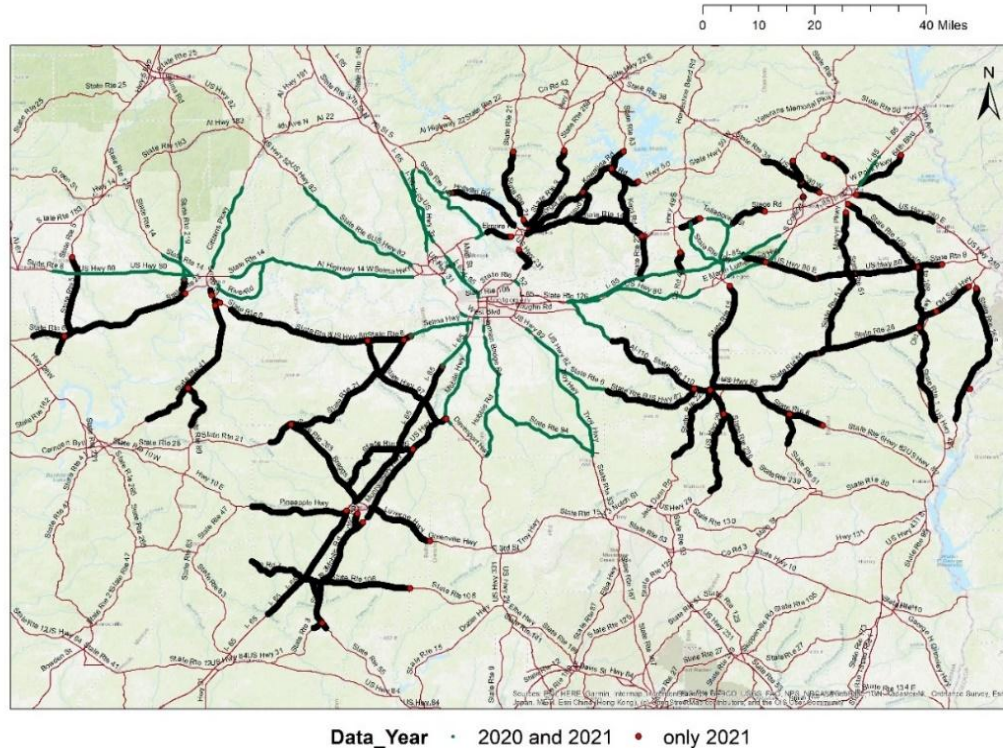


**Figure 3.2 Rural locations of RL measurement in Montgomery**

### 3.2 Crash Data

The Critical Analysis Reporting Environment (CARE) system, developed and maintained by the Center for Advanced Public Safety (CAPS) at the University of Alabama, serves as a comprehensive repository documenting all traffic crashes within Alabama. This system provides extensive data, including location, road, environment, driver, and vehicle characteristics, among other details. In context of this study, a few key road inventory variables available in the crash datasets include posted speed limit, location classification, functional class, road surface type, and number of lanes. This research obtained two years of crash records from 2020 to 2021. The geocoordinate of locations, route identification numbers, and mile marker information associated with crashes are vital for linking crash records to RL data.

### 3.3 Traffic Flow and Road Inventory Data

AADT was obtained from the ALDOT's traffic data website for the entire state of Alabama for 2020 and 2021 (ALDOT, 2023). The original dataset included route identification numbers, milepoints, and county details, which served as key reference points for accurately assigning AADT for each 0.1-mile road segment. Notably, the traffic flow datasets include information on the percentage of truck ADT, allowing for the calculation of truck AADT. However, including both passenger vehicle AADT and truck AADT as separate predictors may influence the model due to their derivation from the same overall AADT variable. This setup often results in truck AADT displaying a negative correlation with RL degradation, given that passenger vehicle AADT typically shows a strong positive correlation with RL degradation. Consequently, researchers usually prefer to incorporate the percentage of trucks rather than percentage of truck in ADT. The percentage of trucks indicates the proportion of trucks within the total vehicle count over a specific period, while the percentage of trucks in ADT reflects the proportion of trucks within the average daily traffic. For these reasons, truck AADT was excluded to avoid multicollinearity. A sample of original traffic flow datasets collected from ALDOT's traffic data website is provided in **Figure 3.3**.

FID	TRNumbe	UCounty	Station	RouteID	FromMeasur	ToMeasure	AADT	KFactor	DFactor
0	0	Randolph	527	AL000022	153.650857	156.8288534	1985	10	55
1	0	Randolph	526	AL000022	149.0878623	153.650857	1985	10	56
2	0	Washingto	809	AL000017	40.5991724	42.9983769	4721	10	53
3	0	Henry	533	AL000134	73.729	75.422107	648	10	52
4	0	Henry	530	AL000134	63.709	64.829	1575	11	67
5	0	Henry	138	AL000173	1.0907556	1.508	2748	10	68
6	0	Henry	136	AL000001	25.72405	26.241515	15733	9	54
7	0	Henry	143	IV0003200	0	0.3125047	2614	15	51
8	0	Henry	451	AL000134	58.885	59.22	3076	9	63

**Figure 3.3 A sample of the original traffic flow datasets**

Currently, there is no comprehensive documentation of road inventory information for Alabama. Relevant horizontal alignment information—such as the presence of curves, curve length, and chord length—was extracted from Google Earth Pro using the geocoordinates for each 0.1-mile road segment. This data was then processed in ArcGIS ‘COGO’ package to obtain additional metrics, including curve angle and curve radius. **Figure 3.4** illustrates a basic example of curve data entry and relevant outputs in ArcGIS.

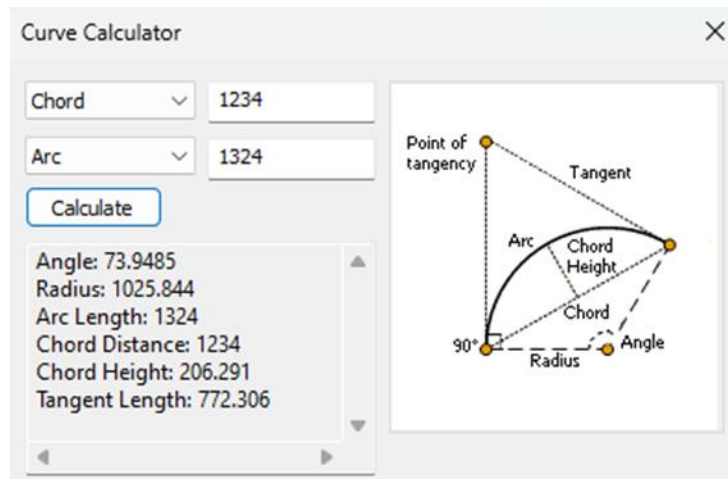


**Figure 3.4 ‘COGO’ package of ArcGIS for obtaining horizontal curve attributes**

The Highway Performance Monitoring System (HPMS) is a nationwide program aimed at providing an inventory of all public roads in the U.S. (FHWA, 2023). HPMS encompasses various roadway feature data such as number of lanes, functional class, speed limit, lane width, shoulder width, vertical alignment, and more. The database includes route identification numbers and mile marker information, which served as reference points for extracting the posted speed limits of each 0.1-mile segment. While assigning speed limits, it was assumed that the same posted speed limit was applicable across an entire 1-mile segment unless the AADT varied within that 1-mile segment. Posted speed limit data for 25% of the roadway segments was sourced from HPMS, and 45% was obtained from crash data. This information was further manually verified using Google

Earth Pro. The remaining 30% of segments posted speed limit information were manually extracted from Google Earth Pro.

The crash database contains route identification numbers and mile marker information, which served as reference points for extracting the location class information for each 0.1-mile segment. It is important to mention that the location class were categorized into two groups: open country and residential/business/mixed areas. For consistency, it was assumed that the same location class was applicable across an entire 1-mile segment unless AADT and posted speed limits varied within that segment. Location class data for 60% of the roadway segments was obtained from the crash datasets and subsequently cross-verified using Google Earth Pro. The remaining 40% of location class information was manually extracted from Google Earth Pro.

Road functional class information was extracted from HPMS and crash data. Given HPMS's comprehensive details on road functional classes, there were very few instances with missing information. Additionally, number of lane information was obtained from both HPMS and Google Earth Pro. Notably, marking line type can also indicate number of lanes, as two-lane roads typically have two marking lines (YCL and WREL), while multilane roads have three (YLEL, WLL, WREL). When extracting road surface type information from the crash datasets, it was found that over 95% of the segments were associated with asphalt surfaces, indicating that this was the predominant surface type. Therefore, road surface type was excluded from further analyses. **Figure 3.5** illustrates the extracted variables from each of the above-mentioned data sources.

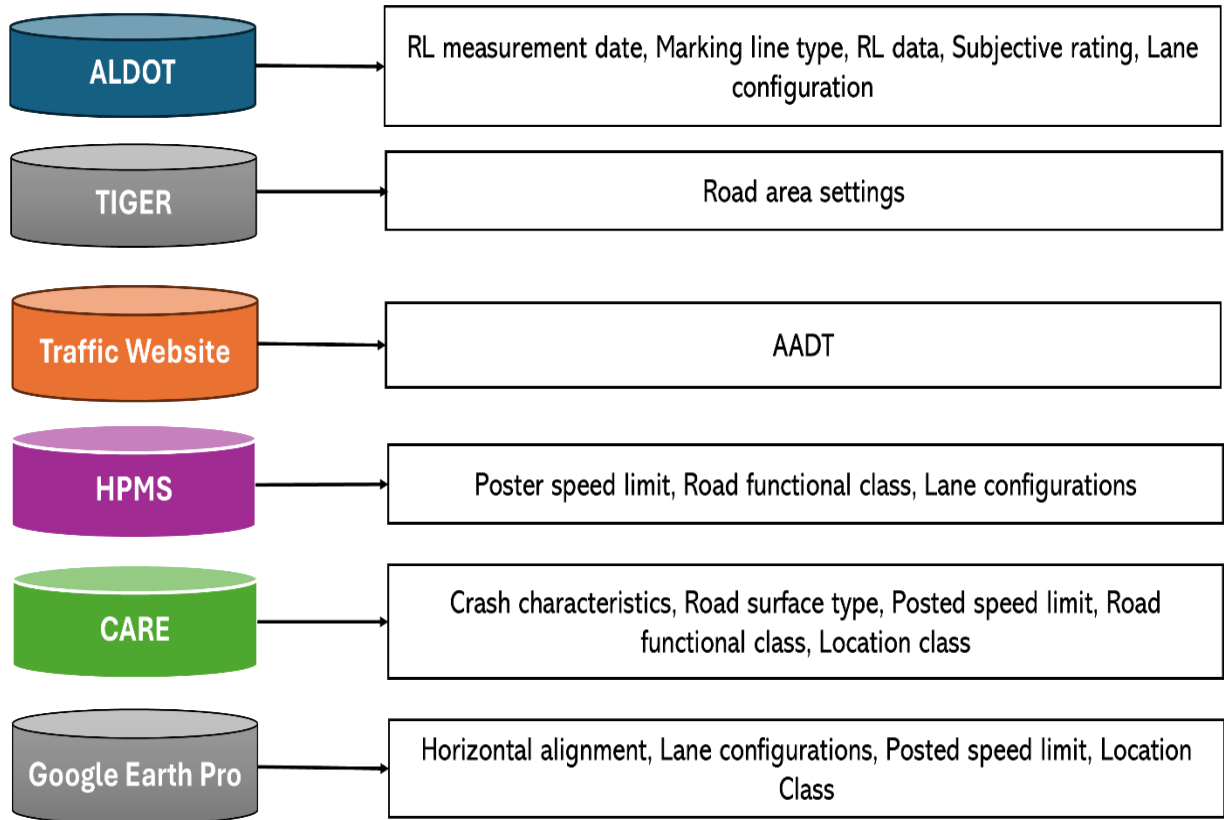


**Figure 3.5** Extracted variables from different data sources

## **Chapter 4     Contributing Factors of RL Degradation**

This section aims to investigate the factors contributing to the degradation of pavement marking RL in relation to marking line type. Regression models are employed to analyze the impact and significance of potential contributing factors on RL degradation. Additionally, the influence of curves on RL degradation is examined by utilizing regression functions and comparing the degradation proportions between curved and adjacent straight road segments. Locations that exhibit a higher proportion of RL degradation than usual, despite having identical marking, road, and traffic flow characteristics, are manually reviewed using Google Earth Street View to identify any additional factors that may contribute to such degradation. These insights are expected to provide a deeper understanding of how influential factors vary regarding marking line type, which can provide valuable guidance for maintaining RL in Alabama.

### **4.1     Data Preprocessing**

Considerable effort has been dedicated to preprocessing the RL data before conducting the analysis. As mentioned earlier, this study exclusively focuses on rural roads. The initial step in processing the RL dataset obtained from ALDOT involves assigning the appropriate marking line type for each measured RL. By manually reviewing lane configurations of each measured RL location using Google Earth Pro, the rural roads were categorized into two lane configurations: two-lane and multilane. For rural two-lane roads, the markings consist of YCL and WREL, while for multilane roads, the markings comprise YLEL, WLL, and WREL. While reviewing the original RL data, it was observed that the marking line types were inaccurately reported in a few instances, such as the transition from two-lane roads to four-lane roads or vice versa. For example, during a transition from two-lane roads to four-lane roads, the measured RL for centerlines was inaccurately

reported as YCL when it should have been recorded as YLEL. Similarly, during transitions from four-lane roads to two-lane roads, the reverse misclassification was observed, with YLEL being reported as YCL. Approximately 15% of 0.1-mile segments contained these inaccuracies, as the errors persisted across multiple continuous segments. Such errors were corrected to ensure the accuracy of further analysis.

The proportion of RL degradation was calculated by comparing data from 2020 and 2021. The basic equation is:

$$\text{Proportion of degradation} = (RL_{2020} - RL_{2021})/RL_{2020}$$

Where,  $RL_{2020}$  represents measured RL in 2020 and  $RL_{2021}$  represents measured RL in 2021. If the RL of a 0.1-mile segment for a specific marking line type was lower in 2020 compared to 2021, it indicates that the segment was restriped during that period. Consequently, such segments were excluded from further analysis. In total, 175 and 112 one-mile segments were identified for rural two-lane and multilane respectively where no restriping activities had been performed. Adjusted AADT (Adj AADT) was computed for each 0.1-mile road segment based on the date of RL measurement. For instance, if RL was measured on September 12, 2020, and November 20, 2021, and the AADT for that road segment in 2020 was 2,455 vpd, and in 2021 was 2,800 vpd, the adj AADT would be calculated as follows:

$$\text{Adjusted AADT (Adj AADT)} = \frac{110 * 2,455 + 323 * 2,800}{110 + 323} = 2,713 \text{ vpd}$$

Where, 110 represents the number of days between September 12, 2020, and December 31, 2020, while 323 represents the number of days from January 1, 2021, to November 20, 2021. Most previous studies have calculated the average RL for each 1-mile segment to develop datasets for degradation modeling. However, this approach does not account for potential variations in road

and traffic characteristics within a 1-mile segment. Recognizing this gap in data preparation, the current study has developed a more refined dataset for RL modeling, ensuring that variations in road, traffic flow, location, and marking characteristics are adequately considered. The detailed steps followed in preparing the dataset for this study are presented below:

- Step 1: Identify 0.1-mile road segments with similar road, traffic flow, and location characteristics. This includes ensuring consistency in factors such as the number of lanes, posted speed limits, location classification, functional classification, horizontal alignment, and Adj AADT
- Step 2: Arrange each group of 0.1-mile segments based on their measured RL values in 2020.
- Step 3: Calculate the moving average of the RL degradation proportion for each group of 0.1-mile segments by measured RL values in 2020 ( $RL_{2020}$ ), following the qualitative states. During this process, it was observed that the degradation proportions exhibited considerable fluctuations in a few instances, even with minimal differences in  $RL_{2020}$ . For example, within the same group, a particular 0.1-mile segment exhibited RL degradation proportion equal to or more than twice, despite having minimal differences in the measured  $RL_{2020}$ . RL data points showing these unexpected changes were excluded to minimize heterogeneity within the final datasets. A threshold of a twofold or greater increase in RL degradation proportion was used for exclusion, based on analytical judgments. It is important to note that less than 5% of the total 0.1-mile segments belonged to this category.

The above steps were applied to prepare the datasets for modeling RL degradation for each pavement marking line type, and horizontal alignment with a specific focus on curved segments. The centrifugal forces experienced by vehicles negotiating curves can cause lateral displacement



of vehicles, leading to more frequent contact with the WREL (Ray and Carrigan, 2023). This constant contact exacerbates the abrasion and friction experienced by the pavement marking, accelerating degradation of RL compared to straight segments. To investigate the influence of curves on the RL degradation of WREL, the average RL of WREL on curve segments was compared with three different types of straight segments: i) straight segments within the same 1-mile segment (s) (SS1), (2) preceding 1-mile straight segment (SS2), and (3) subsequent 1-mile straight segment (SS3). In this context, SS1 primarily represents the tangent section of the curves. For clarity, **Figure 4.1** provides an illustrative example of three different types of segmentation. The first two examples (from the top) illustrate the segmentation of a curve segment, along with SS1, SS2, and SS3, when the curve segment is located within a 1-mile road segment. The third example demonstrates the segmentation of a curve segment, SS1, SS2, and SS3, when the curve spans two 1-mile road segments. For comparison purposes, the curve segment and the adjacent straight segments (SS1, SS2, and SS3) need to satisfy two criteria: i) they share identical road, traffic flow, and location characteristics, and ii) measured  $RL_{2020}$  fall within the same qualitative state. It is important to mention that the qualitative state of white pavement markings was selected from two prior experimental studies provided in **Table 1.1** (Ortiz-García et al., 2006; Porrás-Alvarado et al., 2014).

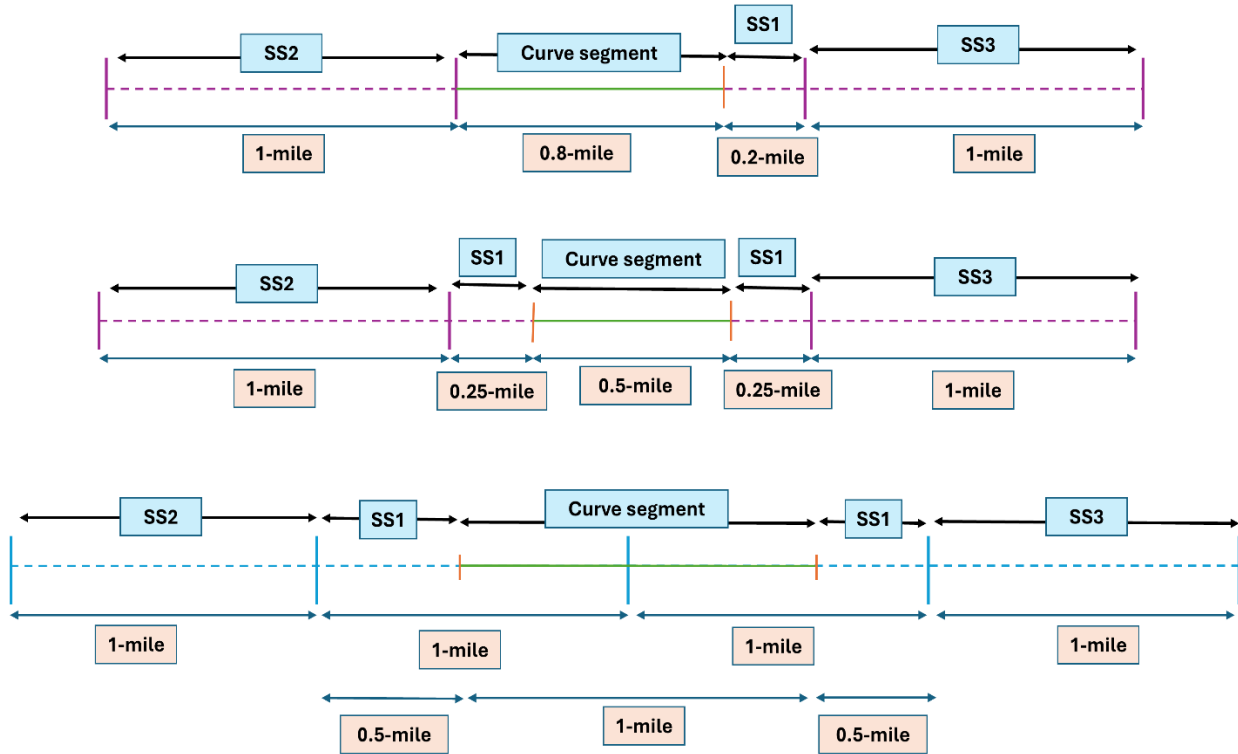


**Figure 4.1 Segmentations between curved and adjacent straight road segments**

In the original RL dataset, the degradation proportions of WREL showed an increase of 1.5 time or more in certain 0.1-mile segments, despite having minimal differences in the  $RL_{2020}$  values and identical road, traffic flow, and location characteristics. These segments were meticulously examined using Google Earth Street View to identify any additional factors contributing to the RL degradation.

## 4.2 Descriptive Statistics

**Table 4.1** presents the total number of observations in the final datasets by marking line type, along with the count of unique 1-mile road segments. Across all datasets, on average, there is more than one observation per 1-mile road segment. This indicates that, in the majority of cases, each observation represents a segment smaller than 1 mile.

**Table 4.1 Observation counts in final datasets for regression analysis**

Marking line type	Number of observations	Count of different 1-mile segments
YCL	209	129
WREL for rural two-lane	347	167
YLEL	177	95
WLL	160	85
WREL for rural multilane	235	108

The following observations provide insights based on **Table 4.2 and Figures 4.2-4.3**, presenting an overview of variables used in modeling RL degradation proportion:

- For rural two-lane roads, the mean degradation proportion of WREL is higher than that of YCL (0.28 and 0.26). A similar trend is observed on multilane roads for WREL (0.32) compared to YLEL (0.30). Among white pavement markings on rural multilane, WREL exhibits a higher mean degradation proportion (0.32) compared to WLL (0.25). Following the distributions, outliers exist in all marking line types except WLL.
- In rural two-lane roads, the mean  $RL_{2020}$  values are higher for WREL (338 mcd/m<sup>2</sup>/lx) than for YCL (224 mcd/m<sup>2</sup>/lx). This is attributed to the relatively higher installation and restriping standards for white pavement markings, resulting in higher RL measurements. The same pattern is observed in rural multilane roads, where WREL exhibits a mean RL of 379 mcd/m<sup>2</sup>/lx, compared to YLEL at 283 mcd/m<sup>2</sup>/lx and WLL at 324 mcd/m<sup>2</sup>/lx. Based on the distributions, outliers are present in all marking line types except WLL.
- The data distribution indicates an expected pattern, with adj AADT being higher on multilane roads compared to two-lane roads.
- In the current version of MUTCD, the minimum RL requirement is based on speed limits of either <35 mph or ≥35 mph. The earlier MUTCD version categorized speed limits into 35-50 mph and ≥55 mph with respect to lane configurations. The RL dataset collected from

ALDOT had a very few segments with a posted speed limit below 35 mph; therefore, for this study, posted speed limit was categorized to  $<55$  mph and  $\geq 55$  mph for two-lane roads, and  $<65$  mph and  $\geq 65$  mph for multilane roads. Given that posted speed limit and road functional class are highly correlated (FHWA, 2000), only one of these variables was used in the regression modeling to satisfy associated assumptions.

- The diversity of data in areas classified as residential, business, or mixed-use is greater for multilane roads (19.41%) compared to two-lane roads (14.57%). Conversely, data diversity on curved road segments is higher for two-lane roads (16.19%) compared to multilane roads (10.84%).

**Table 4.2 Overview of variables used in degradation proportion modeling by marking line type**

Variable attribute	Rural two-lane		Rural multilane		
	YCL (209)	WREL (347)	YLEL (177)	WLL (160)	WREL (235)
RL degradation proportion	Min: 0.04, Max: 0.73, Median: 0.25, Mean: 0.26	Min: 0.03, Max: 0.74, Median: 0.25, Mean: 0.28	Min: 0.04, Max: 0.76, Median: 0.26, Mean: 0.30	Min: 0.05, Max: 0.57, Median: 0.22, Mean: 0.25	Min: 0.06, Max: 0.78, Median: 0.31, Mean: 0.32
<i>RL</i> <sub>2020</sub> (mcd/m <sup>2</sup> /lux)	Min: 91, Max: 451, Median: 216, Mean: 224	Min: 94, Max: 711, Median: 331, Mean: 338	Min: 49, Max: 620, Median: 276, Mean: 283	Min: 99, Max: 639, Median: 301, Mean: 324	Min: 90, Max: 742, Median: 375, Mean: 379
Adj AADT (vpd)	Min: 546, Max: 11,220, Median: 3,556, Mean: 3,447	Min: 546, Max: 13,560, Median: 2,874, Mean: 3,443	Min: 842, Max: 72,187, Median: 16,258, Mean: 21,899	Min: 3,610, Max: 52,638, Median: 15,624, Mean: 18,606	Min: 3,610, Max: 85,257, Median: 16,258, Mean: 22,849
<i>Posted speed limit</i>					
<55mph	17 (8.13%)	46 (13.26%)	-----	-----	-----
≥55mph	192 (91.87%)	301 (86.74%)	-----	-----	-----
<65mph	-----	-----	59 (33.33%)	46 (28.75%)	74 (31.49%)
≥ 65mph	-----	-----	118 (66.67%)	114 (71.25%)	161 (68.51%)
<i>Location class</i>					
open country	178 (85.17%)	297 (85.59%)	144 (81.36%)	133 (83.13%)	184 (78.30%)
residential/business/mixed	31 (14.83%)	50 (14.41%)	33 (18.64%)	27 (16.88%)	51 (21.70%)
<i>Horizontal alignment</i>					
straight	188 (89.95%)	278 (80.12%)	156 (88.14%)	144 (90%)	210 (89.36%)
curve	21 (10.05%)	69 (19.88%)	21 (11.86%)	16 (10%)	25 (10.64%)

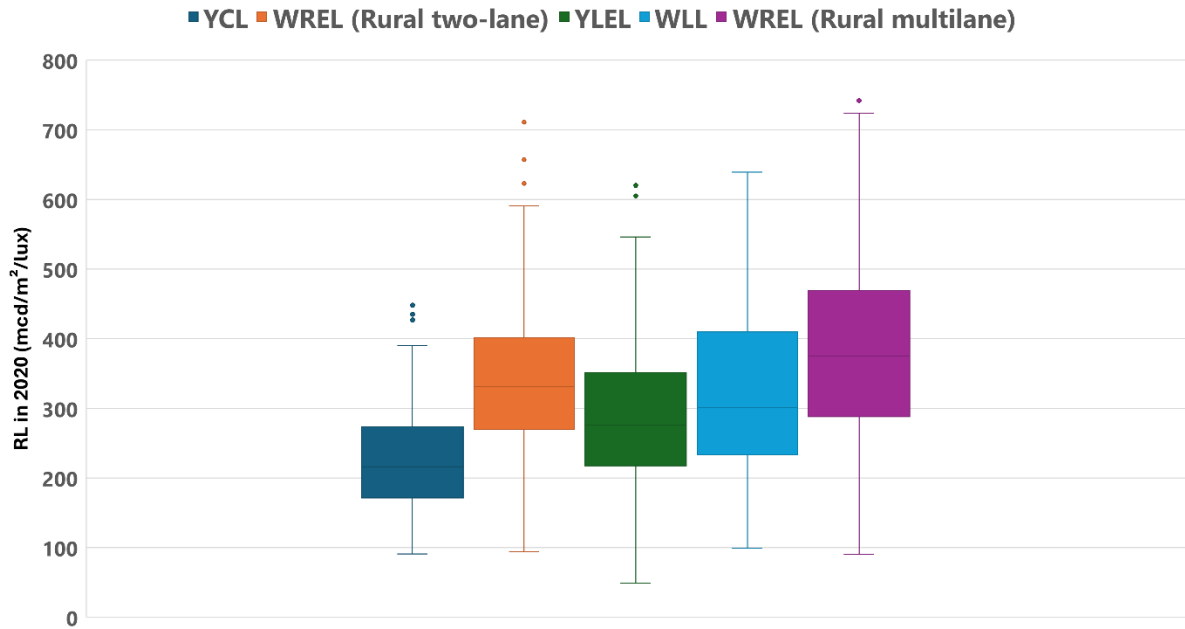


Figure 4.2 Distribution of  $RL_{2020}$  by marking line type

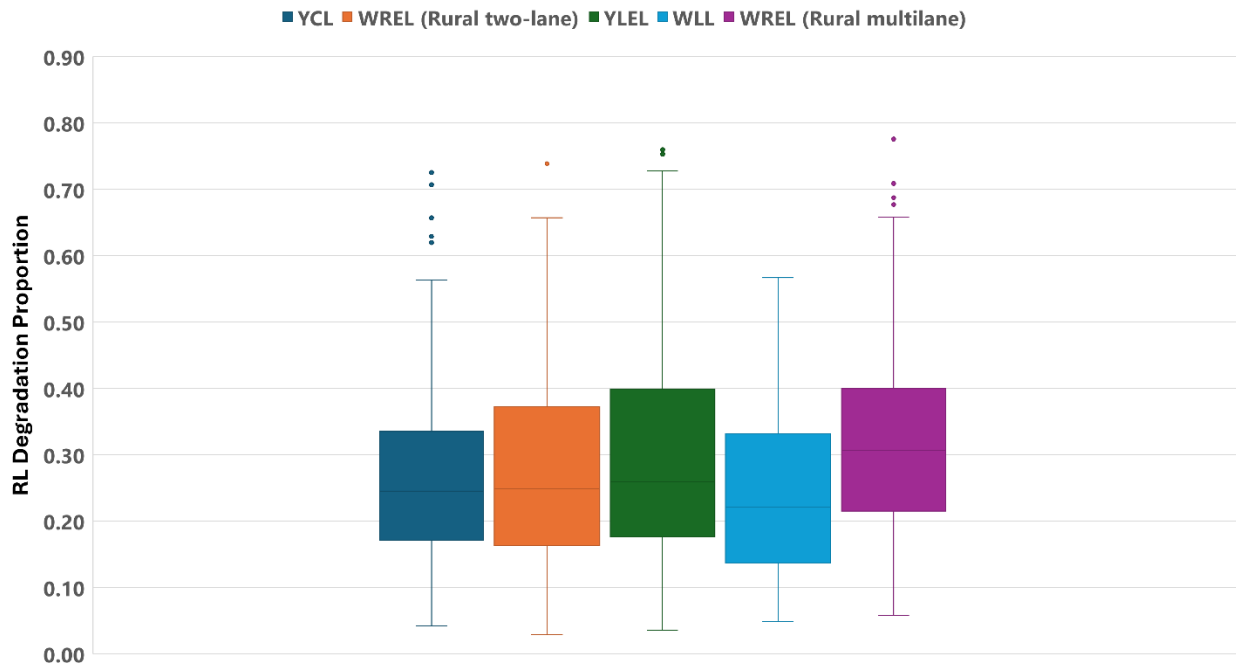


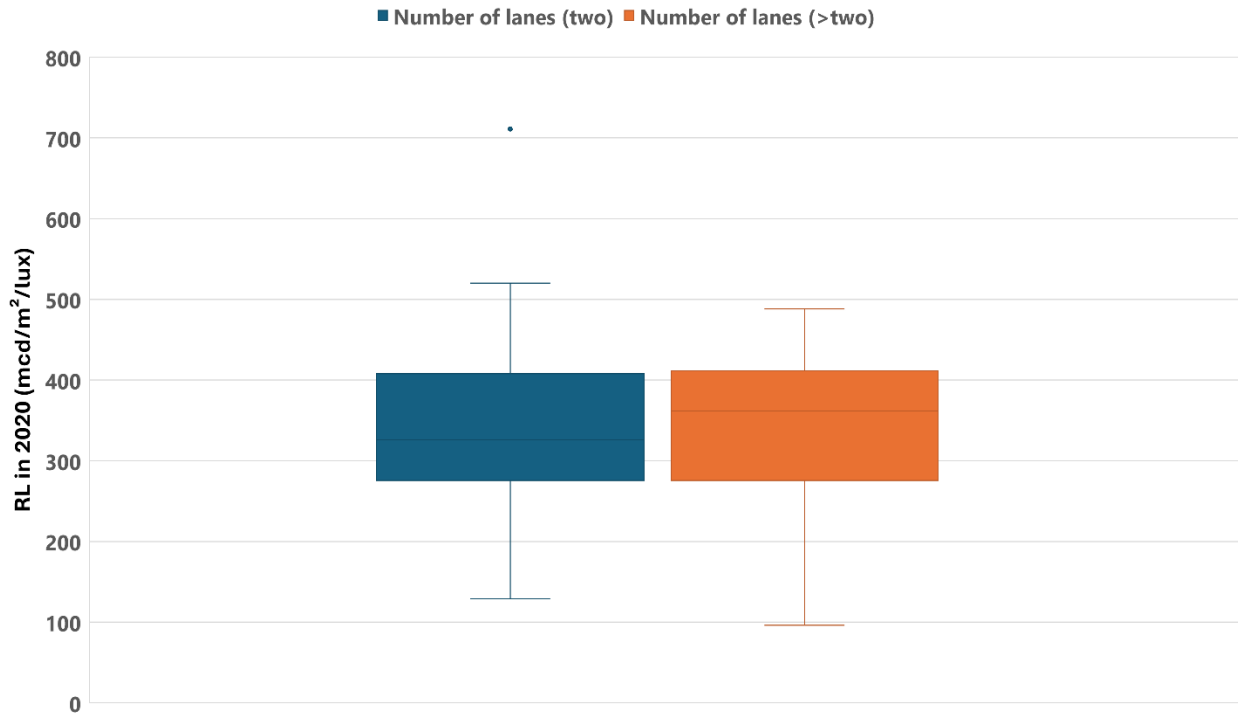
Figure 4.3 Distribution of RL degradation proportion by marking line type

Table 4.3 and Figures 4.4-4.5 provide an overview of variables utilized to model degradation proportion of curved sections specifically related to WREL. The total number of observations is 90. The median  $RL_{2020}$  and RL degradation proportion of curve segments are higher on multilane

roads compared to two-lane roads. The curve angles observed in these segments range from 12.88 degrees to 77.04 degrees. Most of these segments are associated with two-lane roads (72.22%). It is essential to note that during the measurement of curve radius and angle, three segments were identified as compound curves. Consequently, these compound curve segments were excluded from the dataset to ensure consistency and accuracy in the regression analysis for simple curve segments. Since the analysis requires consideration of both two-lane and multilane roads, the road functional class has been chosen for further analysis instead of the posted speed limit due to multicollinearity. The functional class of curve road segments is categorized into three main classifications: major collector (16.67%), arterial (75.56%), and interstate (7.78%).

**Table 4.3 Overview of variables used to model RL degradation proportion of WREL for curved sections**

<b>Variable</b>	<b>Data summary / Proportion</b>
RL degradation proportion	Min: 0.06, Max: 0.59, Median: 0.25, Mean: 0.28
<i>RL</i> <sub>2020</sub> (mcd/m <sup>2</sup> /lux)	Min: 96, Max: 711, Median: 338, Mean: 336
Adj AADT (vpd)	Min: 546, Max: 39,595, Median: 3,610, Mean: 8,761
Curve angle (degree)	Min: 12.88, Max: 77.04, Median: 38.02, Mean: 39.08
Curve radius (ft)	Min: 406.10, Max: 7,272.90, Median: 2,767.20, Mean: 3,045.40
<i>Number of lanes</i>	
two	65 (72.22%)
> two	25 (27.78%)
<i>Functional class</i>	
major collector	15 (16.67%)
arterial	68 (75.56%)
interstate	7 (7.78%)
<i>Location class</i>	
open country	80 (88.89%)
residential/business/mixed	10 (11.11%)



**Figure 4.4 Distribution of  $RL_{2020}$  for curve segments**

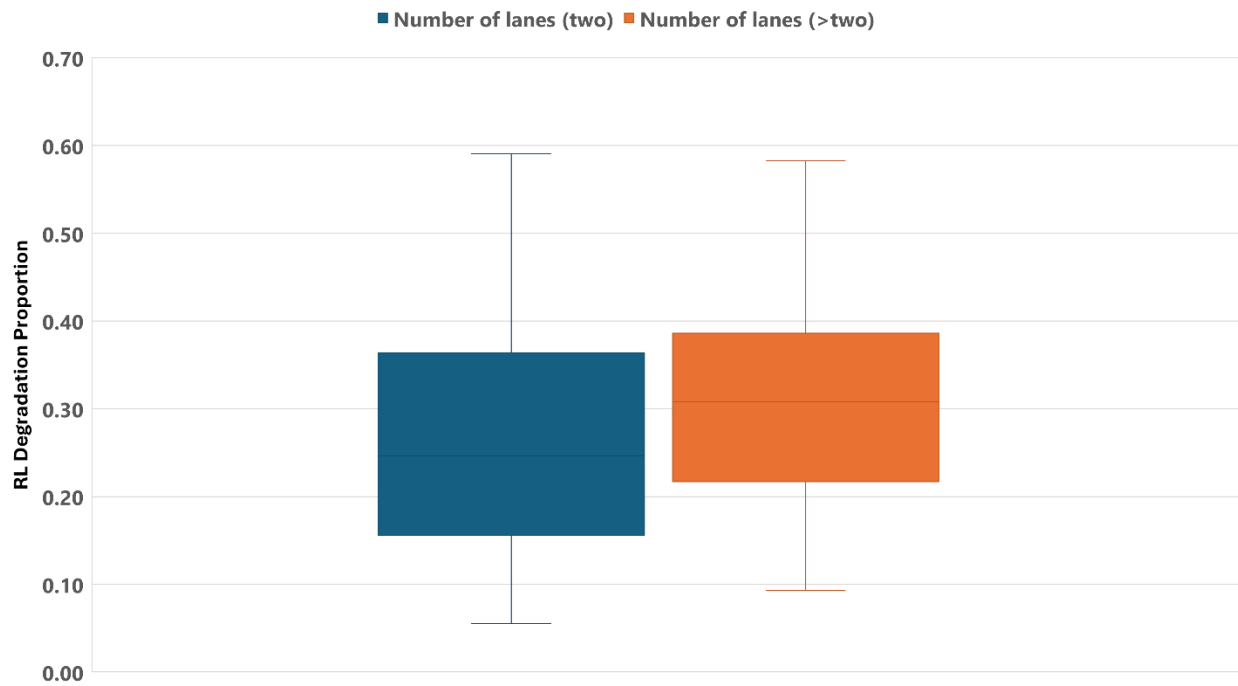


**Figure 4.5 Distribution of RL degradation proportion for curve segments**



**Table 4.4** provides an overview of the datasets used to compare RL degradation proportion of WREL by horizontal alignments. Three distinct datasets are developed for this comparison: i) RL degradation proportion on curve segments compared with the corresponding degradation on straight segments within the same 1-mile segment(s) (Curve-SS1), ii) the RL degradation proportion on curve segments compared with the corresponding degradation on the preceding 1-mile straight segment (Curve-SS2), and iii) the RL degradation proportion on curve segments compared with the corresponding degradation on the subsequent 1-mile straight segment (Curve-SS3). In all three datasets, RL degradation observed in the curved sections is consistently higher than in the corresponding straight sections. This pattern is further evidenced by the percentage of observations in which the RL degradation proportion is greater in the curved sections, with all percentages exceeding 60%. The trend is more frequent when comparing the curved sections with the preceding and subsequent straight sections, where the percentages were 79.41% and 82.93%, respectively.

**Table 4.4 Overview of datasets to compare degradation proportion by horizontal alignment**

<b>Dataset type</b>	<b>Horizontal alignment</b>	<b>Summary</b>	<b>Percentage of observations where curved section RL degradation proportion is higher</b>
Curve-SS1	curve	Min: 0.04, Max: 0.59, Median: 0.26, Mean: 0.26	31 out of 49 (63.27%)
	SS1	Min: 0.03, Max: 0.59, Median: 0.18, Mean: 0.23	
Curve-SS2	curve	Min: 0.04, Max: 0.59, Median: 0.26, Mean: 0.26	27 out of 34 (79.41%)
	SS2	Min: 0.01, Max: 0.52, Median: 0.15, Mean: 0.18	
Curve-SS3	curve	Min: 0.04, Max: 0.55, Median: 0.27, Mean: 0.27	34 out of 41 (82.93%)
	SS3	Min: 0.02, Max: 0.49, Median: 0.18, Mean: 0.21	

### 4.3 Methodology

This study utilized beta regression to identify the statistically significant factors contributing to RL degradation. Furthermore, to determine whether there were statistically significant differences in RL degradation between curve and adjacent straight road segments with similar road, traffic flow, location, and marking characteristics, Paired t-test and Wilcoxon test were conducted based on the RL degradation distribution of road segments.

#### 4.3.1 Beta Regression

Beta regression is a statistical technique designed to model the probability distribution of continuous values within the range of 0 to 1. This makes it particularly well-suited for analyzing proportions or rates, where the dependent variable is naturally bounded (Cribari-Neto and Zeileis, 2010; Ferrari and Cribari-Neto, 2004). In this study, RL degradation proportion was used as the dependent variable in the beta regression analysis. The probability density function of beta regression is presented below:

$$f(y; c, d) = \frac{\Gamma(c + d)}{\Gamma(c)\Gamma(d)} y^{c-1}(1 - y)^{d-1}$$

Where  $0 < y < 1$  and  $\Gamma(\cdot)$  function is the gamma function. The parameters  $c$  and  $d$  are positive integer values, influencing the shape of the curve. By defining  $\mu = \frac{c}{c + d}$  and  $\phi = c + d$ , the function transforms into:

$$f(y; \mu, \phi) = \frac{\Gamma(\phi)}{\Gamma(\mu\phi)\Gamma((1 - \mu)\phi)} y^{\mu\phi-1}(1 - y)^{(1-\mu)\phi-1}$$

Where  $y \sim \beta(\mu, \phi)$ ,  $\mu$  is the mean of distribution ( $0 < \mu < 1$ ), and  $\phi$  represents the variability of distribution. Let  $y_1, \dots, y_n$  be a random sample and  $y_i \sim \beta(\mu_i, \phi)$ ,  $i = 0, 1, 2, \dots, n$ . If  $x_i$  represents the independent variable and  $\beta$  stands for the unknown parameter, the beta regression model is specified with a log link function, as shown below:

$$g(\mu_i) = \log(\mu_i) = x_i^T \beta = \tau_i$$

$$\beta = (\beta_1, \dots, \beta_k)^T$$

$$x_i = (x_{i1}, \dots, x_{ik})^T$$

The coefficients  $\beta$  describe the relationship between the independent variables and the logit of the mean response  $\mu$ . A negative coefficient signifies a decrease in the log-odds of  $\mu$  while a positive coefficient suggests an increase. Odds represent the ratio of the probability of an event occurring to the probability of it not occurring. For instance, if the probability of RL degradation is 0.2, the odds of RL degradation can be calculated as:

$$Odds = \frac{0.2}{1 - 0.2} = 0.25$$

Pseudo  $R^2$  is commonly applied in non-linear models, such as logistic regression, Poisson regression, and beta regression, where the dependent variable is not continuous or normally distributed (Ferrari and Cribari-Neto, 2004; Hu et al., 2006).

$$Pseudo R^2 = 1 - \frac{\ln(L_{full})}{\ln(L_{null})}$$

Where,  $\ln(L_{full})$  is the likelihood of the fitted model and  $\ln(L_{null})$  is the likelihood of the null model.

### 4.3.2 Paired t-test

The upper-tail paired sample t-test is a statistical method used to determine whether the mean difference between two sets of paired observations is significantly greater than zero (Hsu and Lachenbruch, 2014). In this research, the upper-tail paired t-test is suitable for determining whether the mean proportion of RL degradation on curve segments is statistically higher than on adjacent straight road segments. The paired t-test assumes that the differences between paired samples are normally distributed. Therefore, it is essential to conduct the Shapiro-Wilk test

beforehand to verify whether the differences follow a normal distribution, ensuring the validity of the paired t-test results (Kim, 2018). The hypotheses for an upper-tail paired t-test are defined as:

$$\text{Null Hypothesis } H_0: \mu_d \leq 0$$

$$\text{Alternative Hypothesis } H_1: \mu_d > 0$$

Where  $\mu_d$  represents the true mean difference between the paired samples. The test statistic  $t$  is calculated as:

$$t = \frac{\bar{d}}{s_d/\sqrt{n}}$$

Where  $\bar{d}$  = sample mean of differences between paired observation,  $s_d$  = sample standard deviation of the differences, and  $n$  = number of paired samples. The degree of freedom for the paired t-test is  $n - 1$ .

#### 4.3.2 Wilcoxon Signed-Rank Test

The Wilcoxon Signed-Rank test is a non-parametric test used instead of the paired t-test when the assumptions of the paired t-test are not met, particularly the assumption that the differences between paired observations are normally distributed. The hypotheses for upper-tail Wilcoxon Signed-Rank test are defined as follows:

$$\text{Null Hypothesis } H_0: \text{Median } (D) \leq 0$$

$$\text{Alternative Hypothesis } H_1: \text{Median } (D) > 0$$

Where  $D$  represents the differences between the paired samples. The analytical framework of exploring the relationship between two paired samples is provided in **Figure 4.6**.

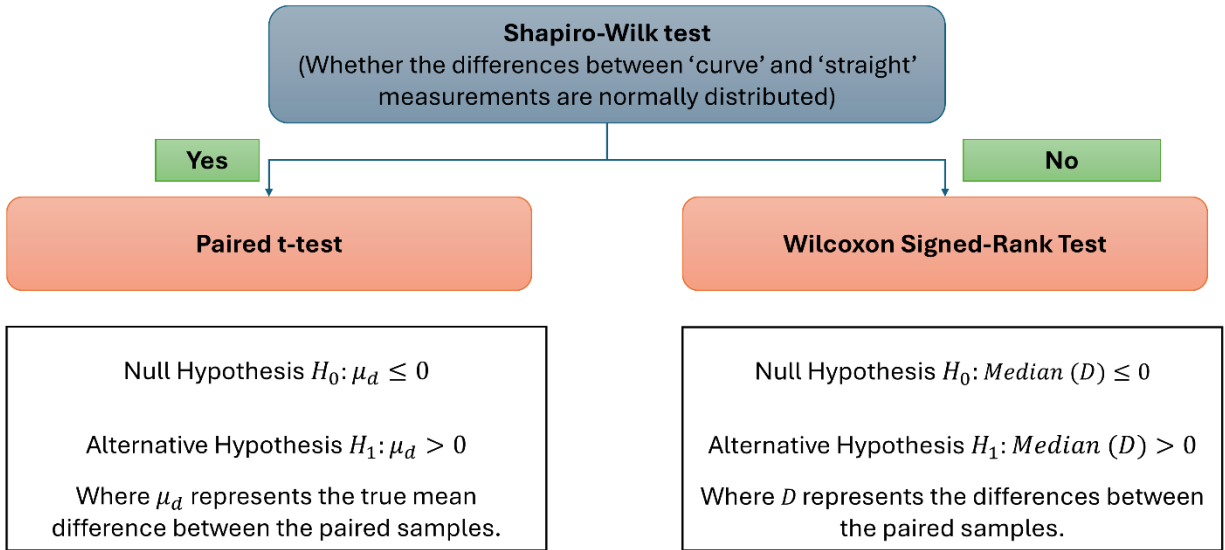


**Figure 4.6 Analytical framework to explore the relationship between curve and adjacent straight road segments in terms of RL degradation proportion**

#### 4.4 Results & Discussions

Initially, beta regression models were applied to datasets representing the RL degradation proportion of different marking line types on rural two-lane and multilane roads. Moreover, a beta regression model was employed to analyze the characteristics of variables on curve road segments. Due to the limited sample size, regression modeling on curved sections was not conducted separately for two-lane and multilane roads. To explore the influence of curved sections on adjacent straight road sections, paired t-test and Wilcoxon test were performed following the distribution of datasets. Finally, locations with relatively high RL degradation proportions were further reviewed to identify any additional factors that may contribute to the degradation. It is important to mention that all regression models were performed at a 95% confidence interval.

##### 4.4.1 RL Degradation Factors by Marking Line Type

**Table 4.5** presents an overview of beta regression results for two different marking line types of rural two-lane roads. In beta regression, coefficients are interpreted in terms of odds ratios.

For YCL, a one-unit increase in  $RL_{2020}$  leads to a 0.15% (calculated as  $e^{0.0015}$ ) increase in RL degradation odds, while for WREL, there is a 0.36% increase. Based on MUTCD guidelines and previous studies, yellow markings typically degrade more slowly than white markings, so white pavement markings have higher initial RL standards. A 1,000-unit increase in adj AADT results in a 3.25% increase in RL degradation odds for YCL and a 4.71% increase for WREL. This statistically higher degradation for WREL is consistent with findings from a previous Alabama study (Ozelim and Turochy, 2014). Previous studies have consistently identified AADT as a significant factor positively correlated with RL degradation (Idris et al., 2024; Migletz et al., 2001; Ozelim and Turochy, 2014). Road segments located in residential, business, or mixed-use areas show statistically higher RL degradation for YCL, with a 36.60% increase in odds. Frequent turning, stopping, accelerating, and higher congestion levels characterize these areas, which can contribute to greater wear on pavement markings. For YCL, road segments with a posted speed limit of  $\geq 55$  mph exhibit lower RL degradation compared to those with a speed limit of  $< 55$  mph, although this is not statistically significant. According to MUTCD guidelines, RL typically degrades more at higher posted speed limits. In the dataset, however, only 8.14% of YCL observations fall under the  $< 55$  mph category. A larger dataset might better capture the true relationship between posted speed limits and RL degradation.

**Table 4.5 Summary of beta regression model for marking line types of rural two-lane (YCL and WREL)**

	YCL				WREL			
	Coef.	SE	z-value	p-value	Coef.	SE	z-value	p-value
Intercept	-2.2048	0.2259	-9.068	<0.001	-1.5100	0.0180	-8.381	<0.001
$RL_{2020}$ (mcd/m <sup>2</sup> /lux)	0.0015	0.0005	6.414	<0.001	0.0036	0.0004	3.980	<0.001
Adj AADT (in 1,000 vpd)	0.0320	0.0210	2.697	0.007	0.0460	0.0240	3.223	0.001
<i>Posted speed limit (ref. &lt;55mph)</i>								
≥55mph	-0.1079	0.1076	-1.004	0.316	0.1396	0.1505	0.927	0.354
<i>Location class (ref. open country)</i>								
residential/business/mixed	0.3119	0.1134	1.994	0.046	0.1024	0.1050	0.975	0.329
<i>Horizontal alignment (ref. straight)</i>								
curve	-0.2354	0.1384	-0.758	0.448	0.0513	0.0892	0.575	0.565
Pseudo $R^2$	0.1822				0.0519			

Note: Coefficient (Coef.) and Standard Error (SE)

**Tables 4.6-4.7** provide an overview of beta regression models for three different pavement markings on rural multilane roads (YLEL, WLL, and WREL). In consistent with rural two-lane roads,  $RL_{2020}$  of YLEL shows statistically lower odds of RL degradation compared to WREL. Among white markings,  $RL_{2020}$  of WREL exhibits statistically higher odds of RL degradation compared to WLL, increasing by 0.22% compared to a 0.07% increase for WLL. Adj AADT increases the odds of degradation less in YLEL compared to WLL and WREL, aligning with previous studies. WLL shows statistically higher RL degradation odds with increasing Adj AADT and on rural road segments with higher posted speed limits, likely due to increased lane-changing behavior. Segments in residential, business, or mixed-use areas exhibit a 1.59 times higher odds of RL degradation for YLEL. This could be due to the greater frequency of U-turns or the use of the left lane to access minor roads, may contribute to increased wear on YLEL in these areas.

**Table 4.6 Summary of beta regression model for WREL of rural multilane**

	<b>Coef.</b>	<b>SE</b>	<b>z value</b>	<b>p-value</b>
Intercept	-1.4340	0.1343	-10.681	<0.001
$RL_{2020}$ (mcd/m <sup>2</sup> /lux)	0.0022	0.0003	4.581	<0.001
Adj AADT (in 1,000 vpd)	0.0041	0.0027	2.597	0.009
<i>Posted speed limit (ref. &lt;65mph)</i>				
>=65mph	0.0985	0.1498	1.325	0.185
<i>Location class (ref. open country)</i>				
residential/business/mixed	0.1685	0.1074	1.569	0.117
<i>Horizontal alignment (ref. straight)</i>				
curve	0.0921	0.1287	0.716	0.474
Pseudo $R^2$ : 0.1192				

Note: Coefficient (Coef.) and Standard Error (SE)



**Table 4.7 Summary of beta regression model for YLEL and WLL of rural multilane**

	YLEL				WLL			
	Coef.	SE	z-value	p-value	Coef.	SE	z-value	p-value
Intercept	-1.5290	0.2010	-7.609	<0.001	-1.3130	0.1876	-6.998	<0.001
$RL_{2020}$ (mcd/m <sup>2</sup> /lux)	0.0014	0.0005	4.140	<0.001	0.0007	0.0004	1.610	0.101
Adj AADT (in 1,000 vpd)	0.0022	0.0035	0.590	0.555	0.0081	0.0047	2.296	0.021
<i>Posted speed limit (ref. &lt;65mph)</i>								
≥65mph	0.0326	0.1489	0.219	0.827	0.0870	0.1325	2.002	0.045
<i>Location class (ref. open country)</i>								
residential/business/mixed	0.4612	0.1690	2.381	0.017	0.1917	0.1537	1.247	0.212
<i>Horizontal alignment (ref. straight)</i>								
curve	0.1010	0.1767	0.571	0.568	-0.2504	0.1765	-1.418	0.156
Pseudo $R^2$	0.2024				0.1056			

Note: Coefficient (Coef.) and Standard Error (SE)

#### 4.4.2 Contributing Factors of RL Degradation on Curve Segments

Since RL degradation of WREL is more likely to be impacted by vehicle encroachment, the analysis focuses specifically on curve segments for WREL. **Table 4.8** provides a summary of the beta regression model results for these curved segments. However, due to the limited sample size (n=90), none of the variables or attributes in the model were found to be statistically significant.

**Table 4.8 Summary of beta regression model for WREL on curve segments**

	<b>Coef.</b>	<b>SE</b>	<b>z value</b>	<b>p-value</b>
(Intercept)	-1.4600	0.4244	-3.440	<0.001
<i>RL<sub>2020</sub></i>	0.0007	0.0007	1.073	0.283
Adj AADT (in 1,000 vpd)	0.0066	0.0125	0.784	0.433
<i>Location class (ref. open country)</i>				
residential/business/mixed	0.1428	0.2370	0.607	0.543
<i>Functional class (ref. major collector)</i>				
arterial	0.2513	0.2084	1.206	0.227
interstate	0.1260	0.4248	0.297	0.767
<i>Number of lanes (ref. &gt;two)</i>				
two	-0.0428	0.2355	-0.182	0.855
curve angle	-0.0011	0.0049	-0.221	0.825
curve radius (in 1,000)	0.0014	0.0430	0.241	0.809
Pseudo $R^2$ : 0.0937				

Note: Coefficient (Coef.) and Standard Error (SE)

#### 4.4.3 RL Degradation by Horizontal Alignment

As discussed in Section 4.2, three datasets were developed to evaluate the impact of curves on RL degradation of WREL in comparison to adjacent straight road segments. To begin the analysis, the Shapiro-Wilk test was employed to assess whether differences between ‘curve’ and ‘straight’ measurements were normally distributed. For the datasets 'Curve-SS1' and 'Curve-SS2', the null hypothesis was accepted (normally distributed), allowing for the use of the paired t-test to determine whether the mean degradation proportion on curve segments was statistically higher

than that of the corresponding straight segments: SS1 and SS2 (defined in Sections 4.1 and 4.2). For the 'Curve-SS3' dataset, the null hypothesis of normality was rejected; therefore, the Wilcoxon test was appropriate to assess whether the median degradation proportion on curve segments was statistically higher than that of the corresponding straight segment. **Table 4.9** presents the results of the paired tests for all three datasets. The findings indicate that the mean/median degradation proportion of RL is statistically higher on curve segments compared to SS1, SS2, and SS3. This suggests that, when road, traffic flow, location, pavement marking, and RL states remain constant, RL of WREL degrades more on curve segments than on adjacent straight segments.

**Table 4.9 Summary of paired tests between curve and corresponding straight road segments**

<b>Dataset type</b>	<b>Test</b>	<b>t-value/V- value</b>	<b>p-value</b>
Curve-SS1	Upper-tail paired t-test	2.126	0.019
Curve-SS2		4.043	<0.001
Curve-SS3	Upper-tail Wilcoxon test	752	<0.001

#### **4.4.4 Additional Factors Contributing to RL Degradation of WREL**

To investigate additional factors contributing to RL degradation of WREL, 0.1-mile road segments with similar road, traffic flow, and location characteristics, as well as identical RL qualitative states, were manually reviewed. The focus was on segments exhibiting a relatively higher RL degradation proportion than expected. To ensure an adequate number of 0.1-mile segments meeting these criteria (similar road, traffic flow, and location characteristics with identical RL qualitative states), segments with RL degradation at least 1.5 times or more than the typical levels were selected, based on engineering judgment. A comprehensive review was conducted on 202 locations, each representing a 0.1-mile segment. Additional logical contributing factors were identified in 100 of these segments through visual observation, providing further insight into the potential influencing factors of increased degradation. In Google Earth Pro, the

majority of street view images for the segments were unavailable for 2021, as these segments were primarily located in open country areas. As a result, street view images from 2022 were used for comparison. Upon reviewing, no significant differences were observed between the 2022 and 2024 images.

Out of the 100 segments with higher RL degradation, 10 segments feature an additional right-turn lane near intersections or ramps. In these areas, vehicles preparing to turn often encroach upon WREL, which can cause increased wear due to tire friction, particularly during braking and deceleration. An example of such locations is illustrated in **Figure 4.7** (Geocoordinates: 32.43941667, -87.35586333). 21% of 0.1-mile segments with U-turn and left-turn facilities to minor roads exhibit higher RL degradation of WREL. The frequent vehicle maneuvers during lane shifts and sharp turns can increase tire contact with WREL, increasing its degradation. Such scenarios are more likely to be found on rural multilane roads. An example is provided in **Figure 4.8** (Geocoordinates: 32.4393683, -87.36104333). Of the 100 segments, 11 are associated with bridges where noticeable differences in surface materials are evident compared to the surrounding asphalt roadways (**Figure 4.9** - Geocoordinates: 32.44584, -87.15954333). Concrete surfaces are usually smoother and less porous than asphalt, which can result in weaker bonding with pavement markings (Romanoschi and Metcalf, 2002). In addition, bridges are exposed to adverse environmental conditions such as temperature fluctuations and use of deicing, which can accelerate RL degradation of WREL.



**Figure 4.7 Additional right-turn lane as potential contributor of RL degradation**

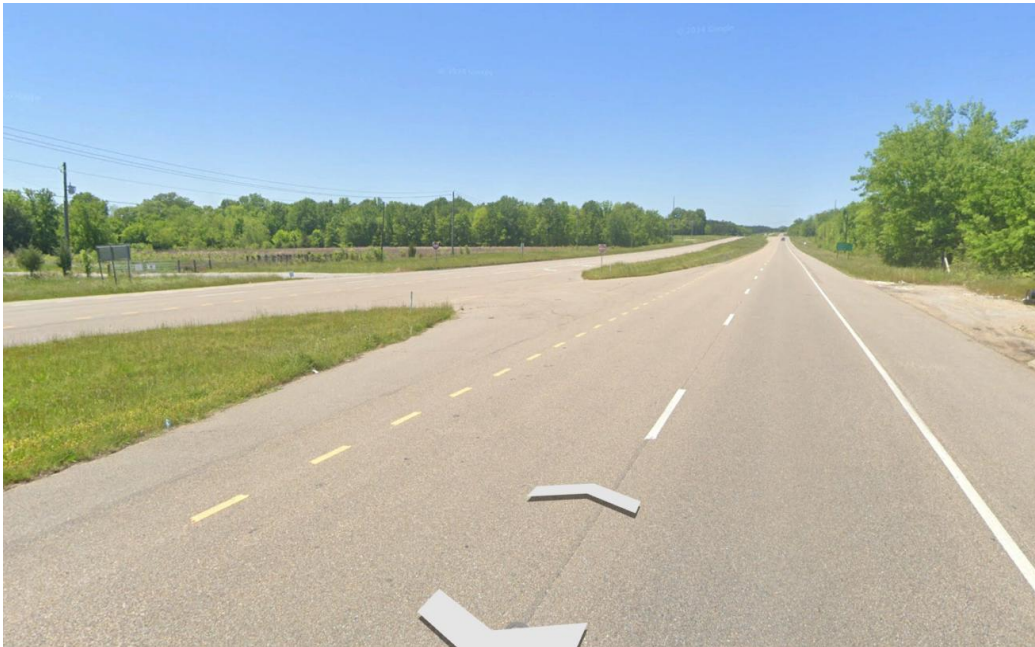


**Figure 4.8 U-turn and left-turn movement as potential contributor of RL degradation**



**Figure 4.9 Bridge as potential contributor of RL degradation**

Out of 100 segments, 2 are associated with the presence of a ramp. It is important to note that vehicles from these ramps merge onto multilane roads. The potential reason for the high RL degradation proportion of WREL in these areas is likely due to the frequent braking and deceleration as vehicles slow down. An example is illustrated in **Figure 4.10** (Geocoordinates: 32.43938167, -87.35928333). 5 out of 100 segments have additional shoulders on the road (**Figure 4.11**- Geocoordinates: 32.43011667, -86.94442333). Shoulders are often used by vehicles during emergencies, which leads to increased tire contact and physical stress on WREL. 51% of the segments are associated with i) residential driveways where vehicles frequently cross the WREL and ii) private roads leading to businesses or other properties. An example of such locations is shown in **Figure 4.12** (Geocoordinates: 32.46460167, -85.59793833). In most of these cases, nearby gravel surfaces have been observed, which can significantly accelerate the degradation of the WREL. Debris from the gravel is frequently displaced onto the roadway, which can lead to additional wear and tear on pavement markings. In similar scenarios where the nearby surface of



WREL is paved, a slightly lower degradation of RL has been observed. This suggests that the surrounding landscape also influences RL degradation.



**Figure 4.10 Presence of ramp as potential contributor of RL degradation**



**Figure 4.11 Shoulder presence as potential contributor of RL degradation**



**Figure 4.12 Residential driveway as potential contributor of RL degradation**

#### **4.5 Key findings**

This section aims to identify the key factors contributing to RL degradation by pavement marking line types. In addition to applying regression models to potential contributing factors identified in previous studies, this research adopts a comprehensive approach by manually reviewing sites and considering the logical impact of vehicle encroachment on curves, particularly focusing on WREL. It is crucial to note that WREL can play a significant role in minimizing lane departures and reducing ROR crashes, making it a focal point for researchers studying pavement markings. As multiple factors and their interactions can influence RL degradation and collecting high-volume data over time is a big challenge in pavement marking research, finding a variable statistically insignificant does not imply that the factor is unimportant. The key findings from this analysis are outlined below:



- Consistent with prior research, AADT plays a crucial role in RL degradation on each marking line type. For two-lane roads, the statistical correlation between adj AADT and RL degradation proportion is higher for WREL than for YCL, aligning with the requirement of higher RL installation or restriping standards for white pavement markings. A similar pattern is observed on multilane roads, where the effect of adj AADT is statistically higher for white markings (WLL and WREL) compared to yellow (YLEL). Moreover, on multilane roads, the RL degradation associated with increasing AADT is statistically higher for WLL than for WREL. Consistent with Adj AADT,  $RL_{2020}$  shows statistically higher RL degradation proportion for white marking compared to yellow.
- Pavement markings in residential, business, or mixed-use areas experience statistically higher RL degradation only for centerlines, YCL on two-lane roads and YLEL on multilane roads.
- The degradation proportion of WLL is found to be statistically significant on roadways with high posted speed limits. On high-speed roads, especially those with multiple lanes, drivers often change lanes to pass slower vehicles.
- RL degradation proportion of WREL is found to be statistically higher on curve segments compared to adjacent straight segments. This is observed when the road, traffic flow, and location characteristics are similar, and both curve and straight segments had the same RL qualitative state in the previous year.
- Several additional factors that may associated with the RL degradation of WREL include the presence of an additional right-turn lane near intersections or ramps, multilane road segments with U-turn and left-turn facilities to minor roads, presence of bridge, presence of ramps/shoulders/residential driveways, and the surrounding landscape.

## **Chapter 5 Relationship between Subjective Rating and Measured RL**

This section provides a detailed understanding of the statistical distribution of measured RL values in relation to subjective RL rating scales, considering the marking line types of rural two-lane and multilane roads. The analyses explore the statistical relationship between subjective ratings and measured RL regarding different marking line types. Moreover, this section examines how the distribution of measured RL varies by marking line type for each subjective rating category. The objective is to evaluate the extent to which subjective RL ratings reflect the measured values, which can provide insights into the reliability of visual evaluations of RL in term of actual RL measurements.

### **5.1 Data Preprocessing**

In Alabama, pavement marking management systems typically conduct daytime visual inspections. The rating of these markings can vary based on the perspectives of observers. Furthermore, visual inspection results may be influenced by factors such as contrast between marking and pavement surface. Since measuring actual RL with specialized equipment can be costly, subjective rating offers a simple and affordable method to evaluate pavement markings to determine if their RL levels meet adequate standards or require restriping. Traditionally, these evaluations involve rating road segments on a scale ranging from 1 to 5, in which 1 indicates poor RL and 5 signifies very good RL.

The original RL dataset comprises both subjective ratings and measured values for each marking line type within 1/10th of a mile segments (in majority of cases), spanning 2020 and 2021. The number of lanes information for each road segment was extracted, as detailed in Chapter 3. While reviewing RL data, it is noted that subjective ratings were scaled from 1 to 4 for 2020, while

the scale was expanded to 5 for 2021. However, there is no information explaining why the rating scale was modified in 2021. To ensure consistency in the final datasets, only the RL data from 2021 was included for further analyses. In addition, as discussed in Section 4.1, there were instances in the original datasets where marking positions were inaccurately reported, such as conversions from two-lane to multilane roads or vice versa. To ensure data accuracy, measured RL values and subjective ratings of road segments without these discrepancies were selected for further analyses.

## **5.2 Descriptive Analysis**

The statistical distributions of measured RL were initially explored in relation to subjective ratings for each marking line type, both with and without outliers. **Table 5.1-5.4** shows the summaries of measured RL by subjective rating for four different marking line types. Since a small fraction of observations (less than 1%) fall within the outlier category, further analyses focus on the calculated statistical distribution of datasets without outliers.

**Table 5.1 Overview of measured RL (mcd/m<sup>2</sup>/lux) for YCL by subjective rating**

Parameter	Rating 1		Rating 2		Rating 3		Rating 4		Rating 5	
	With outlier	Without outlier	With outlier	Without outlier	With outlier	Without outlier	With outlier	Without outlier	With outlier	Without outlier
Number of observations	283	282	2,070	2,060	3,360	3,279	2,686	2,663	399	387
Minimum	66	66	47	47	58	58	60	60	50	96
Maximum	612	390	478	385	845	333	543	381	560	291
1st Quartile	101	101	117	117	135	134	156	156	159	159
Median	132	132	160	160	173	172	199	199	184	182
3rd Quartile	219.50	218.75	225.75	224	215	210	246	245	212	210
Mean	162.31	160.71	173.86	172.65	181.10	175.01	205.07	203.09	189.78	186.07
Standard deviation	74.47	69.60	71.87	69.87	67.72	54.41	63.09	59.48	49.54	38.10

**Table 5.2 Overview of measured RL (mcd/m<sup>2</sup>/lux) for YLEL by subjective rating**

Parameter	Rating 1		Rating 2		Rating 3		Rating 4		Rating 5	
	With outlier	Without outlier	With outlier	Without outlier	With outlier	Without outlier	With outlier	Without outlier	With outlier	Without outlier
Number of observations	91	90	1,033	1,023	1,088	1,062	634	588	355	354
Minimum	43	43	53	53	57	57	79	79	102	102
Maximum	257	175	917	466	706	339	1299	419	846	555
1st Quartile	50	50	126	126	152.75	152	195	191.75	235.50	235.25
Median	81	78.5	175	173	191	189	237.5	232	344	344
3rd Quartile	114	112.50	262	257.50	227.25	224.75	284.75	272.25	406	405.50
Mean	86.69	84.80	206.45	203.01	195.60	189.18	264.28	234.69	325.80	324.33
Standard deviation	41.30	37.353	105.76	99.56	69.31	53.53	142.03	67.64	105.40	101.84

**Table 5.3 Overview of measured RL (mcd/m<sup>2</sup>/lux) for WLL by subjective rating**

Parameter	Rating 1		Rating 2		Rating 3		Rating 4		Rating 5	
	With outlier	Without outlier	With outlier	Without outlier	With outlier	Without outlier	With outlier	Without outlier	With outlier	Without outlier
Number of observations	30	28	960	861	1,733	1,675	426	409	168	166
Minimum	66	66	72	72	65	65	94	94	199	199
Maximum	383	291	785	453	789	459	1126	649	1144	733
1st Quartile	113	111.25	179	172	172	170	227.25	226	327.50	326.50
Median	149	146	244	234	227	223	301	288	404.50	403.50
3rd Quartile	186.25	181.75	290.25	273	287	280	401	384	508.50	506
Mean	164.63	150.25	269.90	229.64	242.17	230.64	337.12	312.41	420.55	413.15
Standard deviation	74.05	51.48	144.14	79.30	101.28	80.28	168.15	116.12	131.35	112.63

**Table 5.4 Overview of measured RL (mcd/m<sup>2</sup>/lux) for WREL by subjective rating**

Parameter	Rating 1		Rating 2		Rating 3		Rating 4		Rating 5	
	With outlier	Without outlier	With outlier	Without outlier	With outlier	Without outlier	With outlier	Without outlier	With outlier	Without outlier
Number of observations	431	429	1,182	1,149	6,701	6,545	3,116	3,075	501	482
Minimum	73	73	73	73	63	63	82	82	167	167
Maximum	524	469	582	440	1037	505	1037	668	992	615
1st Quartile	139.50	139	167.25	165	193	192	264	263	313	310.25
Median	206	204	225	222	253	250	328	326	371	366.50
3rd Quartile	278.50	278	277	269	318	313	429	422	435	427.75
Mean	217.88	216.51	230.45	222.99	262.88	255.48	352.50	346.72	386.63	373.05
Standard deviation	92.84	90.85	91.35	80.85	101.18	89.49	122.06	111.37	112.72	87.72

In relation to YCL, the mean and median measured RL values follow the expected trend for ratings 1-3, increasing with higher subjective ratings (**Figure 5.1**). However, the mean and median measured RL for a subjective rating of 4 (203.09 mcd/m<sup>2</sup>/lux and 199 mcd/m<sup>2</sup>/lux, respectively) are higher than for a rating of 5 (186.07 mcd/m<sup>2</sup>/lux and 182 mcd/m<sup>2</sup>/lux, respectively). This discrepancy may be attributed to factors such as small sample size, human error, pavement contrast, environmental conditions, and so on. In addition, the lower standard deviations of measured RL for YCL in ratings 3-5 compared to ratings 1-2 suggest that YCLs with higher perceived quality may have less variability with actual RL measurements. In addition, the range of the mean measured RL across different rating scales is relatively small for YCL, varying from 160.71 mcd/m<sup>2</sup>/lux to 186.07 mcd/m<sup>2</sup>/lux. In relation to YLEL, the mean measured RL for a subjective rating of 2 (203.01 mcd/m<sup>2</sup>/lux) is higher than for a subjective rating of 3 (189.18 mcd/m<sup>2</sup>/lux) (**Figure 5.2**). However, the median of measured RL increases as subjective ratings improve, following an expected pattern. Moreover, the standard deviations of measured RL do not exhibit a consistent pattern regarding ratings; therefore, variability of measured RL for YLEL may not correlate with subjective ratings.

For WLL, the median measured RL for a subjective rating of 2 (234 mcd/m<sup>2</sup>/lux) is higher than for a rating of 3 (223 mcd/m<sup>2</sup>/lux) (**Figure 5.3**). However, the mean measured RL follows the expected pattern, increasing as subjective ratings improve. Additionally, the standard deviations of measured RL increases with subjective ratings. This indicated that although WLLs with higher perceived quality tend to have more consistency with higher actual RL measurements, there may be greater variability. For WREL, both means and medians of measured RL follow the expected trend, increasing with subjective ratings (**Figure 5.4**). Moreover, the standard deviations of measured RL remain relatively consistent across different subjective ratings.

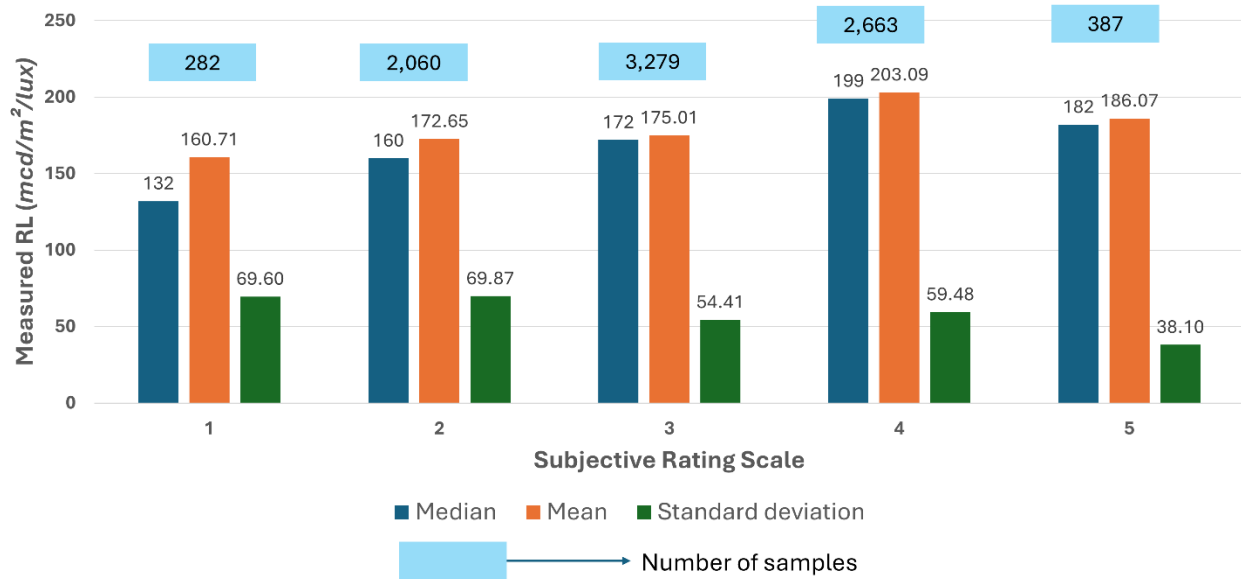


**Figure 5.1 Key descriptive statistics parameters of measured RL (mcd/m<sup>2</sup>/lux) for YCL by subjective rating**

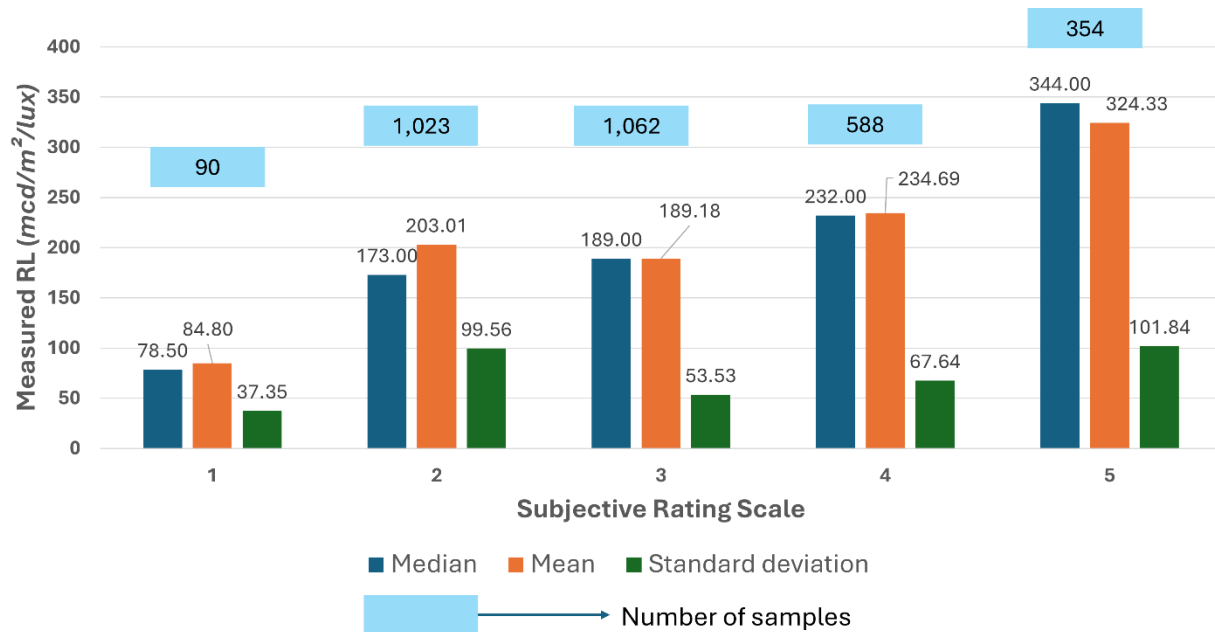


**Figure 5.2 Key descriptive statistics parameters of measured RL (mcd/m<sup>2</sup>/lux) for YLEL by subjective rating**

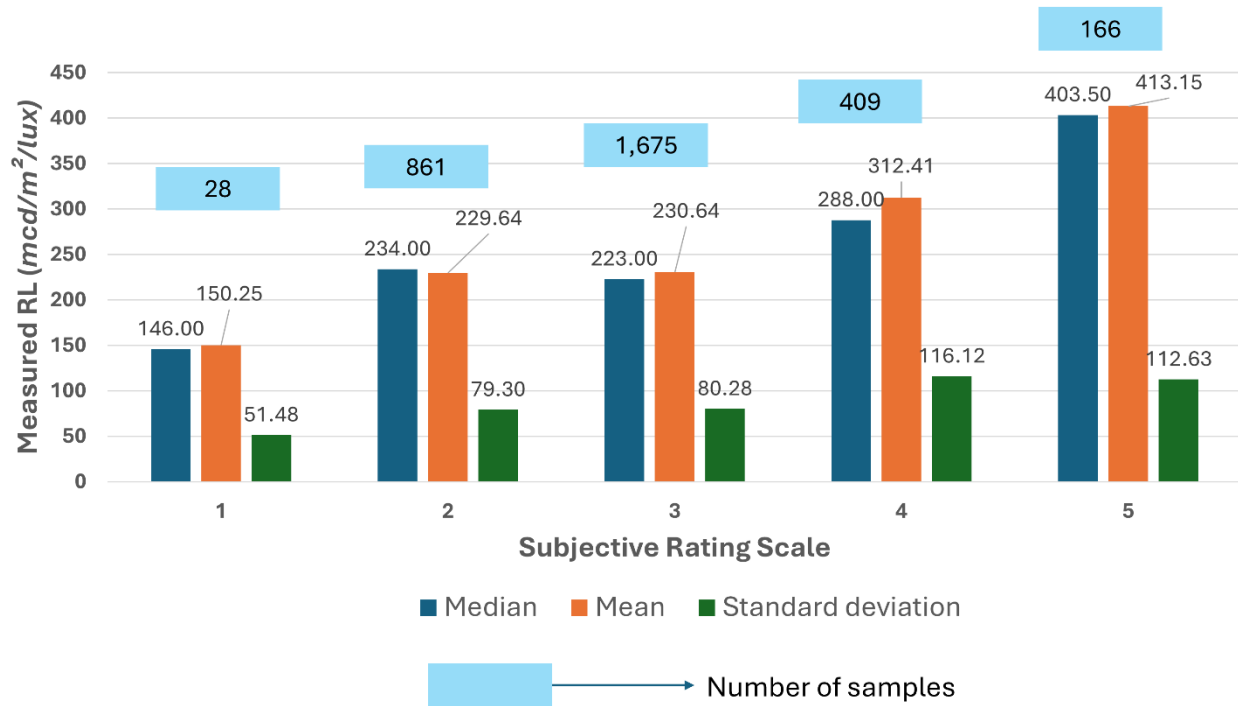


**Figure 5.3 Key descriptive statistics parameters of measured RL (mcd/m<sup>2</sup>/lux) for WLL by subjective rating**

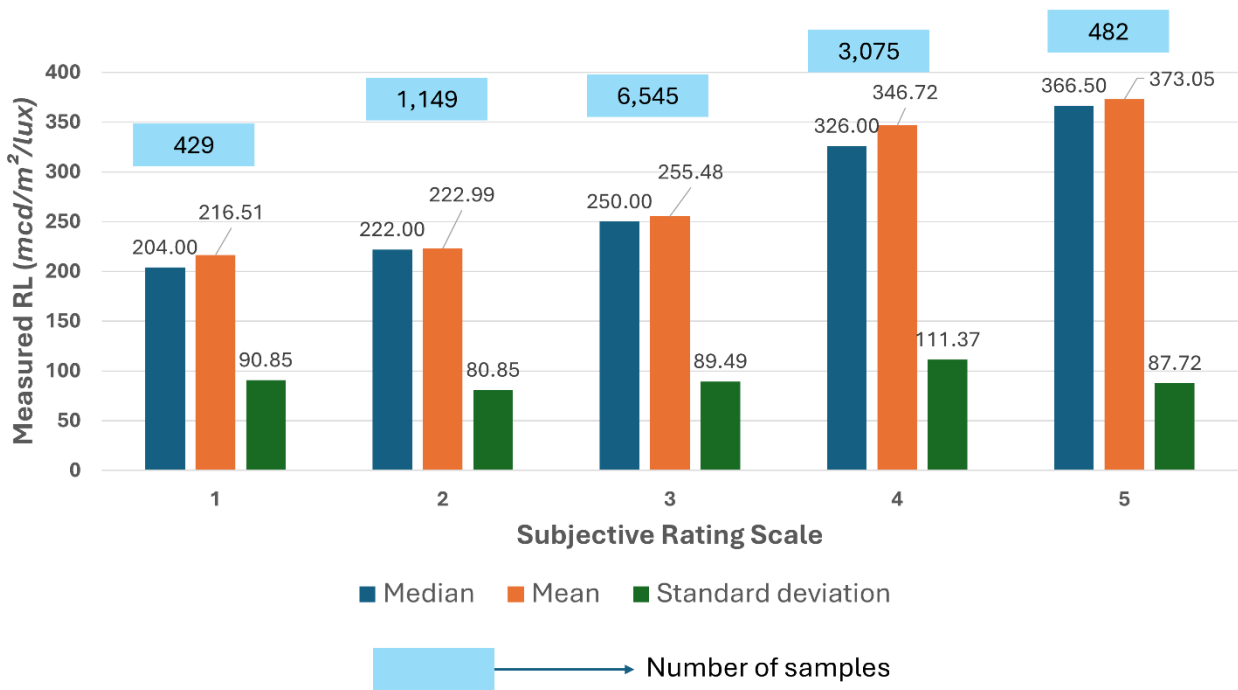


**Figure 5.4 Key descriptive statistics parameters of measured RL (mcd/m<sup>2</sup>/lux) for WREL by subjective rating**



### 5.3 Methodology

Two-sample t-tests were employed to explore the relationship between subjective ratings and marking line type in context of the measured RL values. Before performing the two-sample t-tests, Levene's test was conducted to assess whether the variances of two samples were equal. If Levene's test indicated equal variances, a pooled t-test was performed. If the variances were found to be unequal, Welch's t-test was used instead.

#### 5.3.1 Pooled t-test

The pooled t-test is a two-sample t-test in which the variances of the two groups are the same. This test pools the variances from both groups and uses the pooled variance to estimate the standard error of the mean difference (Land and Chase, 1993). The hypotheses for lower-tail and upper-tail pooled t-test are defined as:

$$\begin{aligned} \text{Lower-tail: } & \begin{cases} \text{Null Hypothesis } (H_0): \mu_1 = \mu_2 \\ \text{alternative Hypothesis } (H_1): \mu_1 < \mu_2 \end{cases} \\ \text{Upper-tail: } & \begin{cases} \text{Null Hypothesis } (H_0): \mu_1 = \mu_2 \\ \text{alternative Hypothesis } (H_1): \mu_1 > \mu_2 \end{cases} \end{aligned}$$

Where,  $\mu_1$  and  $\mu_2$  are the means of two populations. The formula for calculating t-statistics is provided in the following:

$$t = \frac{\bar{X}_1 - \bar{X}_2}{\sqrt{S_p^2 \left( \frac{1}{n_1} + \frac{1}{n_2} \right)}}$$

Where,  $\bar{X}_1$  and  $\bar{X}_2$  are mean of two sample means,  $n_1$  and  $n_2$  are sample sizes, and  $S_p^2$  is the pooled variance.

$$S_p^2 = \frac{(n_1 - 1)S_1^2 + (n_2 - 1)S_2^2}{n_1 + n_2 - 2}$$

Where  $S_1^2$  and  $S_2^2$  are the sample variances.

### 5.3.2 Welch's t-test

The Welch's t-test does not assume equal variances between the two groups. Instead, it estimates the standard error using separate variance estimates for each group. Welch's t-test is appropriate when the variances of two groups are different (Land and Chase, 1993). The hypotheses for lower-tail and upper-tail Welch's t-test are defined as:

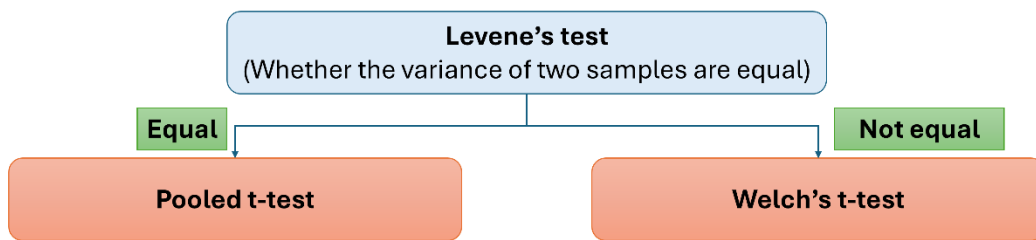
$$\text{Lower-tail: } \begin{cases} \text{Null Hypothesis } (H_0): \mu_1 = \mu_2 \\ \text{alternative Hypothesis } (H_1): \mu_1 < \mu_2 \end{cases}$$

$$\text{Upper-tail: } \begin{cases} \text{Null Hypothesis } (H_0): \mu_1 = \mu_2 \\ \text{alternative Hypothesis } (H_1): \mu_1 > \mu_2 \end{cases}$$

Where,  $\mu_1$  and  $\mu_2$  are the means of two populations. The formula for calculating t-statistics is provided in the following:

$$t = \frac{\bar{X}_1 - \bar{X}_2}{\sqrt{\left(\frac{S_1^2}{n_1} + \frac{S_2^2}{n_2}\right)}}$$

Where,  $\bar{X}_1$  and  $\bar{X}_2$  are mean of two sample means,  $n_1$  and  $n_2$  are sample sizes, and  $S_1^2$  and  $S_2^2$  are the sample variances. The analytical framework of this section is provided in **Figure 5.5**.



$$\text{Lower-tail: } \begin{cases} \text{Null Hypothesis } (H_0): \mu_1 = \mu_2 \\ \text{alternative Hypothesis } (H_1): \mu_1 < \mu_2 \end{cases}$$

$$\text{Upper-tail: } \begin{cases} \text{Null Hypothesis } (H_0): \mu_1 = \mu_2 \\ \text{alternative Hypothesis } (H_1): \mu_1 > \mu_2 \end{cases}$$

Where,  $\mu_1$  and  $\mu_2$  are the means of two populations

**Figure 5.5 Analytical framework of exploring relationship between subjective ratings and marking line type in context of the measured RL values**

## 5.4 Analysis & Discussions

**Figure 5.6** shows the results of two-sample t-tests conducted to examine the statistical relationship between subjective ratings by pavement marking line types, comparing the measured RL values in  $\text{mcd/m}^2/\text{lux}$ . It is important to note that the order of sample 1 and sample 2 for subjective rating scales can be identified using the two row names. The cell colors indicate the statistical relationship between the mean measured RL of population corresponding to samples from one rating and the mean measured RL of population corresponding to samples from another rating. For instance, for YCL, the first cell (from left) indicates that the mean measured RL for the population corresponding to samples with a subjective rating of 1 is statistically lower than that for the population corresponding to samples with a subjective rating of 2. The majority of rating combinations by marking positions follow the expected pattern, where the mean of measured RL statistically decreases as the subjective rating decreases at 90% and 95% confidence intervals. However, as noted in Section 5.2, ratings 4 and 5 for YCL and Ratings 2 and 3 for YLEL show a reverse trend where the mean of measured RL statistically increases significantly, despite a lower subjective rating. It is important to note that both instances involve yellow markings, suggesting that challenges related to evaluating yellow markings may contribute to this. In relation to WLL, the mean of measured RL values for ratings 2 and 3 are statistically equal, indicating no significant difference between these subjective ratings in terms of measured RL values.


Sample 1 (Rating scale)	1				2			3		4
Sample 2 (Rating scale)	2	3	4	5	3	4	5	4	5	5
Marking line type										
YCL										
WREL										
WLL										
YLEL										

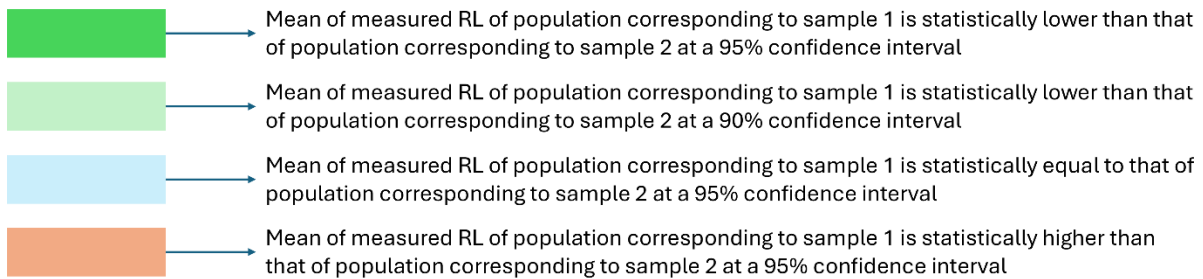



**Figure 5.6 Statistical relationship between subjective ratings with respect to marking positions in terms of measured RL values**

Figure 5.7 presents the results of two-sample t-tests conducted to identify the statistical relationship between pavement marking line types by subjective ratings comparing the measured RL values in mcd/m<sup>2</sup>/lux. The organization concept is similar to Figure 5.7, using the same color coding for results. For Rating 1, the first cell (from the left) indicates that the mean measured RL for the population associated with WREL samples is statistically higher than that for the population associated with YCL samples. The findings reveal that the mean of measured RL for white markings is statistically higher than for yellow markings in almost all subjective rating scales. This aligns with the fact that white pavement markings typically have higher minimum RL standards than yellow markings, which is reflected even in the subjective rating standards. Among white markings, in the majority of rating scales, WREL shows a statistically higher mean measured RL compared to WLL. This indicates higher subjective rating standards for WREL. Among yellow markings, the mean measured RL for YLEL is statistically higher than YCL in most of the subjective ratings.

Sample 1 (line type)	WREL			WLL		YLEL
Sample 2 (line type)	YCL	WLL	YLEL	YCL	YEL	YCL
Rating scale						
1						
2						
3						
4						
5						

 → Mean of measured RL of population corresponding to sample 1 is statistically lower than that of population corresponding to sample 2 at a 95% confidence interval

 → Mean of measured RL of population corresponding to sample 1 is statistically higher than that of population corresponding to sample 2 at a 95% confidence interval

**Figure 5.7 Statistical relationship between marking line types by subjective ratings in terms of measured RL values**

### 5.5 Key Findings

This section examines the statistical relationship between subjective ratings and measured RL, considering pavement marking line types. The findings can provide insights into the consistency of subjective rating in different marking line types in terms of actual RL measurement. One of the purposes of this section is to determine whether the higher RL standards maintained by ALDOT based on marking color, are also reflected in the subjective rating scales. Moreover, the analyses offer insights into the marking line types where observers may encounter difficulties determining subjective rating scales (e.g., 2 or 3), as a range of factors can influence these visual assessments. The key findings of this section are outlined below:

- In the majority of marking line types, the mean measured RL statistically decreases as the subjective rating decreases, which reflects consistency between subjective rating and measured RL. This pattern is more evident in white markings, such as WREL and WLL.

- Yellow markings, such as YCL and YLEL, show an unexpected pattern where the mean measured RL statistically increases despite lower subjective ratings. This may be due to lower sample size and observers encountering difficulties in rating yellow markings accurately because of color contrast.
- Almost in all subjective rating scales, the mean measured RL for white markings is statistically higher than for yellow markings. This reflects a tendency to maintain higher rating standards for white markings in terms of actual RL measurement, as they tend to degrade more over time.
- Among white markings, observers apply higher rating standards for WREL in context of actual RL measurement across most of the subjective rating scales, while YLEL is found to have higher rating standards among yellow markings.

## Chapter 6      RL Prediction Model

This chapter focuses on developing regression models to predict RL for YCL and WREL. Initially, descriptive analyses are conducted to understand the distribution and characteristics of the datasets. Before constructing new models, an existing model is fitted to the datasets to evaluate its goodness of fit. Subsequently, new regression models are developed separately for YCL and WREL, considering different lane configurations. The practical applicability of these new models is then assessed, identifying the limitations in their implementation and potential improvements.

### 6.1      Descriptive Analysis

The datasets prepared for beta regression modeling in Chapter 4 are utilized in this chapter. Prediction models are developed to forecast  $RL_{2021}$  values based on  $RL_{2020}$  and other traffic flow and location characteristics previously identified as significant in degradation proportion modeling. It is important to note that only two RL measurements of each location are available: one taken in September 2020 ( $RL_{2020}$ ) and the other in November 2021 ( $RL_{2021}$ ), providing a 14-month interval. It is noted that  $RL_{2020}$  may be a significant predictor of  $RL_{2021}$ , meaning the distribution of  $RL_{2020}$  can substantially influence model performance. **Table 6.1** provides the distribution of  $RL_{2020}$  for both YCL and WREL, with RL categorization based on the qualitative standards outlined in **Table 1.1**.

**Table 6.1 Distribution of datasets by  $RL_{2020}$**

Marking line type	Count of observations (Percentage of total observations)		
	< 150 mcd/m <sup>2</sup> /lux	150 - 249 mcd/m <sup>2</sup> /lux	>249 mcd/m <sup>2</sup> /lux
WREL for rural two-lane	6 (1.73%)	56 (16.19%)	285 (82.13%)
WREL for rural multilane	8 (3.40%)	32 (13.62%)	195 (82.98%)
	< 100 mcd/m <sup>2</sup> /lux	100 - 199 mcd/m <sup>2</sup> /lux	>199 mcd/m <sup>2</sup> /lux
YCL for rural two-lane	5 (2.29%)	84 (40.19%)	120 (57.52%)

The distribution reveals that the datasets for YCL and WREL contain very few observations where the measured  $RL_{2020}$  values were low based on the qualitative states. Out of the total segments where RL data was collected in 2020, only a small proportion had  $RL_{2020}$  values below 150 mcd/m<sup>2</sup>/lux for WREL and below 100 mcd/m<sup>2</sup>/lux for YCL. This may be because segments are typically restriped before their RL values drop below these thresholds, which several earlier studies have identified as the failure point for pavement markings in terms of RL. For WREL, only 1.73% of observations on two-lane roads and 3.40% on multilane roads fall below 150 mcd/m<sup>2</sup>/lux. Similarly, only 2.29% of YCL observations on two-lane roads are below 100 mcd/m<sup>2</sup>/lux. Compared to WREL, YCL are more evenly distributed with respect to  $RL_{2020}$  values 100 mcd/m<sup>2</sup>/lux and above, with 40.191% of observations ranging between 100 - 199 mcd/m<sup>2</sup>/lux and 57.517% above 199 mcd/m<sup>2</sup>/lux.

## 6.2 Methodology

Earlier RL models utilized multiple linear regression (MNL) models as it provided a good fit for the datasets. The standard format for the linear prediction model can be stated as follows (Marill, 2004):

$$Y = \beta_0 + \beta_1 X_1 + \beta_2 X_2 + \dots + \beta_n X_n + \epsilon$$

Where,  $Y$  is dependent variable;  $\beta_0$  means intercept representing the expected value of  $Y$  when all  $X$  variables are zero;  $\beta_1, \beta_2, \dots, \beta_n$  are the coefficients for each independent variable;  $X_1, X_2, \dots, X_n$  are the independent variables;  $\epsilon$  is the error term capturing the variability in  $Y$  not explained by the independent variables.

$R^2$  or coefficient of determination is a measure used to assess the goodness-of-fit of a MNL model. It represents the proportion of the variance in the dependent variable that is predictable from the independent variables (Quinino et al., 2013).



$$R^2 = 1 - \frac{SS_{residual}}{SS_{total}}$$

Where,  $SS_{residual}$  is the sum of squared residuals (differences between observed and predicted values);  $SS_{total}$  is the total sum of squares (variance of observed values from the mean). An  $R^2$  closer to 1 indicates a better fit, meaning the model explains a larger portion of the variance in  $Y$ .

### 6.3 Results and Discussions

Initially, the MNL models were applied to the existing model by Ozelim and Turochy (2014) to evaluate how well the previous developed equation fits to the current dataset. Since **Section 4.4.1** demonstrates that the contributing factors are significantly influenced by marking line type and lane configuration, separate models were developed for WREL on two-lane and multilane roads. The transformed equations from the earlier models for predicting  $R_{2021}$  for white and yellow markings are provided below:

$$\text{White marking: } TM_w = R_{2020} - 71.82 - 0.00699 * (AADT_{2021} - AADT_{2020})$$

$$\text{Yellow marking: } TM_y = R_{2020} - 69.57 - 0.00217 * (AADT_{2021} - AADT_{2020})$$

The calibrated model predicts the measured RL in 2021 based on the measured RL in 2020 and the AADT difference between 2021 and 2020. Subsequently, new models were developed specifically for YCL on two-lane segments, WREL on two-lane segments, and WREL on multilane segments. It is important to note that, while constructing these prediction models, only variables identified as statistically significant for each marking line type in the degradation proportion modeling (Chapter 4) were included to ensure relevance to each specific line type. The validity and limitations of these models were then discussed using practical examples to illustrate their applicability and potential constraints. It is important to note that, since only two RL measurements

were available for each 0.1-mile segment, the time interval for the RL prediction models was fixed at 14 months. This indicates that the predicted  $R_{2021}$  represents the RL of 14 months after the previous measurement,  $R_{2020}$ .

### 6.3.1 RL Prediction Model for YCL

**Table 6.2** presents the linear regression results for YCL following the previous RL prediction model. The RL prediction model for yellow markings developed by Ozelim and Turochy (2014) shows a good fit with the dataset, achieving an  $R^2$  value of 0.6752, which explains 67.52% of the overall variability.

**Table 6.2 Linear regression results for YCL using the previous RL prediction model**

	<b>Coef.</b>	<b>SE</b>	<b>t-value</b>	<b>p-value</b>
(intercept)	74.6942	4.6589	16.032	<0.001
$TM_y$	0.5957	0.0272	20.773	<0.001
$R^2 = 0.6752$				

Note: Coefficient (Coef.) and Standard Error (SE)

**Table 6.3** presents the MNL results for YCL on rural two-lane roads, aiming to develop a new RL prediction model without initial RL and marking age. Including only  $R_{2020}$  in a simple linear regression model accounts for 65.61% of the variability. Consistent with the degradation proportion model for YCL (Section 4.4.1), all selected variables are found to be statistically significant. A one-unit increase in  $R_{2020}$  (mcd/m<sup>2</sup>/lux) leads to a 0.57 mcd/m<sup>2</sup>/lux increase in  $R_{2021}$  when other predictors are constant. Additionally, 1,000 units increase in AADT decreases  $R_{2021}$  by 1.20 mcd/m<sup>2</sup>/lux, indicating a statistically significant correlation between AADT and RL degradation. For roads in residential, business, or mixed-use areas,  $R_{2021}$  decreases by 14.03 mcd/m<sup>2</sup>/lux, when all other variables remain constant. It is worth noting that, although residential/business/mixed areas are found to be statistically significant in the model, their

inclusion marginally improves model performance, as  $R^2$  increases slightly. Following this, the final RL prediction model is provided below:

$$R_{2021} = 39.35 + 0.578 * R_{2020} - 0.0011 * \text{Adj AADT}$$

**Table 6.3 MNL results for YCL**

	<b>Coef.</b>	<b>SE</b>	<b>t-value</b>	<b>p-value</b>
(intercept)	44.5800	7.8472	5.680	<0.001
$R_{2020}$ (mcd/m <sup>2</sup> /lux)	0.5684	0.0284	19.578	<0.001
Adj AADT (vpd)	-0.0012	0.0013	-5.401	<0.001
<i>Location class (ref. open country)</i>				
residential/business/mixed	-14.0312	5.8432	-2.036	0.043
$R^2 = 0.6824$				
<b>Equation</b>				<b><math>R^2</math></b>
$R_{2021} = 44.58 + 0.568 * R_{2020} - 0.0012 * \text{Adj AADT} - 14.03 * (\text{location class @ residential/business/mixed})$				0.6824
$R_{2021} = 39.35 + 0.578 * R_{2020} - 0.0011 * \text{Adj AADT}$				0.6785

Note: Coefficient (Coef.) and Standard Error (SE)

### 6.3.2 RL Prediction Model for WREL (Rural Two-lane)

**Table 6.4** shows the linear regression results for WREL on rural two-lane following the previous RL prediction model. The RL prediction model for white markings developed by Ozelim and Turochy (2014) shows a good fit with the dataset, explaining 59.34% of the overall variability.

**Table 6.4 Linear regression results for WREL (rural two-lane) using the earlier RL prediction model**

	<b>Coef.</b>	<b>SE</b>	<b>t-value</b>	<b>p-value</b>
(intercept)	83.8771	7.5372	11.131	<0.001
$TM_w$	0.5640	0.0273	22.446	<0.001
$R^2 = 0.5934$				

Note: Coefficient (Coef.) and Standard Error (SE)

**Table 6.5** presents the MNL results for WREL on rural two-lane roads, aiming to develop a new RL prediction model for WREL without initial RL and marking age. A simple linear regression model that includes only  $R_{2020}$  explains 58.55% of the variability. Both  $R_{2020}$  and Adj

AADT are found to be statistically significant predictors. A one mcd/m<sup>2</sup>/lux increase in  $R_{2020}$  results in a 0.56 mcd/m<sup>2</sup>/lux increase in  $R_{2021}$  when other predictors remain constant. Moreover, an increase of 1,000 units in AADT decreases  $R_{2021}$  by 4.90 mcd/m<sup>2</sup>/lux, indicating a statistically significant associations between AADT and RL degradation. Notably, the absolute magnitudes of influence regrading  $R_{2020}$  and Adj AADT are higher for WREL than for YCL. In consistent with earlier studies, this highlights that yellow markings experience less RL degradation over time compared to white markings. The final RL prediction model for WREL on rural two-lane road segments is provided below:

$$R_{2021} = 63.42 + 0.561 * R_{2020} - 0.0049 * \text{Adj AADT}$$

**Table 6.5 MNL results for WREL (rural two-lane)**

	<b>Coef.</b>	<b>SE</b>	<b>t-value</b>	<b>p-value</b>
(intercept)	63.4151	13.7742	5.578	<0.001
$R_{2020}$ (mcd/m <sup>2</sup> /lux)	0.5613	0.0277	21.303	<0.001
Adj AADT (vpd)	-0.0049	0.0016	-4.673	<0.001
$R^2 = 0.6153$				
<b>Equation</b>				<b><math>R^2</math></b>
$R_{2021} = 63.42 + 0.561 * R_{2020} - 0.0049 * \text{Adj AADT}$				0.6153

Note: Coefficient (Coef.) and Standard Error (SE)

### 6.3.3 RL Prediction Model for WREL (Rural Multilane)

**Table 6.6** represents the linear regression results for WREL on rural multilane using the previous RL prediction model for white marking (Ozelim and Turochy, 2014). The earlier RL prediction model shows a good fit with the dataset, explaining 58.92% of the overall variability. The  $R^2$  value for multilane roads is slightly lower than that for two-lane roads, likely due to the limited number of segments on multilane in the previously developed model.

**Table 6.6 Linear regression results for WREL (rural multilane) using the previous RL prediction model**

	<b>Coef.</b>	<b>SE</b>	<b>t-value</b>	<b>p-value</b>
(intercept)	88.4553	9.5126	10.035	<0.001
TM <sub>w</sub>	0.4782	0.0293	18.149	<0.001
$R^2 = 0.5892$				

Note: Coefficient (Coef.) and Standard Error (SE)

**Table 6.7** shows the MNL results for WREL on rural multilane roads, aiming to predict RL without initial RL and marking age. A simple linear regression model that includes only  $R_{2020}$  explains 58.22% of the variability. Both  $R_{2020}$  and Adj AADT are found to be statistically significant predictors. A one mcd/m<sup>2</sup>/lux increase in  $R_{2020}$  results in a 0.46 mcd/m<sup>2</sup>/lux increase in  $R_{2021}$  when other predictors remain constant. Moreover, an increase of 1,000 units in AADT decreases  $R_{2021}$  by 0.7 mcd/m<sup>2</sup>/lux, indicating a statistically significant positive correlation between AADT and RL degradation. It is noteworthy that the impact of AADT in RL degradation for WREL is lower on rural multilane compared to rural two-lane. This is because, on multilane roads, the total vehicle volume is distributed across multiple lanes, which spreads out the wear and reduces pressure on individual markings. The final RL prediction model for WREL on rural multilane road segments is provided below:

$$R_{2021} = 66.75 + 0.464 * R_{2020} - 0.0007 * \text{Adj AADT}$$

**Table 6.7 MNL results for WREL (rural multilane)**

	<b>Coef.</b>	<b>SE</b>	<b>t-value</b>	<b>p-value</b>
(intercept)	66.7492	13.5372	3.314	0.001
$R_{2020}$ (mcd/m <sup>2</sup> /lux)	0.4642	0.0288	18.383	<0.001
Adj AADT (vpd)	-0.0007	0.0003	-3.455	<0.001
$R^2 = 0.6034$				
<b>Equation</b>				<b><math>R^2</math></b>
$R_{2021} = 66.75 + 0.464 * R_{2020} - 0.0007 * \text{Adj AADT}$				0.6034

Note: Coefficient (Coef.) and Standard Error (SE)

### 6.3.4 Prediction Models Limitations

Multiple validation steps are required before finalizing the models to enhance their practical applicability. An established finding in pavement marking research is that yellow markings generally degrade slower compared to white markings. To assess whether the developed models align with this basic concept, the following estimations have been conducted. At both high and low RL levels, yellow markings exhibit lower degradation compared to white markings, which aligns with findings from previous studies.

- i) Assume, measured RL of any given time ( $RL_t$ ) of YCL = 300 mcd/m<sup>2</sup>/lux, AADT = 10,000 vpd, and road setting = rural two-lane  
Predicted RL after 14 months ( $RL_{t+14}$ ) =  $39.35 + 0.578 * 300 - 0.0011 * 10,000 = 201.75 \approx 202$  mcd/m<sup>2</sup>/lux.
- ii) Assume, measured RL of any given time ( $RL_t$ ) of YCL = 100 mcd/m<sup>2</sup>/lux, AADT = 10,000 vpd, and road setting = rural two-lane  
Predicted RL after 14 months ( $RL_{t+14}$ ) =  $39.35 + 0.578 * 100 - 0.0011 * 10,000 = 86.15 \approx 87$  mcd/m<sup>2</sup>/lux.
- iii) Assume, measured RL of any given time ( $RL_t$ ) of WREL = 300 mcd/m<sup>2</sup>/lux, AADT = 10,000 vpd, and road setting = rural two-lane  
Predicted RL after 14 months ( $RL_{t+14}$ ) =  $63.42 + 0.561 * 300 - 0.0049 * 10,000 = 182.72 \approx 183$  mcd/m<sup>2</sup>/lux.
- iv) Assume, measured RL of any given time ( $RL_t$ ) of WREL = 100 mcd/m<sup>2</sup>/lux, AADT = 10,000 vpd, and road setting = rural two-lane  
Predicted RL after 14 months ( $RL_{t+14}$ ) =  $63.42 + 0.561 * 100 - 0.0049 * 10,000 = 70.52 \approx 71$  mcd/m<sup>2</sup>/lux.

Figures 6.1-6.3 show the normal QQ plots and residual vs. fitted plots for the three RL prediction models: YCL, WREL on two-lane roadways, and WREL on multilane roadways, respectively. These plots provide insights into the distribution of residuals and the fit of each model, allowing for a visual assessment of model assumptions. In each case, a few outliers are present in the datasets. Most residuals (represented by the red lines in the residual plots) are close to the dashed line, indicating a high degree of linearity in the prediction model. However, the residual variance changes across the range of fitted values, a phenomenon known as heteroscedasticity. To evaluate the predictive performance of each model in estimating the service life of pavement marking RL, each model was tested across various AADT ranges.

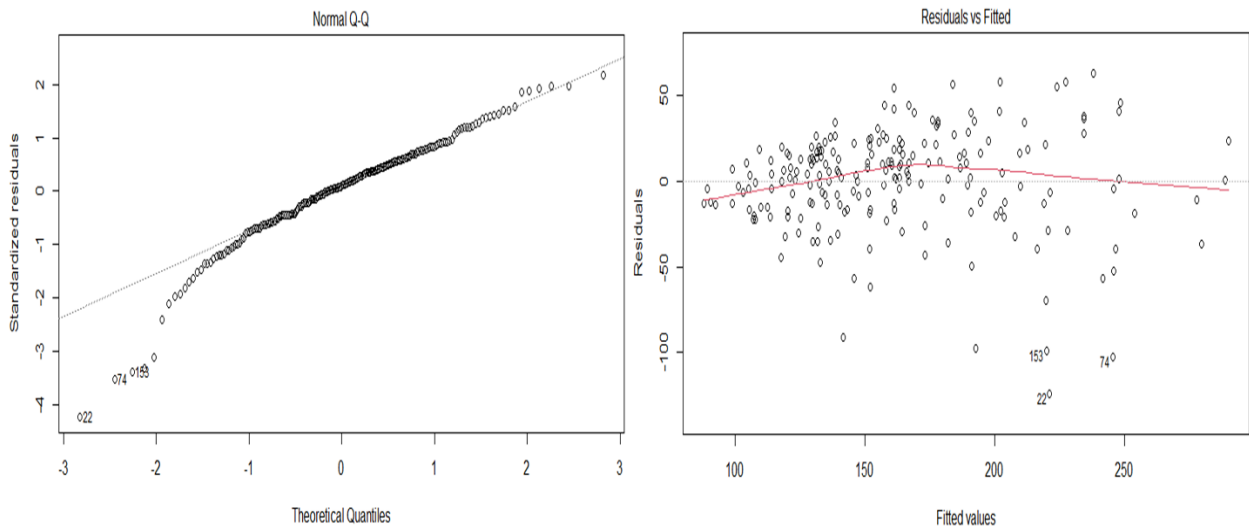


**Figure 6.1 QQ and Residual plots for YCL model**

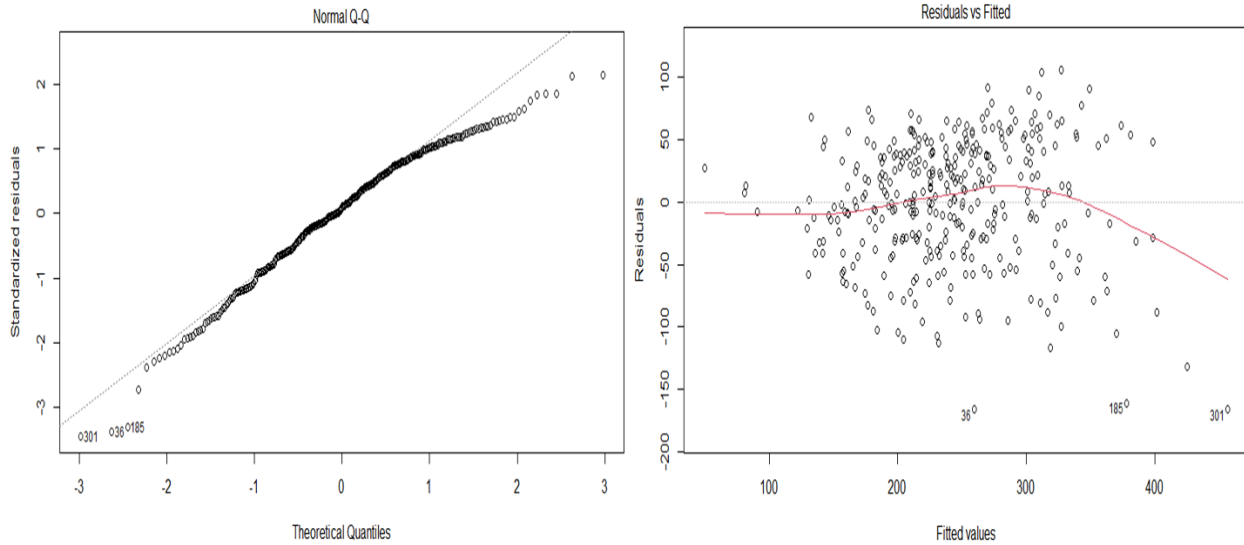


**Figure 6.2 QQ and Residual plots for WREL model (rural two-lane)**

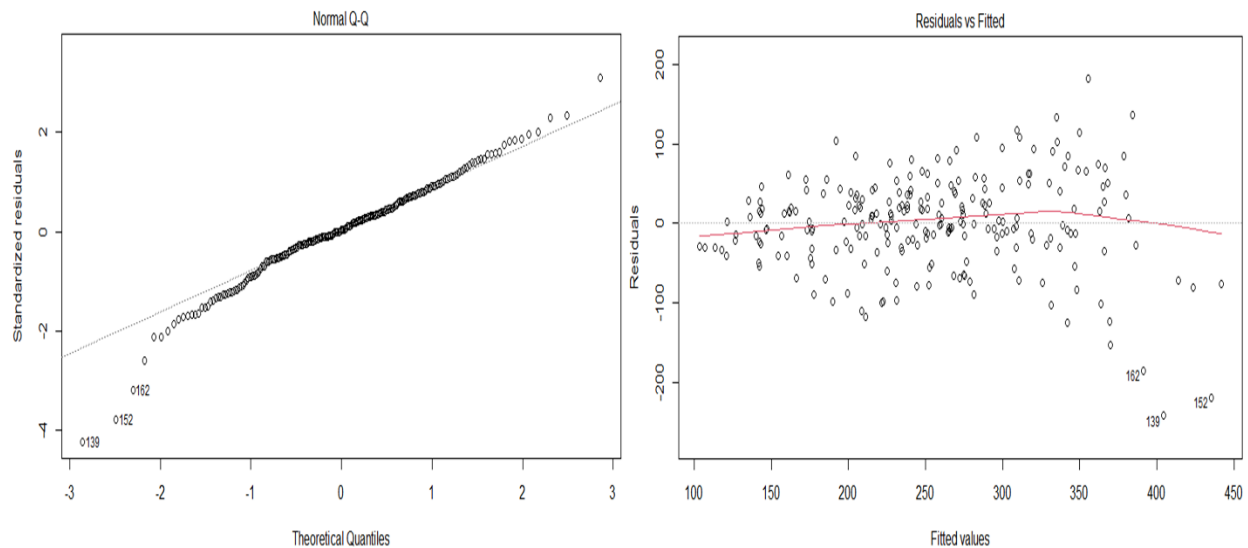


**Figure 6.3 QQ and Residual plots for WREL model (rural multilane)**

In RL predictive modeling, estimating service life can help to reveal the limitations of regression models. Since the MUTCD has lowered the minimum RL requirement to 50 mcd/m<sup>2</sup>/lux, it is crucial to have enough RL data observations within the 50-100 mcd/m<sup>2</sup>/lux range across diverse traffic volumes to develop a model capable of better predicting RL below this threshold. However, in the RL datasets, very few observations fall below 100 mcd/m<sup>2</sup>/lux for YCL (below 3%) and below 150 mcd/m<sup>2</sup>/lux for WREL (less than 4%). As a result, it is anticipated that



the models developed in this research may not perform well when the  $RL_t$  levels falls within such ranges. Ozelim and Turochy (2014) also highlighted such limitations in their study, noting unexpected results while calculating service life using the regression equations of earlier studies. In this study, **Figures 6.4-6.9** illustrate the predicted RL values for YCL and WREL based on minimum RL installation standards and diverse AADT ranges. The two primary issues are: i) RL degradation becomes zero at a certain point, resulting in no further decline, and ii) percentage of degradation is not stable after a certain RL, specifically when  $RL_t$  below 150 mcd/m<sup>2</sup>/lux for WREL and below 100 mcd/m<sup>2</sup>/lux for YCL. For yellow markings, the  $RL_{t+14}$  predictions for YCL are less reliable when  $RL_t$  values fall below 100 mcd/m<sup>2</sup>/lux. Similarly, for white markings, the  $RL_{t+14}$  predictions for WREL are less reliable when  $RL_t$  values fall below 150 mcd/m<sup>2</sup>/lux, for both two-lane and multilane road segments. One primary reason for such limitations is the scarcity of road segments at these low RL levels across a range of traffic volumes, leading to limited data distribution. However, this limitation may have minimal practical impact, as segments are often restriped before reaching 100 mcd/m<sup>2</sup>/lux for yellow markings and 150 mcd/m<sup>2</sup>/lux for white markings. With recent changes in the MUTCD, it is increasingly important to develop models that can more accurately predict future RL levels below 100 mcd/m<sup>2</sup>/lux, as the minimum maintained RL threshold has been reduced from 100 mcd/m<sup>2</sup>/lux to 50 mcd/m<sup>2</sup>/lux for certain road segments.

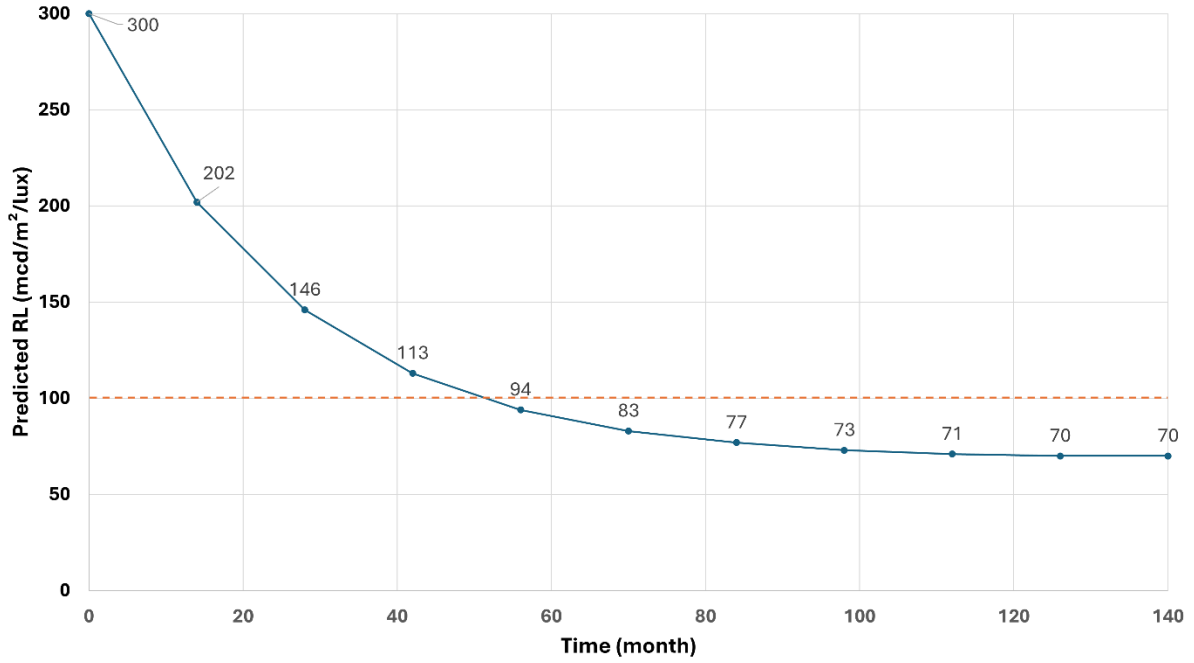


Figure 6.4 Predicted RL of YCL by month ( $RL_t = 300 \text{ mcd/m}^2/\text{lux}$  and  $\text{AADT} = 10,000 \text{ vpd}$ )

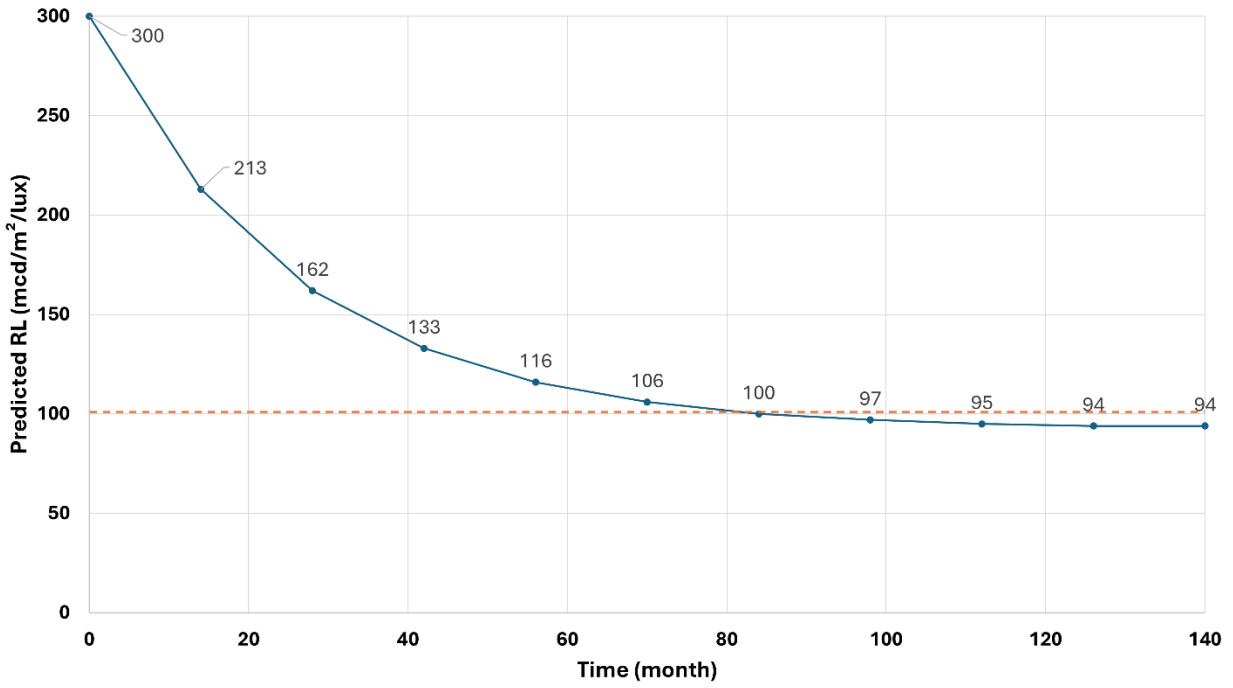


Figure 6.5 Predicted RL of YCL by month ( $RL_t = 300 \text{ mcd/m}^2/\text{lux}$  and  $\text{AADT} = 546 \text{ vpd}$ )

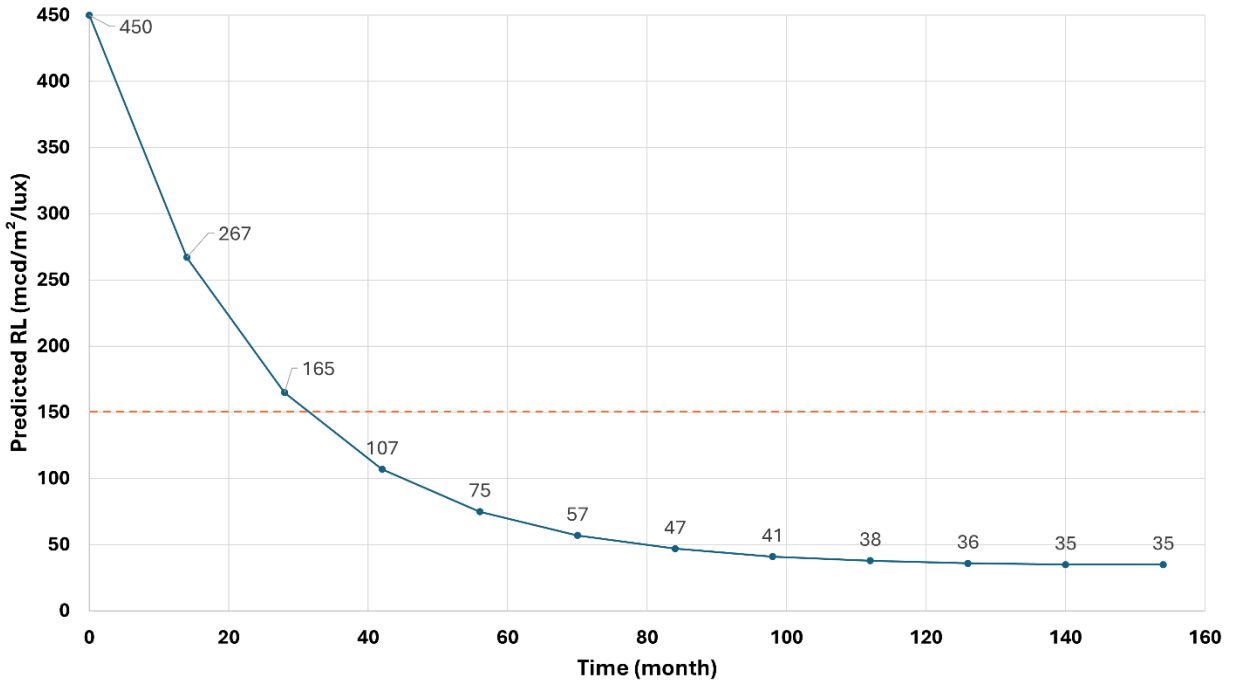


Figure 6.6 Predicted RL of WREL (rural two-lane) by month ( $RL_t = 450 \text{ mcd/m}^2/\text{lux}$  and  $\text{AADT} = 10,000 \text{ vpd}$ )

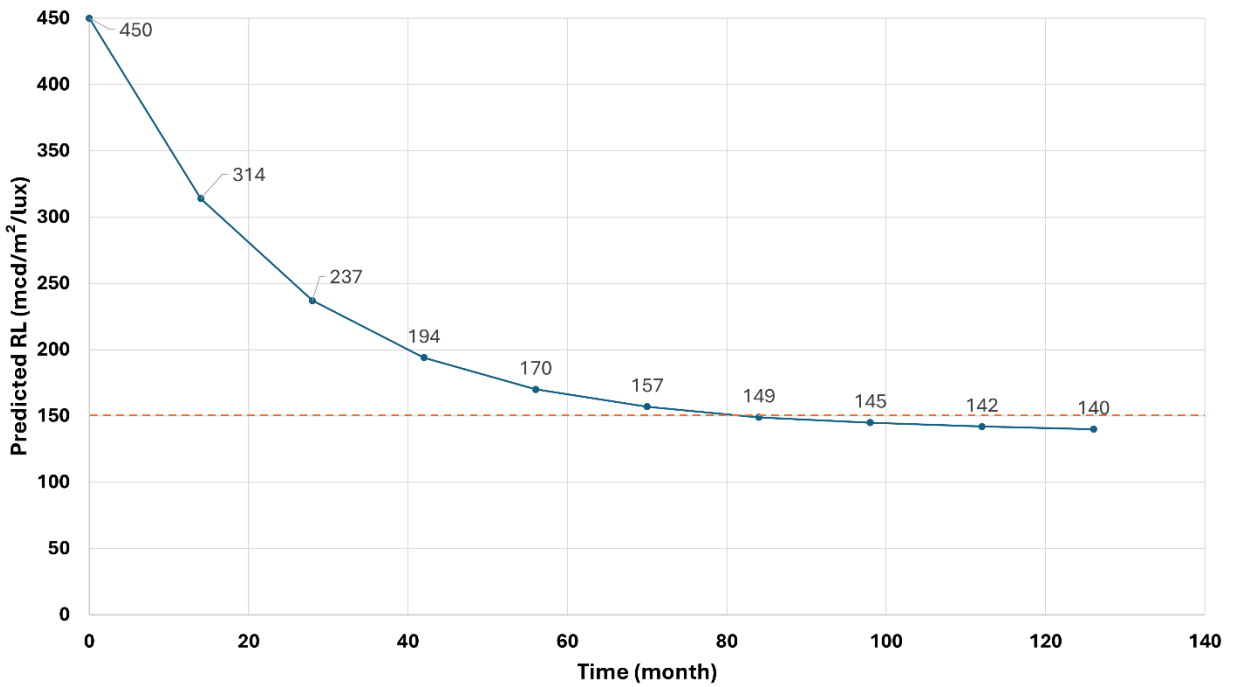


Figure 6.7 Predicted RL of WREL (rural two-lane) by month ( $RL_t = 450 \text{ mcd/m}^2/\text{lux}$  and  $\text{AADT} = 546 \text{ vpd}$ )

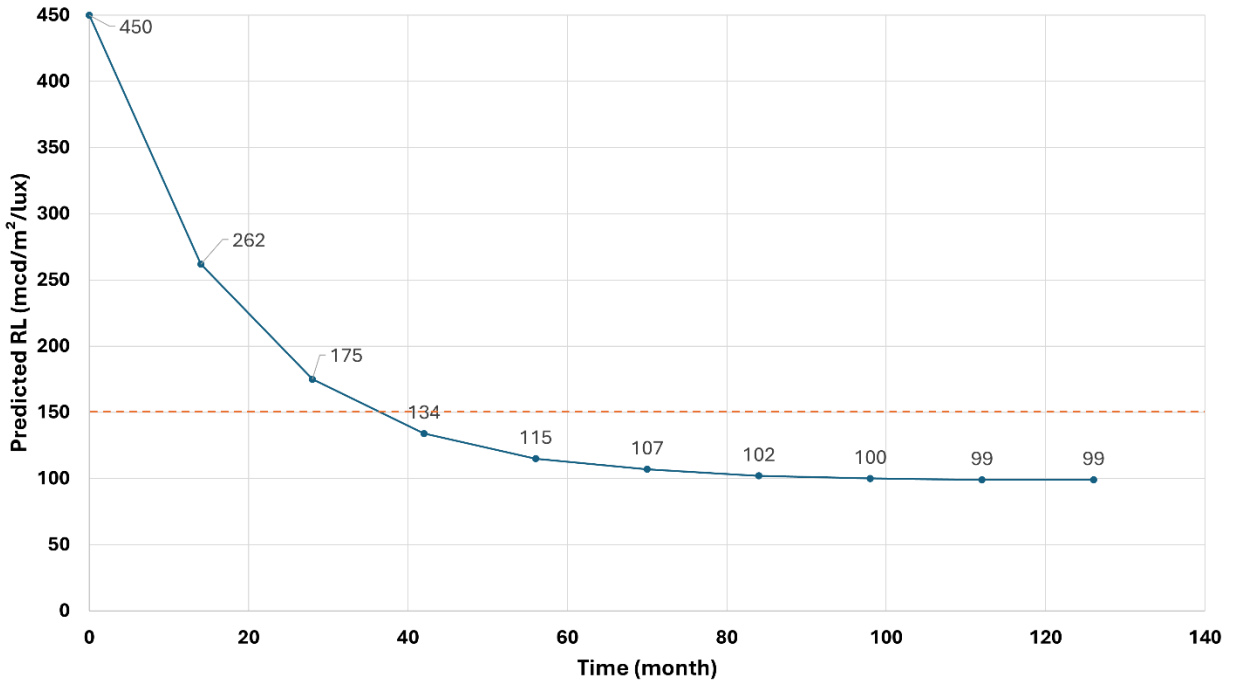


Figure 6.8 Predicted RL of WREL (rural multilane) by month ( $RL_t = 450$  mcd/m<sup>2</sup>/lux and AADT = 20,000 vpd)

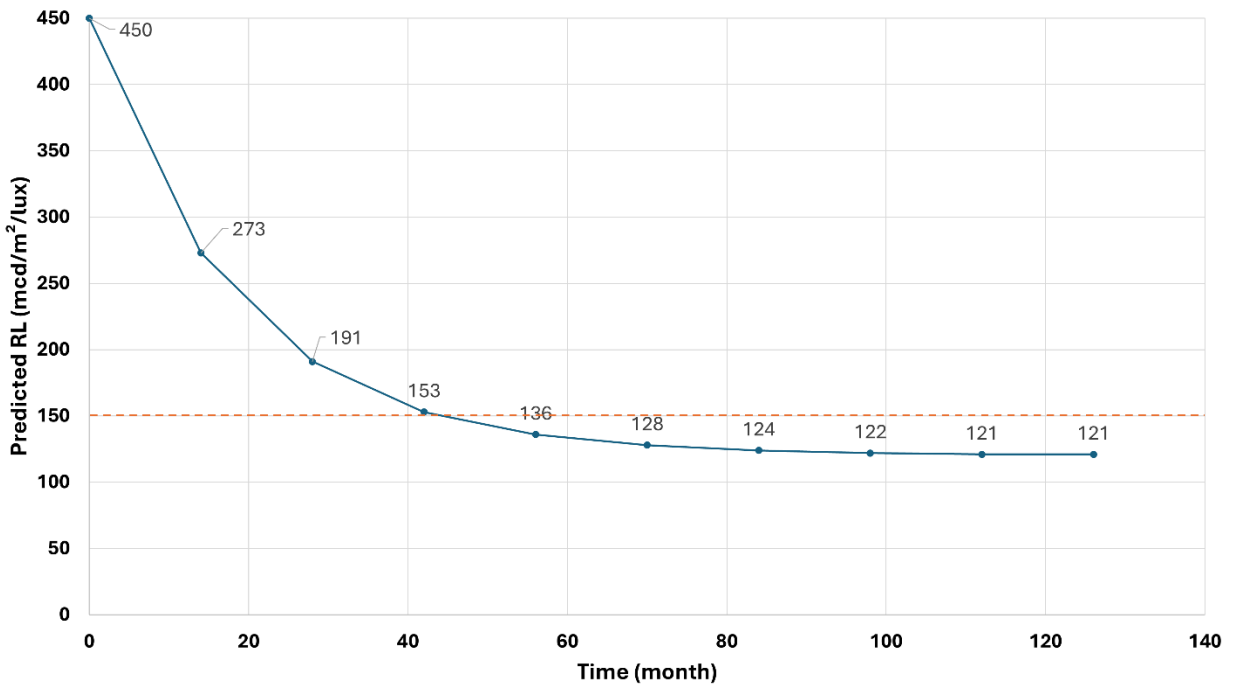


Figure 6.9 Predicted RL of WREL (rural multilane) by month ( $RL_t = 450$  mcd/m<sup>2</sup>/lux and AADT = 3,610 vpd)

## 6.4 Key Findings

This chapter focuses on developing RL prediction models for YCL and WREL without requiring initial RL and pavement marking age information. Using a multiple linear regression approach, this study addresses a gap in the literature by providing separate regression models for WREL on different rural road lane configurations. The newly developed models demonstrate improved goodness-of-fit compared to the calibrated models from a previous Alabama study. However, a limitation arises due to the limited sample size, particularly in lower RL levels, which constrains the accuracy of predicting the service life of pavement markings. The resulting RL prediction equations, along with guidance on their application, are presented below:

$$\text{YCL (rural two-lane): } RL_{t+14} = 39.35 + 0.578 * RL_t - 0.0011 * AADT$$

$$\text{WREL (rural two-lane): } RL_{t+14} = 63.42 + 0.561 * RL_t - 0.0049 * AADT$$

$$\text{WREL (rural multilane): } RL_{t+14} = 66.75 + 0.464 * RL_t - 0.0007 * AADT$$

Where,  $RL_t$  is the measured RL at any given time,  $RL_{t+14}$  is the predicted RL after 14 months of  $t$ . For better accuracy in RL measurements, it is recommended to use these models when  $RL_t \geq 100$  mcd/m<sup>2</sup>/lux for yellow markings and  $RL_t \geq 150$  mcd/m<sup>2</sup>/lux for white markings. Additionally, it is recommended to calculate adj AADT if AADT values vary between years.

## **Chapter 7 Statistical Relationship between RL and Road Safety**

This section aims to examine the statistical relationship between RL and specific types of crashes, including single-vehicle ROR collisions, crashes occurring in dark conditions, and crashes at night with no streetlighting. Since RL measurements for 856 miles of rural road segments were only taken in 2021, prediction models for YCL and WREL have been used to estimate RL for 2020. Within the majority of 1-mile segments, significant variability in measured RL along with road and traffic flow characteristics were observed, highlighting the importance of analyzing shorter segments to more accurately assess safety benefits. Consequently, average RL values are calculated for each 0.5-mile segment, and crash counts of those segments are compiled over a defined period. Finally, regression models are applied to investigate any statistically significant relationship between RL and relevant crash types.

### **7.1 Data Preprocessing**

Investigating the safety implications of pavement marking RL reveals a complexity that goes beyond initial assumptions. RL fluctuates notably due to diverse factors such as location and environmental conditions, complicating safety assessments. To address these complexities, this study focuses specifically on the RL values of WREL and YCL markings on both rural two-lane and multilane roads. The objective is to evaluate the statistical correlation between these RL values and road crashes, providing a clearer understanding of their impact on road safety. There were 856 1-mile rural road segments with RL measurements only available in November 2021. To estimate RL values for 2020 on these segments, prediction models for WREL on two-lane and multilane roads and YCL on two-lane roads, developed in Chapter 6, were utilized. Since road segments are more frequently restriped during summer months, and to accurately assess the statistical

relationship between crashes and RL without the seasonal effects of winter, this analysis focused on a time period between March 2021 and November 2021 (mid spring to late fall). The following steps are performed to assign average RL values to the road segments and select the appropriate road segments for further analyses.

- *Segments with measured RL data in September 2020 and November 2021:* Assuming a linear degradation of RL, the RL were calculated for March 2021. Restriped 0.1-mile segments were removed while comparing two years of measurements. Each 0.1-mile segment was then assigned an average RL value calculated using the following formula:

$$\text{Average RL} = \frac{\text{RL in March 2021} + \text{RL in November 2021}}{2}$$

An example is provided to enhance clarity. For instance, consider a specific 0.1-mile segment where the measured RL in September 2020 was 240 mcd/m<sup>2</sup>/lx, and in November 2021, it was 140 mcd/m<sup>2</sup>/lx. Using this information, the RL in March 2021, as well as the average RL between March 2021 and November 2021, can be calculated as follows:

$$\text{RL in March 2021} = 240 - \left(\frac{100}{14}\right) * 6 = 197 \text{ mcd/m}^2/\text{lx}$$

$$\text{Average RL} = \frac{197 + 140}{2} = 169 \text{ mcd/m}^2/\text{lx}$$

- *Segments with measured RL only in November 2021:* The developed RL prediction models for WREL and YCL were used to estimate the RL values in September 2020 as well as March 2021. To ensure exclusion of restriped segments, thresholds were established beyond which segments are considered restriped during the summer. In Alabama, the minimum RL values required for white and yellow thermoplastic pavement marking for installation and restriping are 450 mcd/m<sup>2</sup>/lx and 300 mcd/m<sup>2</sup>/lx, respectively. Hence, for added precaution, only segments with RL values ≤ 425 mcd/m<sup>2</sup>/lx for WREL and ≤ 275

mcd/m<sup>2</sup>/lx for YCL in March 2021 were considered for further analyses. Subsequently, each segment was assigned an average RL value between March 2021 and November 2021 using the same methodology outlined in the earlier step.

For each 0.1-mile segment, relevant data—including AADT, location classification, road alignment, functional classification, and posted speed limit—were assigned following the procedure outlined in Chapter 3. To address variability in road, traffic flow, and location characteristics more accurately, RL values were assigned to shorter segments. Therefore, 0.5-mile segments were chosen to improve analytical precision. 0.1-mile segments were compiled into a 0.5-mile segment, with the calculated average RL. Since a single curve can span across two 0.5-mile segments, a variable was created to indicate the presence of a curve within each 0.5-mile segment. Although RL was measured in one specific direction of traffic flow, both directions were assumed to have the same RL value to maximize the number of crashes attributed to each 0.5-mile segment. **Table 7.1** presents the number of 0.5-mile segments incorporated into the safety analysis using RL prediction models. More than three times 0.5-mile segments from rural two-lane roads and more than two times 0.5-mile segments from rural multilane roads were included using RL prediction models. **Figure 7.1** illustrates the distribution of 0.5-mile segments on rural two-lane and multilane roads by RL of WREL: < 250 mcd/m<sup>2</sup>/lux and ≥ 250 mcd/m<sup>2</sup>/lux. In both road settings, a higher percentage of segments fall into the ≥ 250 mcd/m<sup>2</sup>/lux category, with 65.13% on rural two-lane roads and 56.78% on rural multilane roads.

**Table 7.1 Summary of 0.5-mile segments for safety analyses in relation to WREL**

Lane configuration	Total segment	Segments attained from actual RL measurements	Segments attained from predictive modeling
Rural two-lane	1,411	288	1,123
Rural multilane	517	152	365



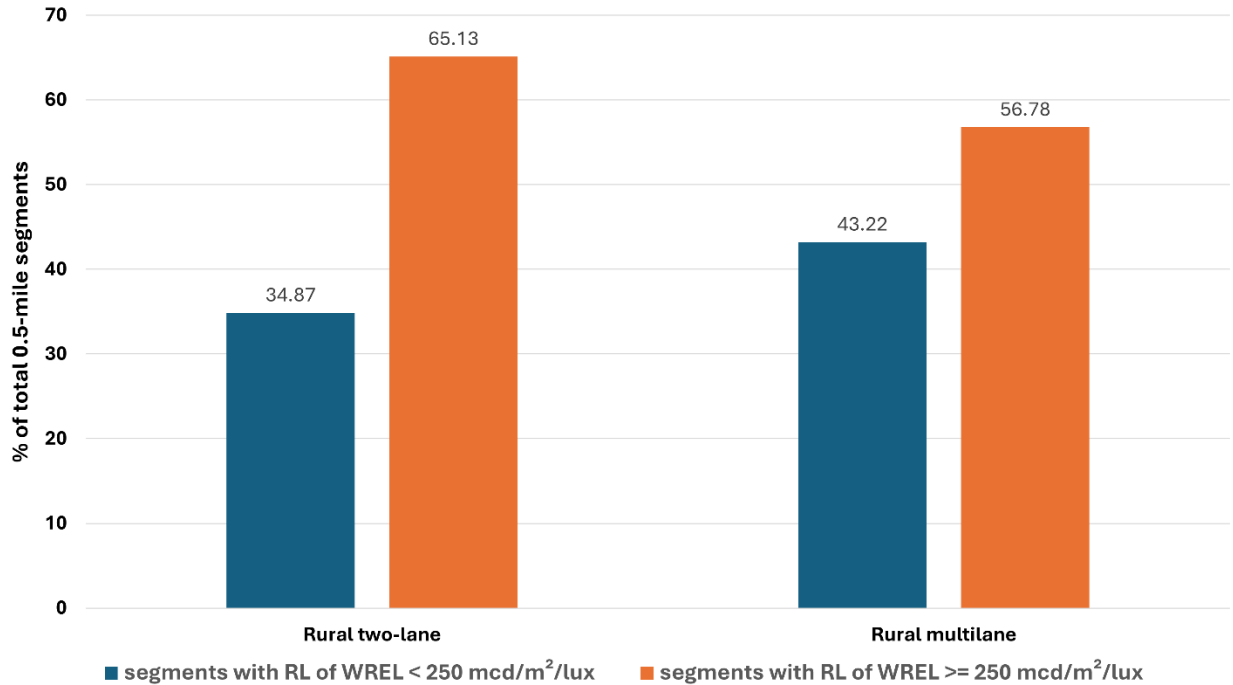


**Figure 7.1 Distribution of 0.5-mile segments by RL of WREL**

While extracting crash data, only crashes occurring between March 2021 and November 2021—covering the Mid Spring to Late Fall seasons—were included. Each measured RL had geocoordinate information, so crashes occurring within 250 feet of a specific 0.1-mile segment were considered to belong to that segment. Crashes involving alcohol impairment were excluded, aligning with previous studies (Donnell et al., 2009; Smadi et al., 2008). Alcohol impairment significantly reduces reaction time, judgment, and attentiveness, resulting in crashes more directly attributed to human error rather than external visibility factors like RL. Both driver condition and primary contributing factors were used to identify and exclude alcohol-impaired crashes. Additionally, intersection crashes were excluded due to the variety of complex factors at intersections—such as traffic signals, signage, pedestrian crossings, and multidirectional vehicle movements—that go beyond pavement marking visibility (Carlson et al., 2013; Masliah et al., 2007). Furthermore, when assigning intersection crashes to the corresponding 0.1-mile segments, misassignments can occur due to the high likelihood of including crashes from minor roads within

a 250-foot radius of the RL measurement point on the major road. An example is provided in **Figure 7.2**.

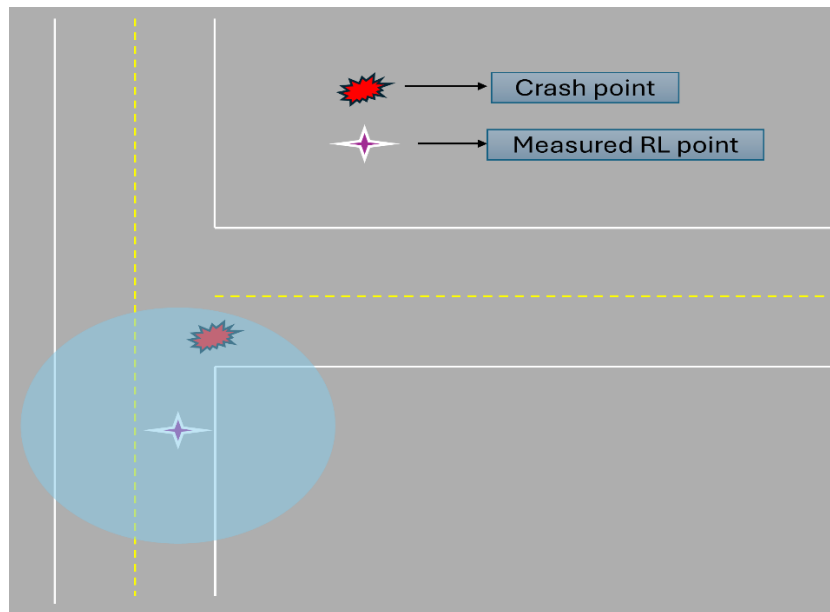


**Figure 7.2 Potential complexities of including intersection crashes**

This study focuses specifically on single-vehicle ROR crashes, which are more likely to be influenced by low RL of WREL. The criteria for selecting single-vehicle ROR crashes are detailed below.

- Exclude from first/most harmful events: crashes with other vehicles, crashes with parked vehicle or pedestrian, crashes with animals, cross-centerline crashes, equipment malfunctions, and other crashes that potentially happened on the roadway.
- Number of vehicle: One (also cross-checked with collision type- single vehicle/non-collision)

The combined effect of WREL and YCL might influence nighttime crashes with no streetlighting conditions. Therefore, in addition to single-vehicle ROR crashes, crashes occurring in dark conditions with no streetlighting were also considered to assess the impact of interactions between RL levels of YCL and WREL. In such cases, crashes involving parked vehicles or

pedestrians, collisions with animals, and equipment malfunctions were excluded; however, cross-centerline crashes and collisions with other vehicles were included. In total, five types of crashes were considered for further analysis, as listed below:

- Single vehicle ROR crashes (rural two-lane and multilane separately)
- Single vehicle ROR crashes on dark, dusk, and dawn conditions (rural two-lane and multilane separately)
- Single vehicle ROR crashes on dark no streetlighting conditions (rural two-lane and multilane separately)
- Crashes on dark no streetlighting conditions (rural two-lane only)
- Single vehicle ROR crashes on curve segments (merging rural two-lane and multilane)

Notably, for single-vehicle ROR crashes occurring on curve segments, the average RL and crash count for each 0.1-mile segment were analyzed, incorporating curve radius and angle as additional covariates. This approach allows for a more comprehensive understanding of the combined impact of curve geometry and RL on crash frequency and the likelihood of crashes.

## **7.2 Descriptive Analysis**

Given the limitations of RL prediction models in estimating lower RL levels, categorizing average RL values into multiple groups offers an effective approach for RL safety analysis. On rural two-lane roads, a small fraction of 0.5-mile segments had RL of WREL below 150 mcd/m<sup>2</sup>/lux. When factoring in the presence of crashes, the number of such segments was even smaller. Therefore, for WREL on rural two-lanes, RL values are grouped into two categories: <250 mcd/m<sup>2</sup>/lux and ≥250 mcd/m<sup>2</sup>/lux. For multilane roads, more detailed categorization is feasible due to a relatively higher proportion of crashes in segments with lower RL values. Categories for multilane roads include <250 mcd/m<sup>2</sup>/lux and ≥250 mcd/m<sup>2</sup>/lux, as well as broader categories of

<150 mcd/m<sup>2</sup>/lux, 150-249 mcd/m<sup>2</sup>/lux, and ≥250 mcd/m<sup>2</sup>/lux. On rural two-lanes, while analyzing crashes at dark with no streetlighting conditions, RL of YCL is categorized as <200 mcd/m<sup>2</sup>/lux and ≥200 mcd/m<sup>2</sup>/lux. Additionally, a separate analysis considers the interaction between RL of WREL and YCL, with the following interaction categories:

- WREL ≥ 250 mcd/m<sup>2</sup>/lux and YCL ≥ 200 mcd/m<sup>2</sup>/lux
- WREL ≥ 250 mcd/m<sup>2</sup>/lux and YCL < 200 mcd/m<sup>2</sup>/lux
- YCL ≥ 200 mcd/m<sup>2</sup>/lux and WREL < 250 mcd/m<sup>2</sup>/lux
- YCL ≥ 200 mcd/m<sup>2</sup>/lux and WREL ≥ 250 mcd/m<sup>2</sup>/lux

**Tables 7.2-7.4 and Figures 7.3-7.7** present an overview of the crash datasets prepared for RL safety analysis. Key observations from these datasets are outlined below:

- The majority of rural two-lane segments are located in open country areas (92.63%) and have posted speed limits of 55 mph or higher (90.645%). Compared to segments with actual RL measurements, the segments included from predictive modeling contain a higher proportion of curves, resulting in a good percentage of curve segments (28.99%) in the overall dataset. On rural two-lanes, the total crash counts by all targeted crash types are equal to or slightly higher than the number of 0.5-mile segments with at least one crash occurrence, indicating that only a few segments experienced multiple crashes (0% to 4.79%). Specifically, there are only 71 segments with RL levels below 150 mcd/m<sup>2</sup>/lux, and further analysis exhibit that only six crashes occurred within these segments.
- In comparison to rural two-lane roadways, the total crash counts by all targeted crash types are considerably higher than the number of 0.5-mile segments with at least one crash occurrence on multilane roads (23.88% to 38.81%), indicating a more dispersed

crash distribution. The proportion of segments with crashes is also higher on multilane roads (12.98% to 32.36%) than on two-lane roads (3.26% to 10.35%), providing a relatively sufficient number of segments with RL levels below 150 mcd/m<sup>2</sup>/lux for modeling. Although segments with curves are less common on multilane roads compared to two-lane roads, the proportion of curved segments with at least one crash occurrence is higher on multilane roadways.

- Among rural two-lane segments where RL measurements are available for both YCL and WREL, a substantial proportion have RL of YCL below 200 mcd/m<sup>2</sup>/lux (68.26%). This may indicate a lower frequency of restriping YCL, potentially due to its slower degradation rate compared to WREL. Rural two-lane segments with low RL levels of YCL and WREL are particularly susceptible to road crashes. For example, there are 42.11% of segments with at least one crashes at dark no streetlighting conditions have RL of below 200 mcd/m<sup>2</sup>/lux and below 250 mcd/m<sup>2</sup>/lux for YCL and WREL, respectively. This percentage is disproportionately high compared to the overall percentage of 0.5-mile segments with low RL levels of YCL and WREL (31.42%).
- When focusing on single-vehicle ROR crashes, the proportion of crashes on curve segments is relatively higher than on straight segments, suggesting that single-vehicle ROR crashes are strongly associated with curve segments. It is important to note that since data for both two-lane and multilane roads have been combined for 0.1-mile curved segments, functional class is used as a covariate instead of posted speed limit.

**Table 7.2 Summary of crash datasets on rural two-lane segments**

Variable	Rural two-lane (Number of 0.5-mile segments = 1,411)		
	Single vehicle ROR	Single vehicle ROR at dark, dusk, and dawn	Single vehicle ROR at dark no streetlighting
Crash count	Min: 0, Max: 2, Median: 0, Mean: 0.11 (Number of crashes = 153)	Min: 0, Max: 2, Median: 0, Mean: 0.04 (Number of crashes = 60)	Min: 0, Max: 1, Median: 0, Mean: 0.03 (Number of crashes = 46)
AADT (vpd)	Min: 229, Max: 13,731, Median: 2,323, Mean: 2,822		
<i>Crash occurrence</i>			
yes	146 (10.35%)	58 (4.11%)	46 (3.26%)
no	1,265 (89.65%)	1,353 (95.89%)	1,365 (96.74%)
<i>Location class</i>			
open country	1,307 (92.63%)		
residential/business/mixed	104 (7.37%)		
<i>Posted speed limit</i>			
< 55mph	132 (9.36%)		
≥ 55mph	1,279 (90.65%)		
<i>Presence of curve</i>			
no	1,002 (71.01%)		
yes	409 (28.99%)		
<i>RL by category (mcd/m<sup>2</sup>/lux)</i>			
<250	492 (34.87%)		
≥ 250	919 (65.13%)		

**Table 7.3 Summary of crash datasets on rural multilane segments**

Variable	Rural multilane (Number of 0.5-mile segments = 516)		
	Single vehicle ROR	Single vehicle ROR at dark, dusk, and dawn	Single vehicle ROR at dark no streetlighting
Crash count	Min: 0, Max: 6, Median: 0, Mean: 0.52 (Number of crashes = 267)	Min: 0, Max: 4, Median: 0, Mean: 0.20 (Number of crashes = 101)	Min: 0, Max: 4, Median: 0, Mean: 0.17 (Number of crashes = 86)
AADT (vpd)	Min: 3,675, Max: 86,009, Median: 19,075, Mean: 22,886		
<i>Crash occurrence</i>			
yes	167 (32.36%)	80 (15.50%)	67 (12.98%)
no	349 (67.64%)	436 (84.50%)	449 (87.02%)
<i>Location class</i>			
open country	464 (89.92%)		
residential/business/mixed	52 (10.08%)		
<i>Posted speed limit</i>			
<65mph	112 (21.71%)		
≥ 65mph	404 (78.29%)		
<i>Presence of curve</i>			
no	443 (85.85%)		
yes	73 (14.15%)		
<i>RL by category (mcd/m<sup>2</sup>/lux)</i>			
<150	83 (16.09%)		
150-249	140 (27.13%)		
<250	223 (43.22%)		
≥ 250	293 (56.78%)		

**Table 7.4 Summary of crash datasets on curve segments and at dark no streetlighting conditions**

<b>Variable</b>	<b>Dark no streetlighting – rural two-lane only (Number of 0.5-mile segments = 1,235)</b>	<b>Single-vehicle ROR crashes on curve segments (Number of 0.1-mile segments = 871)</b>
Crash count	Min: 0, Max: 2, Median: 0, Mean: 0.09 (Number of crashes = 106)	Min: 0, Max: 5, Median: 0, Mean: 0.18 (Number of crashes = 158)
AADT (vpd)	Min: 229, Max: 13,731, Median: 2,404, Mean: 2,851	Min: 229, Max: 140,466, Median: 2,955, Mean: 5,256
Curve angle (degree)	----	Min: 8.96, Max: 84.77, Median: 35.04, Mean: 37.19
Curve radius (ft)	----	Min: 317, Max: 7,968, Median: 2,135, Mean: 2,623
<i>Crash occurrence</i>		
yes	95 (7.69%)	130 (14.93%)
no	1,140 (92.31%)	741 (85.07%)
<i>Location class</i>		
open country	1,147 (92.87%)	777 (89.21%)
residential/business/mixed	88 (7.13%)	94 (10.79%)
<i>Posted speed limit</i>		
< 55mph	117 (9.47%)	----
≥ 55mph	1,118 (90.53%)	----
<i>Presence of curve</i>		
yes	367 (29.72%)	----
no	868 (70.28%)	----
<i>Number of lanes</i>		
two	----	718 (82.43%)
>two	----	153 (17.57%)
<i>RL of WREL by category (mcd/m<sup>2</sup>/lux)</i>		
<250	447 (36.19%)	326 (37.43%)
≥ 250	788 (63.81%)	545 (62.57%)
<i>RL of YCL by category (mcd/m<sup>2</sup>/lux)</i>		
		----



<b>Variable</b>	<b>Dark no streetlighting – rural two-lane only (Number of 0.5-mile segments = 1,235)</b>	<b>Single-vehicle ROR crashes on curve segments (Number of 0.1-mile segments = 871)</b>
<200	843 (68.26%)	----
≥ 200	392 (31.74%)	----
<i>Interaction of RL ((mcd/m<sup>2</sup>/lux)</i>		----
YCL<200 and WREL<250	388 (31.42%)	----
YCL≥200 and WREL<250	59 (4.78%)	----
YCL<200 and WREL≥250	455 (36.84%)	----
YCL≥200and WREL≥250	333 (26.96%)	----
<i>Functional class</i>		
major collector	----	265 (30.43%)
arterial	----	591 (67.85%)
interstate	----	15 (1.72%)

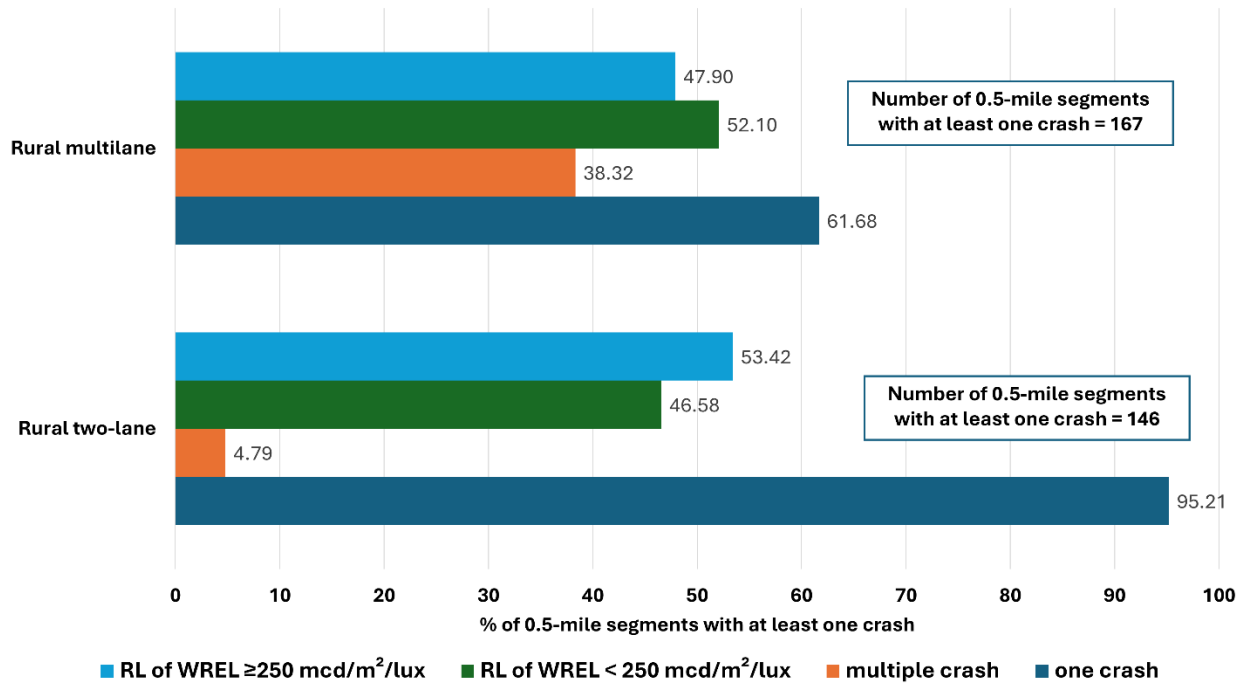


**Figure 7.3 Distribution of 0.5-mile segments with at least one single vehicle ROR crash**

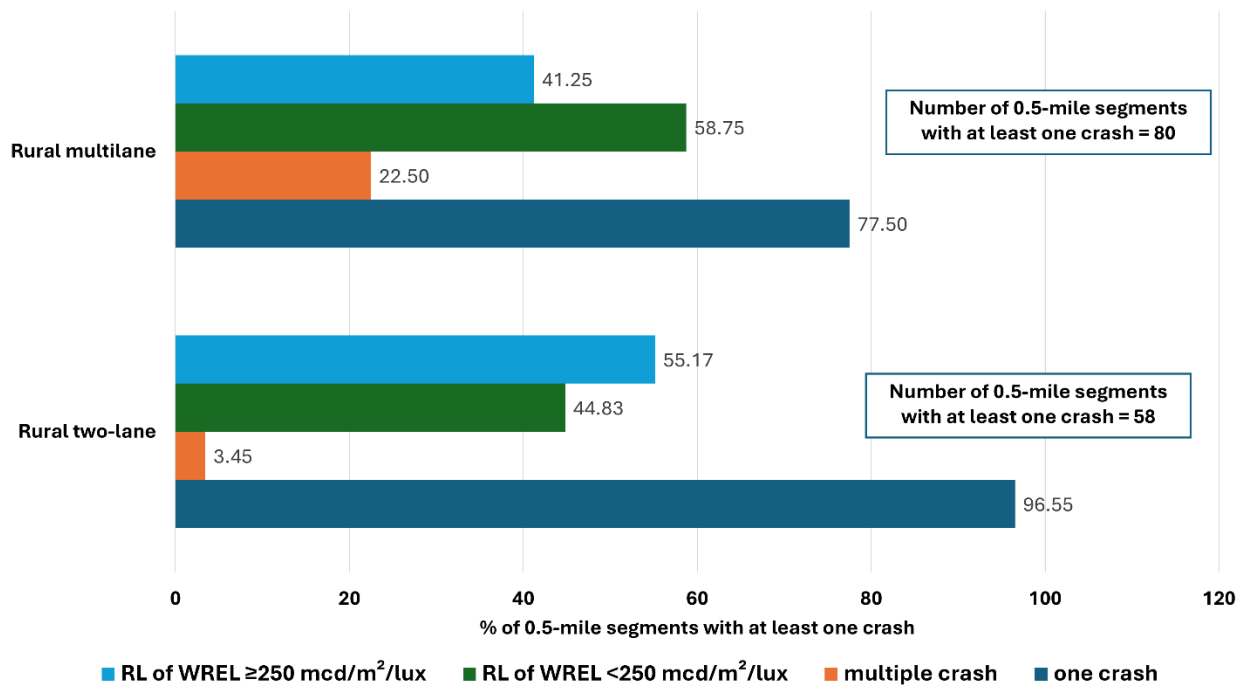


**Figure 7.4 Distribution of 0.5-mile segments with at least one single vehicle ROR crash at dark, dusk, and dawn**

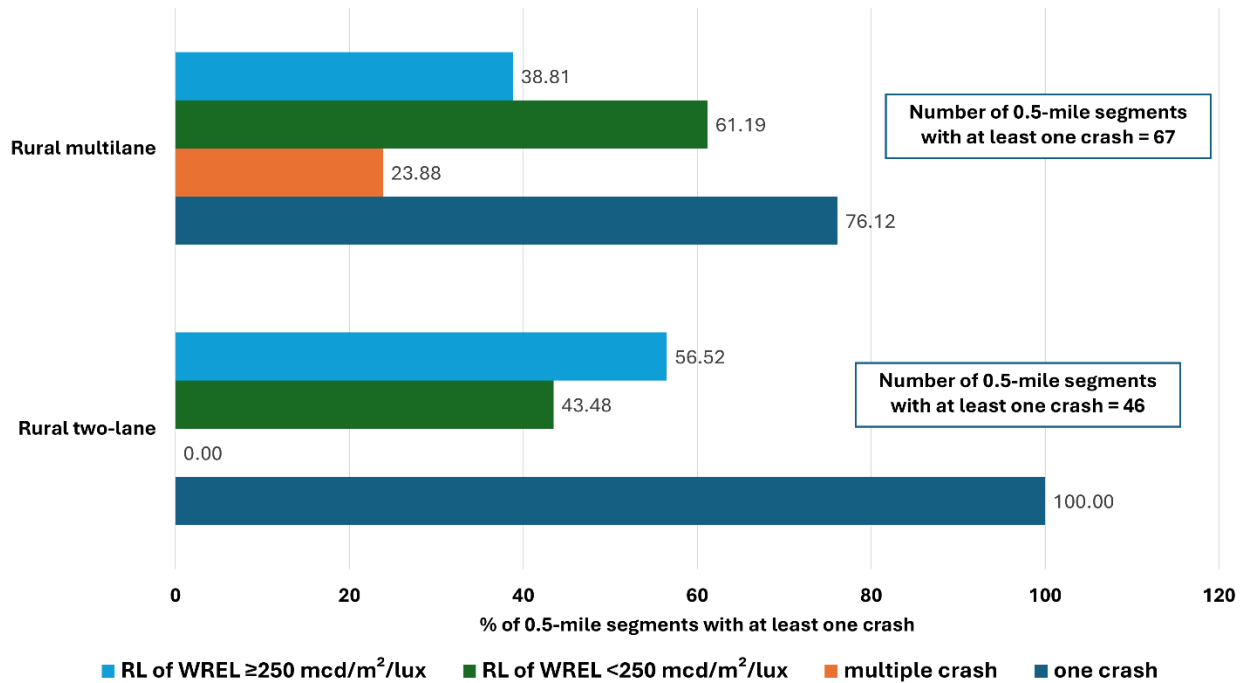


**Figure 7.5 Distribution of 0.5-mile segments with at least one single vehicle ROR crash at dark no streetlighting**

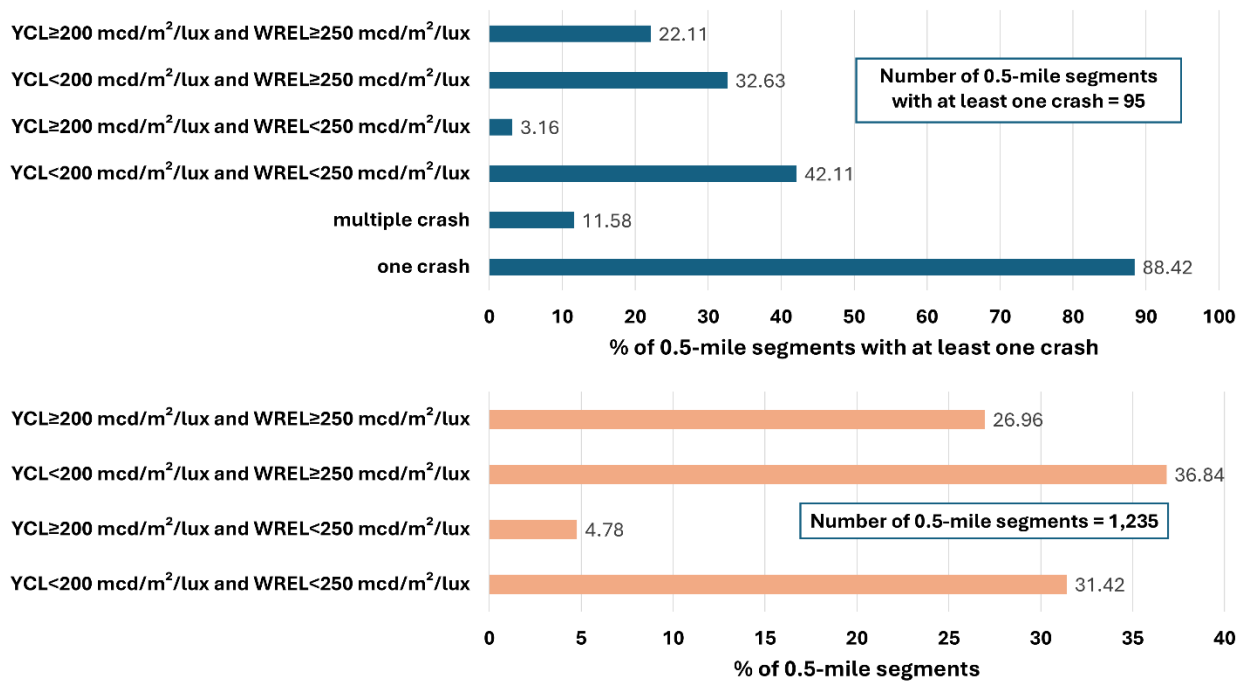


**Figure 7.6 Distribution of 0.5-mile segments with at least one crashes at dark no streetlighting (rural two-lane only)**

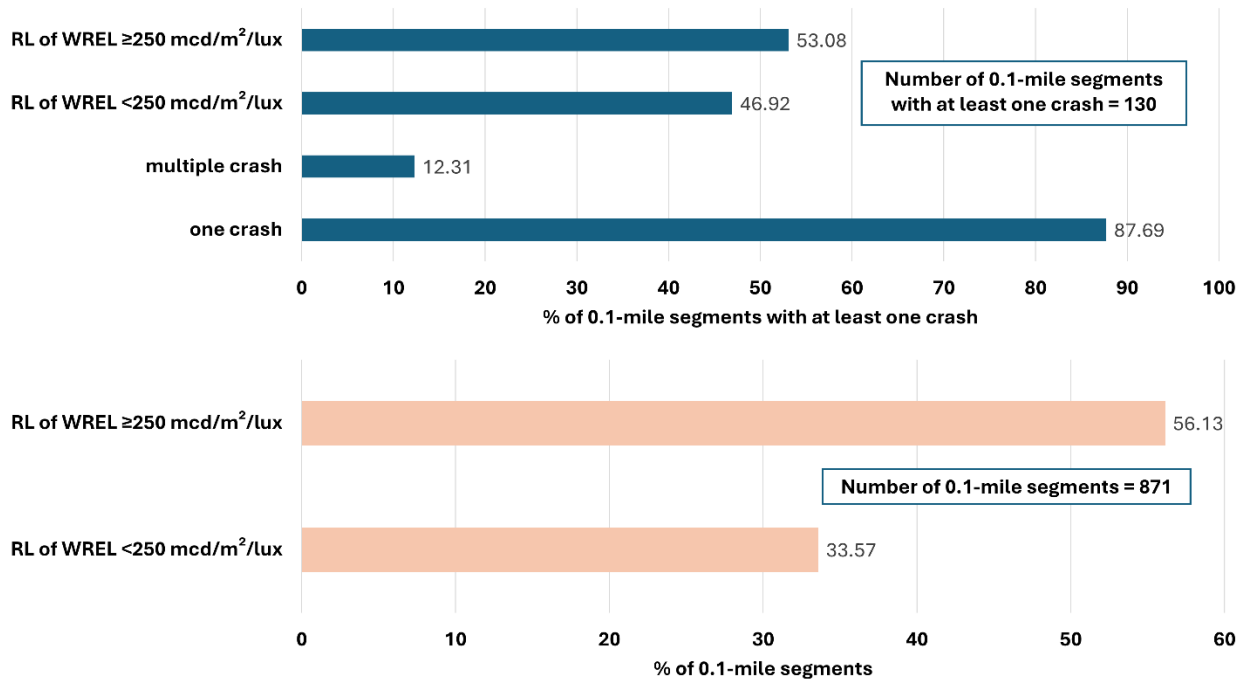


**Figure 7.7 Distribution of 0.1-mile segments with at least one crashes on curve segments**

### 7.3 Methodology

In this research, both binary logit regression and negative binomial (NB) regression are applied to examine the statistical relationship between RL and road crashes. In the binary logit regression model, the dependent variable indicates whether a crash occurred within a segment, providing the probability of crash occurrence. In contrast, the NB regression model utilizes crash frequency as the dependent variable, allowing for the assessment of the percentage increase or decrease in expected crash frequency.

#### 7.3.1 Binary Logit Regression

Binary logit regression has been employed in traffic safety research to examine the association between binary outcome variables and explanatory factors (Rahman et al., 2021). In this study, the dichotomous outcome variable  $y_{in}$  is defined as:

$$y_{in} = \begin{cases} 1, & \text{if presence of crashes} \\ 0, & \text{if no presence of crashes} \end{cases}$$

If the probability of a crash occurring is represented by  $P(y_{in} = 1)$ , then the logistic function can be defined as follows (McFadden, 1981):

$$P(y_{in} = 1) = \frac{\exp(\beta X_{in})}{1 + \exp(\beta X_{in})}$$

In this context,  $X_{in}$  refers to the independent variable vector, while  $\beta$  represents the estimable coefficient vector. The estimation of the coefficients can be achieved by maximizing the following log-likelihood function (Minka, 2001):

$$LL(\beta) = \sum_{i=1}^n \{(y_{in} \ln(P(y_{in})) + (1 - y_{in}) \ln(1 - P(y_{in})))\}$$

The Akaike Information Criterion (AIC) is a statistical measure used to evaluate the relative quality of regression models. It is rooted in information theory and provides a means of comparing multiple models to determine which is the most suitable for explaining the observed data (Bozdogan, 1987; Cavanaugh and Neath, 2019). The AIC assesses both the goodness-of-fit and the complexity of the model, aiming to strike a balance between them to avoid overfitting or underfitting (Petegem and Wegman, 2014).

$$AIC = 2k - 2\ln(L)$$

Where,  $k$  is the number of parameters in the model and  $\ln(L)$  is the natural logarithm of the likelihood of the model.

### 7.3.2 Negative Binomial (NB) Regression

The negative binomial model, also regarded as the Poisson-Gamma model, is an extension of the conventional Poisson model to overcome potential over-dispersion in the data. The model hypothesizes that the Poisson parameter supports a gamma likelihood distribution (Poch and Mannering, 1996). The NB assumes that crash frequencies are independent for an entity for any month. The model outcomes in a closed-form equation and the computation to manipulate the

association between the mean and the variance is relatively straightforward (Lord and Mannering, 2010). The equations of NB regression model are specified below:

$$P(z_i) = \frac{\Gamma\left(\left(\frac{1}{\beta}\right) + z_i\right)}{\Gamma\left(\frac{1}{\beta}\right) z_i!} \left(\frac{\frac{1}{\beta}}{\left(\frac{1}{\beta}\right) + \mu_i}\right)^{\frac{1}{\beta}} \left(\frac{\mu_i}{\left(\frac{1}{\beta}\right) + \mu_i}\right)^{z_i}$$

$$\mu_i = \exp(\gamma Y_i)$$

$$L(\gamma) = \prod_i \frac{\Gamma\left(\left(\frac{1}{\beta}\right) + z_i\right)}{\Gamma\left(\frac{1}{\beta}\right) z_i!} \left(\frac{\frac{1}{\beta}}{\left(\frac{1}{\beta}\right) + \exp(\gamma Y_i)}\right)^{\frac{1}{\beta}} \left(\frac{\exp(\gamma Y_i)}{\left(\frac{1}{\beta}\right) + \exp(\gamma Y_i)}\right)^{z_i}$$

$$LL(\gamma) = \sum_{i=1}^n \left( \ln \left( \frac{\Gamma\left(\left(\frac{1}{\beta}\right) + z_i\right)}{\Gamma\left(\frac{1}{\beta}\right) z_i!} \right) + \left(\frac{1}{\beta}\right) \ln \left( \frac{\frac{1}{\beta}}{\left(\frac{1}{\beta}\right) + \exp(\gamma Y_i)} \right) + z_i \left[ \gamma Y_i - \ln \left( \left(\frac{1}{\beta}\right) + \exp(\gamma Y_i) \right) \right] \right)$$

Where,  $P(z_i)$  = the likelihood of segment  $i$  having  $z_i$  crashes;  $\mu_i$  = the expectation of  $z_i$  conditional on  $Y_i$ ;  $\beta$  = over-dispersion parameter;  $Y_i$  = a vector of explanatory variables;  $\gamma$  = a vector of unknown parameter;  $L(\cdot)$  = likelihood function;  $LL(\cdot)$  = logarithm of likelihood function. Compared to the Poisson distribution, the NB distribution can allow for over-dispersion. If  $\beta \rightarrow 0$ , the NB model converges to the Poisson model as the variance equals the mean (Yang et al., 2021).

Given that crashes are typically infrequent and occur randomly, the zero-inflated negative binomial (ZINB) model can be employed to address segments with zero crashes, which cannot be adequately explained by NB model alone. The probability distribution of ZINB for random variable  $y_k$  is provided below (Garay et al., 2011):

$$P(y_k = j) = \begin{cases} \pi_k + (1 - \pi_k)g(\pi_k = 0), & \text{if } j = 0 \\ (1 - \pi_k)g(y_k), & \text{if } j > 0 \end{cases}$$

$$g(y_k) = P(Y = y_k | \mu_k, \alpha) = \frac{\Gamma(y_k + \alpha^{-1})}{\Gamma(\alpha^{-1}) \Gamma(y_k + 1)} \left(\frac{1}{1 + \alpha\mu_k}\right)^{\alpha^{-1}} \left(\frac{\alpha\mu_k}{1 + \alpha\mu_k}\right)^{y_k}$$

$$\pi_k = \frac{\vartheta_k}{1 + \vartheta_k}$$

Where,  $g(y_k)$  represents the NB distribution and  $\pi_k$  denotes the logistic link function.  $\mu_k$  represents the average crash frequency,  $\alpha$  denotes the over-dispersion parameter,  $\vartheta_k$  represents the probability of segment k being completely safe, i.e., the probability of a true absence of crashes at segment k.

#### 7.4 Analysis & Discussions

As discussed, both binary logistic regression and NB regression were applied to crash datasets, covering various types of targeted crashes along with the corresponding RL values of WREL and YCL for specific length of segments. The analyses were done at a 95% confidence interval ( $\alpha = 0.05$ ). The results indicate that both AIC and Pseudo  $R^2$  values are higher in binary logistic regression compared to NB regression. A high dispersion value was observed in NB models, particularly for rural two-lane segments, suggesting significant overdispersion where the variance is much greater than the mean. In rural two-lane segments, only a small fraction of segments had more than one crash, therefore, ZINB models were also applied. However, these models did not yield any significant improvement in performance or changes in coefficient values. Comparing logistic and NB regression, the coefficients and variable significance were nearly identical, with logistic regression consistently performing better across all crash datasets. In all targeted crashes, binary logit model performs well compared to NB and ZINB in terms of AIC and Pseudo  $R^2$  values. Previously, several highway safety studies have selected the best model outputs by comparing AIC values across multiple regression models (Li et al., 2019; Montella et al., 2008; Chen and Jovanis, 2000). Consequently, the results from logistic regression were selected for further discussion. It is important to note that the F-statistic is used to determine whether adding new predictors significantly enhances a model's explanatory power, rather than to identify the best model by comparing multiple regression models.

#### 7.4.1 Regression Results for Rural Two-Lane Segments

Tables 7.5-7.9 provide a summary of regression results for rural two-lane segments with respect to various targeted crashes, including single-vehicle ROR crashes, single-vehicle ROR crashes at dark, dusk, and dawn conditions, single-vehicle ROR crashes at dark not-lighted, and crashes at dark with no streetlighting. In all crash types, AADT is found to be a significant factor, indicating that higher AADT is associated with increased odds of a crash occurrence. Both single-vehicle ROR crashes and single-vehicle ROR crashes at dark not-lighted conditions show a statistically significant positive correlation with curve segments at a 95% confidence level, aligning with prior studies that highlight a higher likelihood of single-vehicle ROR crashes on curves (Duddu et al., 2020), especially in rural roadways (Gong and Fan, 2017). At a 90% confidence level ( $\alpha = 0.1$ ), the presence of curves is also found to be statistically significant for single-vehicle ROR crashes at dark, dusk, and dawn conditions. Interestingly, at a 90% confidence level, the odds of crashes on rural two-lane road segments at dark not-lighted conditions decrease by 17.66% in residential, business, or mixed-use areas. This reduction may be due to drivers' tendency to lower their speed in these areas because of the increased presence of pedestrians and parked vehicles, particularly during nighttime hours. On rural two-lane segments, RL of WREL below 250 mcd/m<sup>2</sup>/lux increases the odds of single-vehicle ROR crashes by 45.21%. In other crash types, however, lower RL values of WREL are not found to be statistically significant, though they are positively correlated with crash occurrences. This lack of statistical significance could be attributed to the limited observations of rural two-lane segments with crashes. When analyzing the combined influence of both YCL and WREL on crashes at dark with no streetlighting, neither the individual nor the interaction of RL levels is found to be statistically significant. However, lower RL levels are positively associated with crashes in dark not-lighted conditions.



**Table 7.5 Summary of regression results for single-vehicle ROR crashes on rural two-lane segments**

<b>Attribute</b>	<b>Coef.</b>	<b>SE</b>	<b>z-value</b>	<b>p-value</b>
(Intercept)	-3.102	0.178	-17.461	<0.001
<i>RL category (ref. <math>\geq 250</math> mcd/m<sup>2</sup>/lux)</i>				
<250 mcd/m <sup>2</sup> /lux	0.373	0.185	2.021	0.043
AADT (in 1,000 vpd)	0.211	0.031	6.050	<0.001
<i>Location class (ref. open country)</i>				
residential/business/mixed	-0.347	0.359	-0.965	0.335
<i>Posted speed limit (ref. <math>\geq 55</math>mph)</i>				
<55mph	-0.186	0.314	-0.594	0.553
<i>Presence of curve (ref. no)</i>				
yes	0.477	0.188	2.538	0.011
AIC: 901.64, Pseudo R <sup>2</sup> : 0.052				

Note: Coefficient (Coef.) and Standard Error (SE)

**Table 7.6 Summary of regression results for single-vehicle ROR crashes on rural two-lane segments at dark, dusk, and dawn conditions**

<b>Attribute</b>	<b>Coef.</b>	<b>SE</b>	<b>z-value</b>	<b>p-value</b>
(Intercept)	-3.938	0.265	-14.883	<0.001
<i>RL category (ref. <math>\geq 250</math> mcd/m<sup>2</sup>/lux)</i>				
<250 mcd/m <sup>2</sup> /lux	0.296	0.281	1.051	0.293
AADT (in 1,000 vpd)	0.173	0.052	3.416	0.001
<i>Location class (ref. open country)</i>				
residential/business/mixed	-0.762	0.629	-1.211	0.226
<i>Posted speed limit (ref. <math>\geq 55</math>mph)</i>				
<55mph	-0.021	0.455	-0.047	0.963
<i>Presence of curve (ref. no)</i>				
yes	0.474	0.282	1.682	0.093
AIC: 479.79, Pseudo R <sup>2</sup> : 0.039				

Note: Coefficient (Coef.) and Standard Error (SE)

**Table 7.7 Summary of regression results for single-vehicle ROR crashes on rural two-lane segments at dark not-lighted conditions**

<b>Attribute</b>	<b>Coef.</b>	<b>SE</b>	<b>z-value</b>	<b>p-value</b>
(Intercept)	-4.301	0.306	-14.044	<0.001
<i>RL category (ref. <math>\geq 250</math> mcd/m<sup>2</sup>/lux)</i>				
<250 mcd/m <sup>2</sup> /lux	0.216	0.317	0.682	0.496
AADT (in 1,000 vpd)	0.213	0.057	3.762	<0.001
<i>Location class (ref. open country)</i>				
residential/business/mixed	-1.734	1.047	-1.646	0.099

Attribute	Coef.	SE	z-value	p-value
<i>Posted speed limit (ref. <math>\geq 55</math>mph)</i>				
<55mph	-0.547	0.617	-0.887	0.374
<i>Presence of curve (ref. no)</i>				
yes	0.678	0.311	2.179	0.029
AIC: 396.71, Pseudo $R^2$ : 0.051				

Note: Coefficient (Coef.) and Standard Error (SE)

**Table 7.8 Summary of regression results for crashes on rural two-lane segments at dark not-lighted conditions (interaction of line type as a covariate)**

Attribute	Coef.	SE	z-value	p-value
(Intercept)	-3.240	0.265	-12.221	<0.001
<i>RL interaction (ref. <math>YCL \geq 200</math> mcd/m<sup>2</sup>/lux and <math>WREL \geq 250</math> mcd/m<sup>2</sup>/lux)</i>				
$YCL < 200$ mcd/m <sup>2</sup> /lux and $WREL < 250$ mcd/m <sup>2</sup> /lux	0.331	0.291	1.137	0.255
$YCL \geq 200$ mcd/m <sup>2</sup> /lux and $WREL < 250$ mcd/m <sup>2</sup> /lux	-0.409	0.651	-0.629	0.529
$YCL < 200$ mcd/m <sup>2</sup> /lux and $WREL \geq 250$ mcd/m <sup>2</sup> /lux	0.048	0.295	0.163	0.870
AADT (in 1,000 vpd)	0.201	0.040	4.994	<0.001
<i>Location class (ref. open country)</i>				
residential/business/mixed	-0.021	0.411	-0.050	0.959
<i>Posted speed limit (ref. <math>\geq 55</math>mph)</i>				
<55mph	-0.916	0.488	-1.878	0.060
<i>Presence of curve (ref. no)</i>				
yes	0.121	0.238	0.510	0.610
AIC: 654.40, Pseudo $R^2$ : 0.048				

Note: Coefficient (Coef.) and Standard Error (SE)

**Table 7.9 Summary of regression results for crashes on rural two-lane segments at dark not-lighted conditions**

Attribute	Coef.	SE	z-value	p-value
(Intercept)	-3.325	0.257	-12.917	<0.001
<i>YCL (ref. <math>\geq 200</math> mcd/m<sup>2</sup>/lux)</i>				
<200 mcd/m <sup>2</sup> /lux	0.195	0.260	0.749	0.454
<i>WREL (ref. <math>\geq 250</math> mcd/m<sup>2</sup>/lux)</i>				
<250 mcd/m <sup>2</sup> /lux	0.177	0.235	0.753	0.452
AADT (in 1,000 vpd)	0.208	0.040	4.988	<0.001
<i>Location class (ref. open country)</i>				
residential/business/mixed	-0.033	0.412	-0.080	0.936
<i>Posted speed limit (ref. <math>\geq 55</math>mph)</i>				
<55mph	-0.909	0.486	-1.871	0.061

Attribute	Coef.	SE	z-value	p-value
<i>Presence of curve (ref. no)</i>				
yes	0.114	0.237	0.481	0.630
AIC: 653.49, Pseudo $R^2$ : 0.045				

Note: Coefficient (Coef.) and Standard Error (SE)

#### 7.4.2 Regression Results for Rural Multilane Segments

Tables 7.10-7.15 exhibit a summary of regression results for rural multilane segments with respect to various targeted crash types, including single-vehicle ROR crashes, single-vehicle ROR crashes at dark, dusk, and dawn conditions, and single-vehicle ROR crashes at dark not-lighted, categorized by different RL levels of WREL. Consistent with findings for rural two-lane segments, AADT shows a statistically significant correlation with crash occurrences in relation to all targeted crash types. At a 95% confidence interval, the odds of single-vehicle ROR crashes on rural multilane segments decreases by over 30% in residential, business, or mixed-use areas. Similar statistically significant correlations are observed for single-vehicle ROR crashes at dark, dusk, and dawn conditions at an 85% confidence interval ( $\alpha = 0.15$ ), and for single-vehicle ROR crashes at dark not-lighted conditions at an 80% confidence interval ( $\alpha = 0.2$ ).

Under dark, dusk, and dawn conditions, rural multilane segments with RL of WREL below 150 mcd/m<sup>2</sup>/lux experience a 76.84% increase in the odds of single-vehicle ROR crashes at a 90% confidence interval. In similar lighting conditions, if RL values of WREL fall between 150 and 249 mcd/m<sup>2</sup>/lux, the odds of single-vehicle ROR crashes increase by 51.77% at an 80% confidence interval. When analyzing only two RL categories,  $\geq 250$  mcd/m<sup>2</sup>/lux and  $< 250$  mcd/m<sup>2</sup>/lux, the odds of single-vehicle ROR crashes at dark, dusk, and dawn conditions increases by 61.08% for segments with RL below 250 mcd/m<sup>2</sup>/lux at a 90% confidence interval. In dark conditions with no streetlighting, rural multilane segments with RL levels below 150 mcd/m<sup>2</sup>/lux show a 116.19% increase in the odds of single-vehicle ROR crashes at a 95% confidence interval. When examining

only two RL categories,  $\geq 250$  mcd/m<sup>2</sup>/lux and  $< 250$  mcd/m<sup>2</sup>/lux, the odds of single-vehicle ROR crash occurrences at dark not-lighted conditions rise by 77.89% on segments with RL below 250 mcd/m<sup>2</sup>/lux at a 90% confidence interval.

**Table 7.10 Summary of regression results for single-vehicle ROR crashes on rural multilane segments (RL category 1)**

Attribute	Coef.	SE	z-value	p-value
(Intercept)	-1.975	0.258	-7.652	<0.001
<i>RL category (ref. <math>\geq 250</math> mcd/m<sup>2</sup>/lux)</i>				
<150 mcd/m <sup>2</sup> /lux	0.226	0.277	0.817	0.414
150-249 mcd/m <sup>2</sup> /lux	0.045	0.242	0.187	0.852
AADT (in 1,000 vpd)	0.051	0.013	6.451	<0.001
<i>Location class (ref. open country)</i>				
residential/business/mixed	-1.002	0.445	-2.250	0.025
<i>Posted speed limit (ref. <math>\geq 65</math>mph)</i>				
<65mph	-0.087	0.329	-0.265	0.791
<i>Presence of curve (ref. no)</i>				
yes	0.123	0.318	0.386	0.700
AIC: 593.64, Pseudo R <sup>2</sup> : 0.108				

Note: Coefficient (Coef.) and Standard Error (SE)

**Table 7.11 Summary of regression results for single-vehicle ROR crashes on rural multilane segments (RL category 2)**

Attribute	Coef.	SE	z-value	p-value
(Intercept)	-1.972	0.258	-7.654	<0.001
<i>RL category (ref. <math>\geq 250</math> mcd/m<sup>2</sup>/lux)</i>				
<250 mcd/m <sup>2</sup> /lux	0.116	0.212	0.546	0.585
AADT (in 1,000 vpd)	0.058	0.017	6.455	<0.001
<i>Location class (ref. open country)</i>				
residential/business/mixed	-1.006	0.445	-2.261	0.024
<i>Posted speed limit (ref. <math>\geq 65</math>mph)</i>				
<65mph	-0.089	0.329	-0.272	0.786
<i>Presence of curve (ref. no)</i>				
yes	0.126	0.318	0.395	0.693
AIC: 592.02, Pseudo R <sup>2</sup> : 0.107				

Note: Coefficient (Coef.) and Standard Error (SE)

**Table 7.12 Summary of regression results for single-vehicle ROR crashes on rural multilane segments at dark, dusk, and dawn conditions (RL category 1)**

Attribute	Coef.	SE	z-value	p-value
(Intercept)	-2.815	0.342	-8.230	<0.001
<i>RL category (ref. <math>\geq 250</math> mcd/m<sup>2</sup>/lux)</i>				
<150 mcd/m <sup>2</sup> /lux	0.570	0.332	1.719	0.086
150-249 mcd/m <sup>2</sup> /lux	0.417	0.294	1.417	0.156
AADT (in 1,000 vpd)	0.043	0.011	4.176	<0.001
<i>Location class (ref. open country)</i>				
residential/business/mixed	-0.912	0.609	-1.497	0.135
<i>Posted speed limit (ref. <math>\geq 65</math>mph)</i>				
<65mph	-0.182	0.462	-0.394	0.693
<i>Presence of curve (ref. no)</i>				
yes	0.099	0.424	0.234	0.815
AIC: 425.44, Pseudo $R^2$ : 0.076				

Note: Coefficient (Coef.) and Standard Error (SE)

**Table 7.13 Summary of regression results for single-vehicle ROR crashes on rural multilane segments at dark, dusk, and dawn conditions (RL category 2)**

Attribute	Coef.	SE	z-value	p-value
(Intercept)	-2.812	0.341	-8.236	<0.001
<i>RL category (ref. <math>\geq 250</math> mcd/m<sup>2</sup>/lux)</i>				
<250 mcd/m <sup>2</sup> /lux	0.477	0.261	1.829	0.067
AADT (in 1,000 vpd)	0.042	0.015	4.175	<0.001
<i>Location class (ref. open country)</i>				
residential/business/mixed	-0.918	0.609	-1.507	0.132
<i>Posted speed limit (ref. <math>\geq 65</math>mph)</i>				
<65mph	-0.185	0.462	-0.399	0.690
<i>Presence of curve (ref. no)</i>				
yes	0.103	0.424	0.242	0.809
AIC: 423.64, Pseudo $R^2$ : 0.075				

Note: Coefficient (Coef.) and Standard Error (SE)

**Table 7.14 Summary of regression results for single-vehicle ROR crashes on rural multilane segments at dark not-lighted conditions (RL category 1)**

Attribute	Coef.	SE	z-value	p-value
(Intercept)	-2.941	0.367	-8.016	<0.001
<i>RL category (ref. <math>\geq 250</math> mcd/m<sup>2</sup>/lux)</i>				
<150 mcd/m <sup>2</sup> /lux	0.771	0.347	2.223	0.026
150-249 mcd/m <sup>2</sup> /lux	0.445	0.319	1.394	0.163
AADT (in 1,000 vpd)	0.033	0.009	3.484	<0.001

Attribute	Coef.	SE	z-value	p-value
<i>Location class (ref. open country)</i>				
residential/business/mixed	-0.901	0.679	-1.326	0.185
<i>Posted speed limit (ref. ≥65mph)</i>				
<65mph	-0.288	0.514	-0.559	0.576
<i>Presence of curve (ref. no)</i>				
yes	-0.034	0.475	-0.071	0.943
AIC: 383.22, Pseudo R <sup>2</sup> : 0.073				

Note: Coefficient (Coef.) and Standard Error (SE)

**Table 7.15 Summary of regression results for single-vehicle ROR crashes on rural multilane segments at dark not-lighted conditions (RL category 2)**

Attribute	Coef.	SE	z-value	p-value
(Intercept)	-2.934	0.365	-8.031	<0.001
<i>RL category (ref. ≥250 mcd/m<sup>2</sup>/lux)</i>				
<250 mcd/m <sup>2</sup> /lux	0.576	0.280	2.055	0.039
AADT (in 1,000 vpd)	0.032	0.009	3.478	<0.001
<i>Location class (ref. open country)</i>				
residential/business/mixed	-0.918	0.681	-1.349	0.177
<i>Posted speed limit (ref. ≥65mph)</i>				
<65mph	-0.292	0.515	-0.566	0.571
<i>Presence of curve (ref. no)</i>				
yes	-0.024	0.475	-0.051	0.959
AIC: 382.05, Pseudo R <sup>2</sup> : 0.071				

Note: Coefficient (Coef.) and Standard Error (SE)

### 7.4.3 Regression Results for Curve Segments

**Table 7.16** summarizes the regression results for curve segments in relation to single-vehicle ROR crashes. For this analysis, the dataset was prepared using average values for each 0.1-mile segment, and both two-lane and multilane roads were merged, resulting in the inclusion of a ‘number of lanes’ variable. Similar to previous segments, AADT is found to be a significant factor. The odds of single-vehicle ROR crashes on curve segments increase with higher road functional classifications, rising by 144% for arterial roads and 373.04% for interstates, which may be associated with higher posted speed limits. No significant correlation has been observed with respect to curve angle and radius. On curve segments, RL values of WREL below 250 mcd/m<sup>2</sup>/lux

are associated with a 59.89% increase in the odds of single-vehicle ROR crashes. Low RL levels on curves can reduce drivers' ability to clearly perceive lane boundaries, making it more challenging to navigate curves safely, which can increase the risk of vehicles veering off the roadway.

**Table 7.16 Summary of regression results for single-vehicle ROR crashes on curve segments**

<b>Attribute</b>	<b>Coef.</b>	<b>SE</b>	<b>z-value</b>	<b>p-value</b>
(Intercept)	-3.240	0.573	-5.655	<0.001
<i>Number of lanes (ref. &gt;two)</i>				
two	0.262	0.374	0.703	0.482
<i>RL category (ref. <math>\geq 250</math> mcd/m<sup>2</sup>/lux)</i>				
<250 mcd/m <sup>2</sup> /lux	0.469	0.201	2.337	0.019
AADT (in 1,000 vpd)	0.052	0.023	2.567	0.010
<i>Location class (ref. open country)</i>				
business/residential/mixed	-0.037	0.312	-0.118	0.906
<i>Functional class (ref. major collector)</i>				
arterial	0.892	0.282	3.165	0.002
interstate	1.554	0.779	1.994	0.046
Curve angle	0.006	0.007	0.920	0.358
Curve radius (in 1,000)	-0.065	0.070	-0.950	0.342
AIC:703.28, Pseudo R <sup>2</sup> : 0.079				

Note: Coefficient (Coef.) and Standard Error (SE)

## 7.5 Key Findings

This chapter aims to investigate the statistical relationship between RL and road crashes. To expand the dataset, the RL prediction models developed in Chapter 6 were applied to estimate RL of WREL and YCL for additional segments, increasing the sample size significantly. Unlike previous studies that calculated average RL over 1-mile segments, this study used shorter segments, specifically 0.5-mile, for more granular analysis. Practical assumptions were made based on the available data and the limitations of the predictive models. Several covariates were considered to improve the validity of the model results by considering the effect of other factors, such as AADT, posted speed limit, location class, road functional class, and horizontal alignment.

Two widely used regression models, binary logit model and NB model, were applied to all prepared crash datasets. Binary logit model demonstrated better performance in terms of AIC and Pseudo  $R^2$ , particularly given the zero-inflated nature of the datasets. The key findings from these analyses are summarized below:

- RL level of WREL below 250 mcd/m<sup>2</sup>/lux statistically increases the likelihood of single-vehicle ROR crashes on rural two-lane road segments.
- On rural multilane segments in dark, dusk, and dawn conditions, both RL levels of WREL below 150 mcd/m<sup>2</sup>/lux and below 250 mcd/m<sup>2</sup>/lux increase the likelihood of single-vehicle ROR crashes.
- Lower RL of WREL, specifically below 250 mcd/m<sup>2</sup>/lux, play a significant role in increasing the probability of single-vehicle ROR crashes on rural multilane segments at dark not-lighted conditions.
- On curve segments, RL of WREL below 250 mcd/m<sup>2</sup>/lux are associated with a statistically significant increase in the likelihood of single-vehicle ROR crashes.



## **Chapter 8    Conclusions**

This chapter aims to highlight the contributions of this research by providing in-depth aspects of RL degradation factors, subjective ratings of pavement marking, RL prediction modeling, and the statistical relationship between RL and crash frequency. The key findings are also presented in alignment with the research objectives, contextualizing the contributions of this study. This discussion further provides practical implementation ideas and recommendations, highlighting the significance of these findings. Additionally, study limitations are addressed, offering insights and potential directions for future research.

### **8.1    Research Contributions**

Based on the literature review, no prior research has examined the factors contributing to RL degradation in relation to different pavement marking line types. Furthermore, while some studies have considered various factors in RL degradation models, very few have focused on road geometry characteristics, such as horizontal alignment. Horizontal alignment may significantly contribute to RL degradation due to increased vehicle encroachment on curves, yet its influence remains underexplored. Other potential contributors to RL degradation exist, but due to limited sample sizes, these variables may not show statistical significance within regression models. Consequently, identifying the importance of such variables through alternative approaches beyond traditional regression modeling is essential - a gap that still needs to be addressed in the current literature. This research examined how the effects of potential contributing factors on RL degradation varies by pavement marking line type. For instance, in relation to yellow markings, locations such as residential, business, and mixed-use areas were found to be statistically significant, exhibiting a high probability of RL degradation. Moreover, WLL markings on

roadways with high posted speed limits (65 mph or higher) showed a greater likelihood of RL degradation. While curve segments were not found to be statistically significant in the regression models, higher RL degradation proportions of WREL were observed on curve segments while compared with adjacent straight segments. Further analysis was conducted to identify locations with higher RL degradation of WREL than expected, revealing several influential factors. These included the presence of additional right-turn lanes near intersections or ramps, multilane segments with U-turn and left-turn access to minor roads, presence of bridges/ramps/shoulders/residential driveways, and surrounding landscape features (e.g., gravel land). These findings can assist ALDOT's pavement management system in identifying locations with high RL degradation, enabling more targeted restriping at these specific segments. This targeted strategy could improve road safety while reducing maintenance costs by focusing on areas with a greater need for RL restoration.

While the correlation between subjective ratings and measured RL has been previously explored, further research is needed to examine this relationship by specific marking line types. Analyzing the measured RL distribution across each subjective rating scale can help to address challenges often encountered in subjective assessment of markings. This study investigated the distribution of measured RL values within each subjective rating scale in relation to different marking line types and found evidence supporting the hypothesis that officers may struggle to assign accurate ratings, particularly for yellow markings. A prevailing hypothesis suggests that darker pavement markings appear brighter than lighter markings, even at similar RL levels. The findings of this study provide evidence supporting this hypothesis. Additionally, the study explored the subjective rating standards of marking line type in terms of measured RL, demonstrating the

practical alignment of rating scales with actual RL measurements. Overall, the study found consistency between subjective rating and actual RL measurements.

Local transportation agencies often do not have initial RL measurements and marking age information when assessing the RL of pavement markings on specific segments. This gap creates a need for models that can predict RL without relying on initial RL measurements taken after installation or restriping and knowing when the markings were installed or restriped. It is crucial that prediction models should remain practical and usable, incorporating only the key variables that contribute to RL degradation to avoid unnecessary complexity. This study is the first in existing literature to take such an approach in developing regression models for predicting RL of YCL and WREL, considering lane configurations of rural roads. While the model showed some limitations, particularly in predicting future RL at lower levels, it provides valuable contributions. The latest MUTCD version lowers the minimum RL standard to 50 mcd/m<sup>2</sup>/lux, meaning transportation agencies need to prioritize collecting more data on segments with RL levels between 50 and 100 mcd/m<sup>2</sup>/lux. This data can be vital for developing predictive models that can better estimate the service life of marking up to 50 mcd/m<sup>2</sup>/lux. Despite limitations in predicting RL at lower levels, the developed RL prediction models of this research offer agencies a useful tool for forecasting RL on segments that previously showed high RL values. A practical application of the developed RL prediction models is demonstrated in the Appendix Section (**Tables A2 and A3**). By utilizing one year of RL data, agencies can predict future RL values and rank road segments accordingly, from lowest to highest predicted RL. This ranking enables ALDOT to efficiently identify and prioritize segments with lower RL levels, ensuring timely restriping and maintaining road safety standards.

This research demonstrates an effective approach for examining the statistical relationship between RL and road crashes by increasing the sample size through predicting RL following a single measured RL value. Employing an appropriate statistical modeling approach, which accounts for the logarithmic relationship of crashes, and strategic RL categorization have strengthened the validity of this research findings. Unlike previous studies that calculated average RL over 1-mile or 2-mile segments, this research considered smaller segment sizes, such as 0.5-mile segments in general and 0.1-mile segments specifically for curves. Moreover, multiple covariates such as posted speed limit, AADT, location classification, and curve presence, were incorporated to validate the correlations. The results revealed a statistically significant relationship between lower RL of WREL and single-vehicle ROR crashes, confirming that this refined approach effectively highlights the significance of maintaining RL in terms of road safety. Furthermore, the findings highlighted the vulnerability associated with lower RL levels on curve segments and low lighting conditions, underscoring their combined impact on road safety. Overall, the findings of this research align with one of the core principles of the Safe System Approach: ‘Making Our Roads Safer’ (FHWA, 2022).

## **8.2 Recommendations**

This study discusses recommendations from three key perspectives: i) the need for additional and expanded datasets to enable more granular analysis, ii) alignment with current MUTCD guidelines, and iii) the key findings related to this research objectives. A summary of the key recommendations is provided in the following:

- This study identified that only a limited number of segments had RL levels below 100 mcd/m<sup>2</sup>/lux for both rural two-lane and multilane roadways. To develop a more robust and comprehensive model capable of accurately predicting the service life of thermoplastic

pavement markings, additional RL data from segments with lower RL levels is required. This need is especially important given the recent changes to the MUTCD guidelines, which have reduced the minimum RL requirement to 50 mcd/m<sup>2</sup>/lux. Therefore, ALDOT needs to implement a more systematic approach to RL data collection. One potential strategy is to conduct an initial subjective rating of specific segments, identifying those likely to have low RL levels, and then prioritize those segments for precise RL measurement.

- To create a comprehensive RL degradation dataset for modeling, it is essential to include detailed road characteristics, such as lane width, shoulder width, and other relevant features. These attributes can vary within a one-mile segment, making precise calculation through tools like Google Earth Pro difficult. Most states maintain road inventory databases that contain such information, particularly for major roadways. It is recommended that ALDOT improve accessibility to Alabama road inventory data to ensure that critical road characteristics are readily available for further research.
- While analyzing the measured RL data, it was observed that RL of YCL and YLEL were often misassigned when lane transitions occurred, such as when transitioning from a rural two-lane to a three-lane configuration or vice versa. To address this issue, closer monitoring and quality control are required to ensure the correct assignment of marking line type to each of the measured RL.
- The current version of MUTCD reduces the minimum RL requirement to 50 mcd/m<sup>2</sup>/lux. This research found that lower RL levels, particularly below 250 mcd/m<sup>2</sup>/lux for WREL, significantly increases the likelihood of crash occurrences. Additionally, vehicles equipped with ADAS rely on adequate RL levels for optimal sensor performance, and a few studies

have concluded that RL levels below 88 mcd/m<sup>2</sup>/lux can significantly reduce sensor accuracy. Therefore, continuous monitoring is essential to ensure that this lower RL requirement does not compromise road safety. While high vehicle automation is still in its early stages with limited penetration, it is important to balance these considerations without overemphasizing automation concerns and benefits.

- The current MUTCD guidelines for minimum RL standards do not consider low lighting conditions. However, higher RL levels are particularly beneficial in nighttime driving, as they help guide drivers to stay within the correct travel lane. Given this, developing a standardized method for determining RL under adverse and low lighting conditions, such as bad weather or dark with no streetlighting, would be more practical.
- This research identified challenges in assigning subjective rating scales to yellow pavement markings. To address this issue, continuous monitoring is needed to determine the underlying causes of these difficulties, thereby enhancing the reliability and consistency of the rating process through improved rating criteria and training.
- This study applied a segment-based approach to examine the statistical relationship between RL and crashes. However, each crash is associated with a combination of multiple factors. As a result, investigating individual crashes with measured RL values, rather than focusing solely on segments, could reveal hidden patterns among variables. It is recommended that RL values be measured at specific hotspot locations over a period of time to enable a more in-depth analysis of the relationship between RL and other crash contributing factors.

### **8.3 Study Limitations and Future Scope**

This research has several limitations that can be addressed in future studies. The study utilized RL data exclusively from the Montgomery region, limiting the sample size. Expanding the dataset to include additional regions would increase the sample size, helping to extend the minimum thresholds for both marking colors. Typically, RL degrades more rapidly after installation until it reaches a certain level, after which it declines at a more stable rate. This degradation pattern could be more effectively captured through machine learning algorithms. However, due to the limited number of observations, machine learning techniques were not applied in this study (Brodley et al., 2012). In the future, machine learning algorithms, such as random forests, could be applied to larger datasets to develop more practical RL prediction models. Additionally, factors like weather conditions, material composition, and quality of installation may influence RL degradation. Future research could explore these variables to better understand their impact on the transition of RL between qualitative states. The research findings and conclusions derived from rural Alabama roads warrant further investigation to ascertain their applicability to other states sharing similar climatic conditions. Future research could delve into more material-specific modeling to capture the distinct effects of various independent variables on RL degradation. Additionally, conducting a human-factors study on the correlation between pavement marking RL and speed could shed light on questions such as whether drivers perceive increased comfort with higher RL values, potentially leading to higher speeds. In this research, temporal variability in AADT was not accounted for in the safety analyses. The findings highlighted significant differences in how various factors contribute to RL degradation between WLL and WREL. Consequently, further research is needed to explore these variations in greater depth and to compare the safety impacts of RL for WLL and WREL.

## References

- Alabama Department of Transportation (ALDOT), 2023. TDM Public: Alabama Traffic Data.  
Alabama Department of Transportation. <https://aldotgis.dot.state.al.us/TDMPublic/>
- Abboud, N., Bowman, B.L., 2002. Cost- and longevity-based scheduling of paint and thermoplastic striping. *Transp. Res. Rec.* 1794(1), 55–64. doi:10.3141/1794-07
- Aktan, F., Schnell, T., 2004. Performance evaluation of pavement markings under dry, wet, and rainy conditions in the field. *Transp. Res. Rec.* 1877(1), 38–49. doi:10.3141/1877-05
- Alabama Department of Transportation (ALDOT), 2022. Standard Specifications for Highway Construction, Alabama Department of Transportation.  
<https://www.dot.state.al.us/publications/Construction/Specifications.html>  
<https://www.dot.state.al.us/publications/construction/pdf/Specifications/2022/SpecBookComplete.pdf>
- Andrady, A.L. Anthony L., 1997. Pavement marking materials : assessing environment friendly performance. National Cooperative Highway Research Program (NCHRP Report 392), Transportation Research Board.  
[https://onlinepubs.trb.org/Onlinepubs/nchrp/nchrp\\_rpt\\_392.pdf](https://onlinepubs.trb.org/Onlinepubs/nchrp/nchrp_rpt_392.pdf)
- Avelar, R., Carlson, P., 2014. Link between pavement marking retroreflectivity and night crashes on Michigan two-lane highways. *Transp. Res. Rec.* 2404 (1), 59–67. doi:10.3141/2404-07
- Babić, D., Babić, D., Fiolić, M., Eichberger, A., Magosi, Z.F., 2022. Impact of Road Marking Retroreflectivity on Machine Vision in Dry Conditions: On-Road Test. *Sensors* 22(4), 1303. doi:10.3390/s22041303
- Bahar, G., Masliah, M., Erwin, T., Tan, E., 2006. Pavement Marking Materials and Markers: Real-World Relationship Between Retroreflectivity and Safety Over Time. National



Cooperative Highway Research Program, Transportation Research Board.

doi:10.17226/23255

Bektas, B.A., Gkritza, K., Smadi, O., 2016. Pavement marking retroreflectivity and crash frequency: Segmentation, line type, and imputation effects. *J. Transp. Eng.* 142(8).

doi:10.1061/(ASCE)TE.1943-5436.0000863

Benz, R.J., Pike, A.M., Kuchangi, S.P., Brackett, Q., 2008. Serviceable pavement marking retroreflectivity levels: technical report. Texas Department of Transportation.

<http://tti.tamu.edu/documents/0-5656-1.pdf>

Bowman, B., 2001. Estimating the Effective Life of Pavement Marking Based on Crash History.

Auburn University. <https://lightspeed.eng.auburn.edu/files/centers/hrc/IR-01-02.pdf>

Bozdogan, H., 1987. Model Selection and Akaike's Information Criterion (AIC): The General Theory and its Analytical Extensions. *Psychometrika* 52(3), 345–370. doi:

10.1007/BF02294361

Brodley, C.E., Rebbapragada, U., Small, K., Wallace, B.C., 2012. Challenges and opportunities in applied machine learning. *AI Mag.* 33(1), 11–24. doi:10.1609/aimag.v33i1.2367

Burghardt, T.E., Popp, R., Helmreich, B., Reiter, T., Böhm, G., Pitterle, G., Artmann, M., 2021. Visibility of various road markings for machine vision. *Case Stud. Constr. Mater.* 15.

doi:10.1016/j.cscm.2021.e00579

Cafiso, S., Pappalardo, G., 2020. Safety effectiveness and performance of lane support systems for driving assistance and automation – Experimental test and logistic regression for rare events. *Accid. Anal. Prev.* 148. doi:10.1016/j.aap.2020.105791

Carlson, P.J., Park, E.S., Kang, D.H., 2013. Investigation of longitudinal pavement marking retroreflectivity and safety. *Transp. Res. Rec.* 2337(1), 59–66. doi:10.3141/2337-08

- Cavanaugh, J.E., Neath, A.A., 2019. The Akaike information criterion: Background, derivation, properties, application, interpretation, and refinements. *Wiley Interdiscip. Rev. Comput. Stat.* 11(3). doi:10.1002/wics.1460
- Chen, W.H. and Jovanis, P.P., 2000. Method for Identifying Factors Contributing to Driver-Injury Severity in Traffic Crashes. *Transp. Res. Rec.* 1717(1). doi: 10.3141/1717-01
- Chimba, D., Kidando, E., Onyango, M., 2018. Evaluating the Service Life of Thermoplastic Pavement Markings: Stochastic Approach. *J. Transp. Eng. Part B Pavements* 144(3). doi:10.1061/jpeodx.0000055
- Cribari-Neto, F., Zeileis, A., 2010. Beta regression in R. *J. Stat. Softw.* 34(2), 1–24. doi:10.18637/jss.v034.i02
- Davies, C., 2017. Effects of Pavement Marking Characteristics on Machine Vision Technology. Transportation Research Board 96th Annual Meeting, Washington DC, United States. <https://trid.trb.org/View/1438482>
- De Land, P.N., Chase, W.W., 1993. Statistics notebook: Entry IV.B: (3) two-sample pooled variance t-test and (4) two-sample separate variance t-test. *Optom. Vis. Sci.* 70(12), 1065–1068. doi:10.1097/00006324-199312000-00014
- Donnell, E.T., Karwa, V., Sathyanarayanan, S., 2009. Analysis of effects of pavement marking retroreflectivity on traffic crash frequency on highways in North Carolina. *Transp. Res. Rec.* 2103(1), 50–60. doi:10.3141/2103-07
- Dravitzki, V.K., Wilkie, S.M., Lester, T.J., 2006. The safety benefits of brighter roadmarkings. Land Transport New Zealand (Report 310), 41. <https://www.nzta.govt.nz/assets/resources/research/reports/310/docs/310.pdf>
- Duddu, V.R., Pulugurtha, S.S., Kukkapalli, V.M., 2020. Variable categories influencing single-

vehicle run-off-road crashes and their severity. *Transp. Eng.* 2.

doi:10.1016/j.treng.2020.100038

Federal Highway Administration (FHWA), 2022. Public Roads - Winter 2022: Making our Roads Safer through a Safe System Approach. <https://highways.dot.gov/public-roads/winter-2022/01>

Federal Highway Administration (FHWA), 2023. Highway Performance Monitoring System (HPMS). <https://www.fhwa.dot.gov/policyinformation/hpms.cfm>

Ferrari, S.L.P., Cribari-Neto, F., 2004. Beta regression for modelling rates and proportions. *J. Appl. Stat.* 31(7), 799–815. doi:10.1080/0266476042000214501

Federal Highway Administration (FHWA), 2022. National Standards for Traffic Control Devices; the Manual on Uniform Traffic Control Devices for Streets and Highways; Maintaining Pavement Marking Retroreflectivity. Federal Highway Administration (FHWA-2009-0139). <https://www.federalregister.gov/documents/2022/08/05/2022-16781/national-standards-for-traffic-control-devices-the-manual-on-uniform-traffic-control-devices-for>

Federal Highway Administration (FHWA), 2000. Road Function Classifications. Federal Highway Administration, U.S Department of Transportation.

[https://safety.fhwa.dot.gov/speedmgt/data\\_facts/docs/rd\\_func\\_class\\_1\\_42.pdf](https://safety.fhwa.dot.gov/speedmgt/data_facts/docs/rd_func_class_1_42.pdf)

Federal Highway Administration (FHWA), 2017. Nighttime Visibility. Federal Highway Administration, U.S. Department of Transportation.

<https://highways.dot.gov/safety/other/visibility/nighttime-visibility>

Fu, H., Wilmot, C.G., 2013. Evaluating Alternative Pavement Marking Materials. *Public Work. Manag. Policy* 18(3), 279–297. doi:10.1177/1087724X12451844

- Garay, A.M., Hashimoto, E.M., Ortega, M.M., and Lachos, V.H, 2011. On Estimation and Influence Diagnostics for Zero-Inflated Negative Binomial Regression Models. *Computational Statistics and Data Analysis*. 55(3), 1304-1318. doi: 10.1016/j.csda.2010.09.019
- Gong, L., Fan, W., 2017. Modeling single-vehicle run-off-road crash severity in rural areas: Accounting for unobserved heterogeneity and age difference. *Accid. Anal. Prev.* 101, 124–134. doi:10.1016/j.aap.2017.02.014
- Hadi, M., Sinha, P., 2011. Effect of pavement marking retroreflectivity on the performance of vision-based lane departure warning systems. *J. Intell. Transp. Syst. Technol. Planning, Oper.* 15(1), 42–51. doi:10.1080/15472450.2011.544587
- Hollingsworth, J.D., 2008. Understanding the Impact of Bead Type on Paint and Thermoplastic Pavement Markings. *Theses and Dissertations*. 1267. <https://scholar.afit.edu/etd/1267/>
- Hsu, H., Lachenbruch, P.A., 2014. Paired t Test . *Wiley Online*. doi:10.1002/9781118445112.stat05929
- Hu, B., Palta, M., Shao, J., 2006. PSEUDO-R 2 in logistic regression model. *Stat. Sin.* 16, 847–860. [https://www.researchgate.net/publication/228463155\\_PSEUDO-R\\_2\\_in\\_logistic\\_regression\\_model](https://www.researchgate.net/publication/228463155_PSEUDO-R_2_in_logistic_regression_model)
- Hummer, J.E., Rasdorf, W., Zhang, G., 2011. Linear Mixed-Effects Models for Paint Pavement-Marking Retroreflectivity Data. *J. Transp. Eng.* 137(10), 705–716. doi:10.1061/(ASCE)TE.1943-5436.0000283
- Hussein, M., Sayed, T., El-Basyouny, K., de Leur, P., 2020. Investigating safety effects of wider longitudinal pavement markings. *Accid. Anal. Prev.* 142. doi:10.1016/j.aap.2020.105527
- Idris, I.I., Mousa, M., Hassan, M., 2024. Modeling retroreflectivity degradation of pavement

- markings across the US with advanced machine learning algorithms. *J. Infrastruct. Preserv. Resil.* 5(1). doi:10.1186/s43065-024-00094-z
- Kopf, J., 2004. Reflectivity of Pavement Markings: Analysis of Retroreflectivity Degradation Curves. Washington State Department of Transportation, U.S. Department of Transportation. <https://depts.washington.edu/trac/bulkdisk/pdf/592.1.pdf>
- Karwa, V., Donnell, E.T., 2010. Predicting pavement marking retroreflectivity using artificial neural networks: Exploratory analysis. *J. Transp. Eng.* 137(2), 91–103. doi:10.1061/(ASCE)TE.1943-5436.0000194
- Lee, J.T., Maleck, T.L., Taylor, W.C., 1999. Pavement marking material evaluation study in Michigan. *ITE J.* 69(7). <https://www.semanticscholar.org/paper/Pavement-Marking-Material-Evaluation-Study-in-Lee-Maleck/ec901e630a6c6a5132692e45e965760ba90ebed0>
- Lee, Y.J., 2009. Life Cycle and Economic Efficiency Analysis: Durable Pavement Markings. Maryland Department of Transportation. [https://www.roads.maryland.gov/OPR\\_Research/MD-11-SP808B4P\\_Life-Cycle-and-Economic-Efficiency-Analysis-Phase%20II\\_Durable-Pavement-Markings\\_REPORT.pdf](https://www.roads.maryland.gov/OPR_Research/MD-11-SP808B4P_Life-Cycle-and-Economic-Efficiency-Analysis-Phase%20II_Durable-Pavement-Markings_REPORT.pdf)
- Li, Z., Ci, Y., Chen, C., Zhang, G., Wu, Q., Zhen, Q., Presendouros, P.D., and Ma, D.T., 2019. Investigation of driver injury severities in rural single-vehicle crashes under rain conditions using mixed logit and latent class models. *Acc. Anal. Prev.* 124, 219-229. doi: 10.1016/j.aap.2018.12.020
- Lindly, J.K., Wijesundera, R., 2004. Evaluation of Profiled Pavement Markings. University Transportation Center for Alabama. <https://rosap.ntl.bts.gov/view/dot/39758>
- Lord, D., Mannering, F., 2010. The statistical analysis of crash-frequency data: A review and assessment of methodological alternatives. *Transp. Res. Part A Policy Pract.* 44(5), 291–

305. doi:10.1016/j.tra.2010.02.001

Malyuta, D.A., 2015. Analysis of Factors Affecting Pavement Markings and Pavement Marking Retroreflectivity in Tennessee Highways. MS thesis, The University of Tennessee at Chattanooga.

<https://scholar.utc.edu/cgi/viewcontent.cgi?referer=&httpsredir=1&article=1321&context=theses>

Marill, K.A., 2004. Advanced Statistics: Linear Regression, Part II: Multiple Linear Regression. *Acad. Emerg. Med.* 11(1), 94–102. doi:10.1197/j.aem.2003.09.006

Masliyah, M., Bahar, G., Hauer, E., 2007. Application of innovative time series methodology to relationship between retroreflectivity of pavement markings and crashes. *Transp. Res. Rec.* 2019(1), 119–126. doi:10.3141/2019-15

Matowicki, M., Pribyl, O., Pribyl, P., 2016. Analysis of possibility to utilize road marking for the needs of autonomous vehicles. 2016 Smart Cities Symp. Prague (SCSP). doi:10.1109/SCSP.2016.7501026

McFadden, D., 1981. Econometric models of probabilistic choice, Structural Analysis of Discrete Data with Econometric Applications. MIT Press. Cambridge, MA. [https://eml.berkeley.edu/~mcfadden/discrete/front\\_matter.pdf](https://eml.berkeley.edu/~mcfadden/discrete/front_matter.pdf)

Migletz, J., Graham, J.L., Harwood, D.W., Bauer, K.M., 2001. Service life of durable pavement markings. *Transp. Res. Rec.* 1749(1), 13–21. doi:10.3141/1749-03

Minka, T.P., 2001. Algorithms for maximum-likelihood logistic regression. Carnegie Mellon University. <https://tminka.github.io/papers/logreg/minka-logreg-old.pdf>

Mohamed, M., Skinner, A., Abdel-Rahim, A., Kassem, E., Chang, K., 2019. Deterioration Characteristics of Waterborne Pavement Markings Subjected to Different Operating

- Conditions. *J. Transp. Eng. Part B Pavements* 145(2). doi:10.1061/jpeodx.0000101
- Montella, A., Colantuoni, L., and Lamberti, R., 2008. Crash Prediction Models for Rural Motorways. *Transp. Res. Rec.* 2083(1). doi: 10.3141/2083-21
- Mousa, M.R., Mousa, S.R., Hassan, M., Carlson, P., Elnaml, I.A., 2021. Predicting the retroreflectivity degradation of waterborne paint pavement markings using advanced machine learning techniques. *Transp. Res. Rec.* 2675(9), 483–494.  
doi:10.1177/03611981211002844
- Mull, D.M., Sitzabee, W.E., 2012. Paint Pavement Marking Performance Prediction Model. *J. Transp. Eng.* 138(5), 618–624. doi:10.1061/(ASCE)TE.1943-5436.0000360
- Ortiz-García, J.J., Costello, S.B., Snaith, M.S., 2006. Derivation of transition probability matrices for pavement deterioration modeling. *J. Transp. Eng.* 132(2).  
doi:10.1061/(ASCE)0733-947X(2006)132:2(141)
- Ozelim, L., Turochy, R.E., 2014. Modeling retroreflectivity performance of thermoplastic pavement markings in Alabama. *J. Transp. Eng.* 140(6). doi:10.1061/(ASCE)TE.1943-5436.0000661
- Pike, A.M., Barrette, T.P., Carlson, P.J., 2018. Evaluation of the Effects of Pavement Marking Characteristics on Detectability by ADAS Machine Vision. National Cooperative Highway Research Program (Report 20-102), Transportation Research Board.  
<https://onlinepubs.trb.org/onlinepubs/nchrp/docs/NCHRP20-102-06finalreport.pdf>
- Pike, A.M., Songchitruksa, P., 2015. Predicting pavement marking service life with transverse test deck data. *Transp. Res. Rec.* 2482(1), 16–22. doi:10.3141/2482-03
- Poch, M., Mannering, F., 1996. Negative binomial analysis of intersection-accident frequencies. *J. Transp. Eng.* 122(2), 105–113. doi:10.1061/(ASCE)0733-947X(1996)122:2(105)

- Porras-Alvarado, J., Zhang, Z., Salazar, L., 2014. Probabilistic Approach to Modeling Pavement Performance Using IRI Data. *Environmental Science Engineering*.  
<https://www.semanticscholar.org/paper/Probabilistic-Approach-to-Modeling-Pavement-Using-Porras-Alvarado-Zhang/5c5a1d420a431c5a806392990083d49fd8ae36bd>
- Quinino, R.C., Reis, E.A., Bessegato, L.F., 2013. Using the coefficient of determination R<sup>2</sup> to test the significance of multiple linear regression. *Teach. Stat.* 35(2), 84–88.  
doi:10.1111/j.1467-9639.2012.00525.x
- Rahman, M.A., Sun, X., Das, S., Khanal, S., 2021. Exploring the influential factors of roadway departure crashes on rural two-lane highways with logit model and association rules mining. *Int. J. Transp. Sci. Technol.* 10(2), 167–183. doi:10.1016/j.ijtst.2020.12.003
- Rasdorf, W.J., 2009. Pavement marking performance analysis. North Carolina Department of Transportation. <https://connect.ncdot.gov/projects/research/RNAProjDocs/2008-05FinalReport.pdf>
- Ray, M.H., Carrigan, C.E., 2023. Six Decades of Roadside Encroachment Modeling. *Transp. Res. Rec.* 2677(1), 708–719. doi:10.1177/03611981221101026
- Robertson, J., Sarasua, W., Johnson, J., Davis, W., 2013. A Methodology for Estimating and Comparing the Lifecycles of High-Build and Conventional Waterborne Pavement Markings on Primary and Secondary Roads in South Carolina. *Public Work. Manag. Policy* 18(4), 360–378. doi:10.1177/1087724X12451441
- Romanoschi, S., Metcalf, J., 2002. Characterization of Pavement Layer Interfaces. PhD Dissertation, Louisiana State University.  
[https://repository.lsu.edu/gradschool\\_disstheses/7008/](https://repository.lsu.edu/gradschool_disstheses/7008/)
- Sarasua, W.A., Clarke, D.B., Davis, W.J., 2003. Evaluation of Interstate Pavement Marking



- Retroreflectivity. South Carolina Department of Transportation (Rep. No. FHWA-SC-03-01). <https://trid.trb.org/View/660929>
- Sasidharan, L., Karwa, V., Donnell, E.T., 2009. Use of pavement marking degradation models to develop a pavement marking management system. *Public Work. Manag. Policy* 14(2), 148–173. doi:10.1177/1087724X09349513
- Satterfield, C., Pike, A., Schertz, G., 2022. Assessment of Economic Impacts of SNPA Proposed Minimum Levels of Pavement Marking Retroreflectivity. Federal Highway Administration. <https://rosap.ntl.bts.gov/view/dot/49515>
- Sauter, G., Doring, M., Nyttens, R., 2021. High Performance Pavement Markings Enhancing Camera And LiDAR Detection. *IOP Conf. Ser.: Mater. Sci. Eng.* 1202. doi: 10.1088/1757-899X/1202/1/012033
- Sitzabee, W.E., Hummer, J.E., Rasdorf, W., 2009. Pavement Marking Degradation Modeling and Analysis. *J. Infrastruct. Syst.* 15(3), 190–199. doi:10.1061/(asce)1076-0342(2009)15:3(190)
- Sitzabee, W.E., White, E.D., Dowling, A.W., 2013. Degradation Modeling of Polyurea Pavement Markings. *Public Work. Manag. Policy* 18(2), 185–199. doi:10.1177/1087724X12462831
- Smadi, O., Souleyrette, R.R., Ormand, D.J., Hawkins, N., 2008. Pavement marking retroreflectivity analysis of safety effectiveness. *Transp. Res. Rec.* 2056(1), 17–24. doi:10.3141/2056-03
- Tae Kyun Kim, 2018. T test as a parametric statistic. *Korean J. Anesthesiol. Stat.* 2, 167–206.
- Thamizharasan, A., Sarasua, W.A., Clarke, D.B., Davis, W.J., 2003. A Methodology for Estimating the Lifecycle of Interstate Highway Pavement Marking Retroreflectivity. TRB

- 2003 Annual Meeting, Washington DC, United States.  
[https://www.researchgate.net/publication/228391454\\_A\\_Methodology\\_for\\_Estimating\\_the\\_Lifecycle\\_of\\_Interstate\\_Highway\\_Pavement\\_Marking\\_Retroreflectivity](https://www.researchgate.net/publication/228391454_A_Methodology_for_Estimating_the_Lifecycle_of_Interstate_Highway_Pavement_Marking_Retroreflectivity)
- Thomas, G.B., Schloz, C., 2001. Durable, cost-effective pavement markings. Phase I: synthesis of current research. Iowa Department of Transportation (Project TR-454).  
<https://rosap.ntl.bts.gov/view/dot/23741>
- Van Petegem, J.W.H., Wegman, F., 2014. Analyzing road design risk factors for run-off-road crashes in the Netherlands with crash prediction models. *J. Safety Res.* 49, 121.  
doi:10.1016/j.jsr.2014.03.003
- Wang, C., Wang, Z., Tsai, Y.C., 2016. Piecewise multiple linear models for pavement marking retroreflectivity prediction under effect of winter weather events. *Transp. Res. Rec.* 2551, 52–61. doi:10.3141/2551-07
- Xu, L., Chen, Z., Li, X., Xiao, F., 2021. Performance, environmental impact and cost analysis of marking materials in pavement engineering, the-state-of-art. *J. Clean. Prod.* 294.  
doi:10.1016/j.jclepro.2021.126302
- Yang, J., Yamamoto, T., Ando, R., 2021. The impact of mandating a driving lesson for elderly drivers in Japan using count data models: Case study of Toyota City. *Accid. Anal. Prev.* 153. doi:10.1016/j.aap.2021.106015
- Zhang, Y., Wu, D., 2010. Methodologies to Predict Service Lives of Pavement Marking Materials. *J. Transp. Res. Forum.* doi:10.5399/osu/jtrf.45.3.601
- Zuur, A.F., Ieno, E.N., Walker, N.J., Saveliev, A.A., Smith, G.M., 2009. Mixed effects models and extensions in ecology with R: Dealing with Heterogeneity. *Statistics for Biology and Health.* doi:10.1007/978-0-387-87458-6\_4

Zwahlen, H.T., Schnell, T., 1997. Visibility of new centerline and edge line pavement markings.

*Transp. Res. Rec.* 1605(1), 49–61. doi:10.3141/1605-07

## Appendix

**Table A1 Used R packages with descriptions**

Package	Description
betareg	Estimating and interpreting regression models designed for beta-distributed dependent variables.
tidyverse	Streamlining data manipulation, visualization, and analysis for multiple linear regression models
MASS	Providing the function for fitting negative binomial regression models

**Table A2 Ranking of rural two-lane 0.5-mile road segments with average RL of WREL  $\geq 450$  mcd/m<sup>2</sup>/lux in November 2021, sorted by predicted RL values for December 2024 (from lowest to highest)**

Rank	Route Identification Number	Starting point of 0.5-mile segment		Direction	RL of WREL (mcd/m <sup>2</sup> /lux)	
		Latitude	Longitude		Nov-21	Dec-24
1	AL0000030000	32.52648167	-86.45536833	SB	496	150
2	AL0002290000	32.42678167	-85.898285	SB	470	156
3	AL0002290000	32.523365	-85.89472	SB	535	159
4	AL0002290000	32.51616667	-85.89552833	SB	544	161
5	AL0002290000	32.50171667	-85.89380667	SB	485	162
6	AL0002290000	32.49449	-85.89281667	SB	503	166
7	AL0002290000	32.465725	-85.890285	SB	509	167
8	AL0002290000	32.50892	-85.89485167	SB	549	168
9	AL0000150000	32.73247833	-85.23268667	NB	479	168
10	AL0002290000	32.48732667	-85.89183833	SB	521	170
11	AL0002290000	32.480115	-85.89086167	SB	526	172
12	AL0002290000	32.47289667	-85.88985167	SB	537	174
13	AL0000030000	32.21785167	-86.348755	SB	465	175
14	AL0000150000	32.68367833	-85.309975	NB	501	176
15	AL0002290000	32.45893667	-85.89340833	SB	566	179
16	AL0002290000	32.58672333	-85.93828333	SB	458	180
17	AL0000150000	32.67988333	-85.31719167	NB	522	181
18	AL0000030000	32.51213	-86.45646333	SB	625	182
19	AL0000210000	32.25147833	-86.52353	SB	450	183
20	AL0000030000	32.51936833	-86.45704167	SB	631	183
21	AL0000090000	32.74713667	-86.10081667	NB	470	184
22	AL0002290000	32.45223667	-85.89656667	SB	621	185
23	AL0000140000	32.580055	-85.71172167	EB	460	187
24	AL0000030000	32.505	-86.45648	SB	652	188

Rank	Route Identification Number	Starting point of 0.5-mile segment		Direction	RL of WREL (mcd/m <sup>2</sup> /lux)	
		Latitude	Longitude		Nov-21	Dec-24
25	AL0000140000	32.581775	-85.7199	EB	466	188
26	AL0000090000	32.71542167	-86.10802833	NB	493	189
27	AL0000210000	32.22625167	-86.54039333	SB	485	191
28	AL0000140000	32.55879	-85.79491167	EB	533	192
29	AL0002290000	32.69239333	-85.96013667	SB	478	194
30	AL0000210000	32.257995	-86.51976667	SB	498	194
31	AL0000060000	32.113505	-85.58548333	WB	457	194
32	AL0002290000	32.60675833	-85.94304333	SB	512	195
33	AL0000140000	32.57779	-85.69498167	EB	479	195
34	AL0002290000	32.60089333	-85.93858833	SB	516	196
35	AL0000090000	32.71076167	-86.10147333	NB	525	196
36	AL0000090000	32.72896667	-86.112645	NB	523	196
37	AL0000030000	32.66191833	-86.489725	SB	451	196
38	AL0000030000	32.67638333	-86.49105333	SB	451	196
39	AL0000210000	32.23238167	-86.53589833	SB	512	197
40	AL0000150000	32.17816667	-85.70785333	SB	461	197
41	AL0000140000	32.58069333	-85.751615	EB	489	198
42	AL0000060000	32.12004667	-85.58910667	WB	512	199
43	AL0002290000	32.69623167	-85.96742833	SB	508	200
44	AL0000210000	32.24493333	-86.52730667	SB	527	200
45	AL0000090000	32.66703333	-86.10888667	NB	549	200
46	AL0000030000	32.497845	-86.45509833	SB	684	200
47	AL0002290000	32.593655	-85.93888333	SB	541	201
48	AL0002290000	32.660535	-85.94316667	SB	484	201
49	AL0000150000	32.19936833	-85.70809167	SB	475	201
50	AL0001650000	32.13932667	-85.06619	NB	450	202
51	AL0002290000	32.67470333	-85.94450667	SB	485	202
52	AL0002290000	32.70121667	-85.97352333	SB	517	202
53	AL0000150000	32.21391667	-85.70868167	SB	481	202
54	AL0000030000	32.64763	-86.48727167	SB	479	202
55	AL0001990000	32.47929	-85.72642667	NB	450	203
56	AL0000030000	32.127095	-86.39189	SB	532	203
57	AL0002230000	32.07999167	-85.77110167	SB	452	204
58	AL0000210000	32.06235167	-86.71920667	SB	456	204
59	AL0000030000	32.66911833	-86.49094333	SB	489	204
60	AL0001990000	32.486015	-85.73956833	NB	467	206
61	AL0000970000	32.079415	-86.44395667	NB	460	206
62	AL0000210000	32.05117	-86.80467667	SB	460	206
63	AL0000150000	32.206675	-85.70840167	SB	501	206
64	AL0000140000	32.579535	-85.70320833	EB	528	206

Rank	Route Identification Number	Starting point of 0.5-mile segment		Direction	RL of WREL (mcd/m <sup>2</sup> /lux)	
		Latitude	Longitude		Nov-21	Dec-24
65	AL0002290000	32.44682333	-85.899855	SB	717	207
66	AL0000210000	32.03850333	-86.824805	SB	459	207
67	AL0000150000	31.87721833	-85.72134833	SB	455	207
68	AL0000140000	32.561445	-85.78701167	EB	528	207
69	AL0000090000	32.72178833	-86.11206333	NB	577	208
70	AL0000140000	32.57251	-85.68919333	EB	537	208
71	AL0002290000	32.57318833	-85.93954167	SB	585	209
72	AL0002230000	32.03085167	-85.77407833	SB	464	209
73	AL0000030000	32.69084833	-86.49180167	SB	493	209
74	AL0002930000	32.34752667	-86.06412	SB	455	210
75	AL0000940000	32.01664167	-86.07472667	EB	457	210
76	AL0000100000	31.83578833	-86.87680833	EB	468	210
77	AL0002630000	31.994745	-86.74017	SB	470	211
78	AL0002630000	32.00597	-86.75097167	SB	469	211
79	AL0000210000	32.04841833	-86.81227667	SB	474	211
80	AL0001650000	32.13257	-85.06937667	NB	492	212
81	AL0002630000	32.01752	-86.761175	SB	474	212
82	AL0000210000	32.06568	-86.72674667	SB	490	212
83	AL0002630000	31.90277833	-86.678015	SB	477	213
84	AL0002630000	31.93408833	-86.69787167	SB	482	213
85	AL0002630000	31.94739167	-86.70493667	SB	477	213
86	AL0000210000	32.04345667	-86.81853667	SB	483	213
87	AL0000140000	32.56959333	-85.77314333	EB	555	213
88	AL0002930000	32.35417333	-86.06757667	SB	476	214
89	AL0002230000	31.995945	-85.77464167	SB	480	214
90	AL0002230000	32.016885	-85.771975	SB	481	214
91	AL0002630000	31.90784333	-86.68404	SB	488	215
92	AL0000140000	32.564575	-85.77931667	EB	571	216
93	AL0002630000	31.94075667	-86.70148	SB	496	217
94	AL0002630000	31.96145	-86.70880667	SB	494	217
95	AL0002630000	31.978145	-86.72367333	SB	496	217
96	AL0000970000	32.06065667	-86.43154667	NB	508	217
97	AL0002630000	32.040635	-86.79321167	SB	491	217
98	AL0002290000	32.633485	-85.95402833	SB	553	217
99	AL0000030000	32.19192	-86.35847833	SB	601	217
100	AL0002230000	31.98417167	-85.79548667	SB	500	218
101	AL0002230000	32.009675	-85.77097167	SB	499	218
102	AL0000210000	32.007515	-86.844435	SB	504	218
103	AL0002290000	32.6534	-85.944935	SB	563	219
104	AL0000210000	32.012655	-86.83854833	SB	508	219

Rank	Route Identification Number	Starting point of 0.5-mile segment		Direction	RL of WREL (mcd/m <sup>2</sup> /lux)	
		Latitude	Longitude		Nov-21	Dec-24
105	AL0002630000	32.04435667	-86.80054	SB	505	220
106	AL0000140000	32.57756167	-85.75897833	EB	585	220
107	AL0002630000	31.92077	-86.691375	SB	517	221
108	AL0002630000	31.927585	-86.69438833	SB	514	221
109	AL0002630000	31.98921167	-86.73471667	SB	515	221
110	AL0002290000	32.62693833	-85.95028167	SB	572	221
111	AL0000210000	32.02576167	-86.83122667	SB	519	221
112	AL0002290000	32.64073833	-85.95324833	SB	575	222
113	AL0002630000	31.88690833	-86.66061667	SB	550	224
114	AL0002290000	32.620215	-85.94791167	SB	585	224
115	AL0000140000	32.57298333	-85.765575	EB	603	224
116	AL0002630000	32.03321167	-86.77860333	SB	529	225
117	AL0000210000	32.00430167	-86.85191167	SB	538	225
118	AL0000210000	32.0192	-86.83486667	SB	538	225
119	AL0002630000	31.88104833	-86.65593333	SB	564	226
120	AL0002630000	31.897685	-86.67194667	SB	539	226
121	AL0002230000	32.00250333	-85.77154833	SB	531	226
122	AL0000210000	32.03293333	-86.829975	SB	541	226
123	AL0000150000	32.22115333	-85.709005	SB	601	229
124	AL0002290000	32.66773833	-85.94238333	SB	614	230
125	AL0002630000	32.023365	-86.76635333	SB	553	231
126	AL0002290000	32.64706333	-85.94905167	SB	626	233
127	AL0002630000	31.913995	-86.68842667	SB	601	240
128	AL0002630000	32.03690833	-86.78587167	SB	604	243
129	AL0002630000	31.89262	-86.66593833	SB	645	250

**Table A3 Ranking of rural multilane 0.5-mile road segments with average RL of WREL  $\geq 450$  mcd/m<sup>2</sup>/lux in November 2021, sorted by predicted RL values for December 2024 (from lowest to highest)**

Rank	Route Identification Number	Starting point of 0.5-mile segment		Direction	RL of WREL (mcd/m <sup>2</sup> /lux)	
		Latitude	Longitude		Nov-21	Dec-24
1	IN0000650000	32.39204667	-86.32639667	SB	451	81
2	IN0000650000	32.37867833	-86.32205667	SB	573	84
3	IN0000650000	32.407365	-86.34465167	SB	477	84
4	IN0000650000	32.40229167	-86.33859833	SB	537	93
5	IN0000650000	32.422925	-86.36274667	SB	467	96
6	IN0000650000	32.42950833	-86.36844	SB	492	99
7	IN0000650000	32.461355	-86.388885	SB	498	112

Rank	Route Identification Number	Starting point of 0.5-mile segment		Direction	RL of WREL (mcd/m <sup>2</sup> /lux)	
		Latitude	Longitude		Nov-21	Dec-24
8	IN0000850000	32.37596333	-86.02723167	NB	450	124
9	IN0000850000	32.71716	-85.30358	NB	469	129
10	IN0000850000	32.71063667	-85.30725667	NB	485	131
11	IN0000850000	32.68462667	-85.32244333	NB	530	137
12	IN0000850000	32.536215	-85.54773167	NB	516	141
13	IN0000850000	32.532865	-85.55535167	NB	527	143
14	AL0000380000	32.68786667	-85.49692833	WB	457	156
15	AL0000030000	32.54097167	-86.45686	SB	452	159
16	IN0000650000	32.41759333	-86.356855	SB	940	160
17	AL0000030000	32.53378167	-86.45575167	SB	456	160
18	AL0000080000	32.26218833	-86.67040667	WB	465	163
19	AL0000060000	32.29251833	-86.19132	EB	554	165
20	AL0000080000	32.44389	-87.193655	WB	456	166
21	AL0000080000	32.43920833	-87.38155	WB	460	168
22	AL0000080000	32.44105833	-87.38979	WB	463	169
23	AL0000080000	32.43974667	-87.31307	WB	469	169
24	AL0000080000	32.44336833	-87.21938167	WB	467	169
25	AL0000080000	32.44349333	-87.21083667	WB	478	169
26	AL0000080000	32.44008667	-87.27023667	WB	486	172
27	AL0000080000	32.44026	-87.25310667	WB	492	173
28	AL0000090000	32.15447833	-86.27141333	SB	498	173
29	AL0000080000	32.44466167	-87.40626833	WB	509	175
30	AL0000080000	32.44344167	-87.39788167	WB	505	175
31	AL0000080000	32.43984333	-87.29596667	WB	506	175
32	AL0000080000	32.43991	-87.28734833	WB	508	175
33	AL0000080000	32.44017667	-87.261675	WB	512	175
34	AL0000380000	32.68201	-85.49179	WB	610	175
35	AL0000410000	32.39862833	-86.99261667	SB	543	175
36	AL0000550000	31.63597833	-86.74899833	NB	527	176
37	AL0000080000	32.43955667	-87.33867	WB	516	177
38	AL0000080000	32.43981167	-87.30447167	WB	520	177
39	AL0000550000	31.62195167	-86.744725	NB	548	179
40	AL0000550000	31.62896	-86.746885	NB	544	179
41	AL0000380000	32.67658	-85.48615333	WB	661	180
42	AL0000080000	32.26221167	-86.67892333	WB	592	181
43	AL0000550000	31.60821667	-86.739155	NB	575	182
44	AL0000080000	32.31661	-86.88712167	WB	590	182
45	AL0000080000	32.26780833	-86.70340333	WB	612	183
46	AL0000550000	31.64300333	-86.75114667	NB	589	184
47	AL0000550000	31.61501667	-86.74210667	NB	592	185



Rank	Route Identification Number	Starting point of 0.5-mile segment		Direction	RL of WREL (mcd/m <sup>2</sup> /lux)	
		Latitude	Longitude		Nov-21	Dec-24
48	AL0000080000	32.26454	-86.68701167	WB	635	187
49	AL0000080000	32.267165	-86.69494	WB	790	208

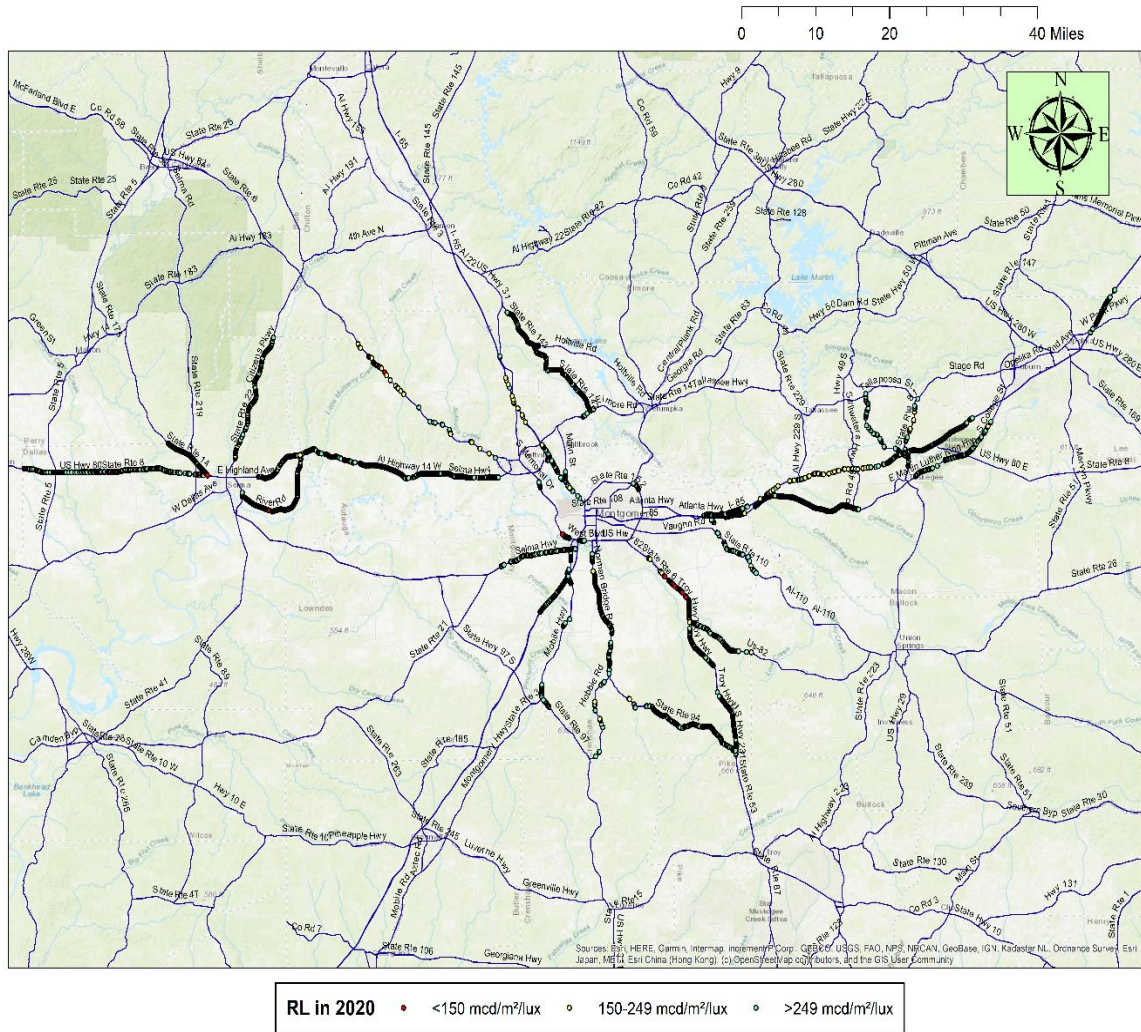
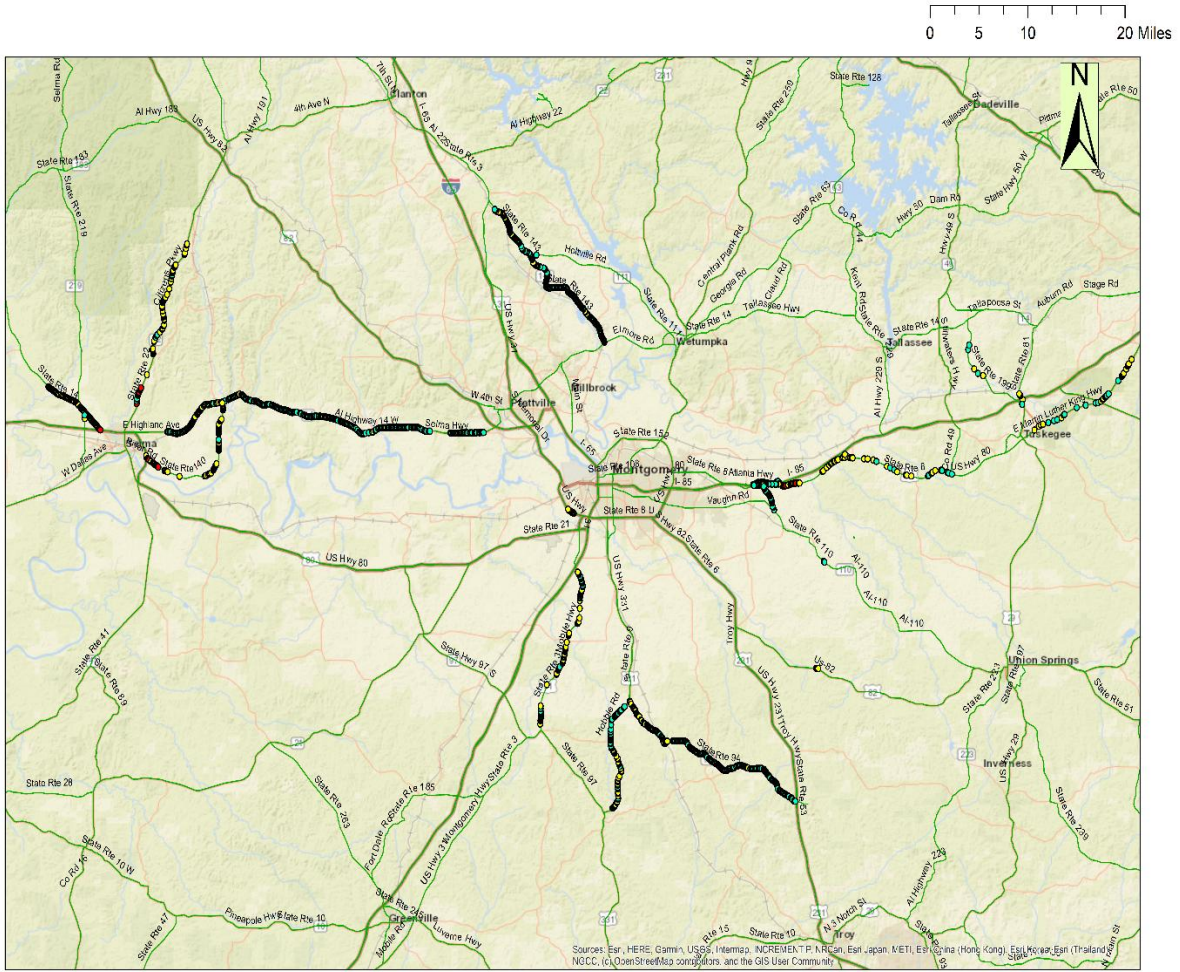


**Figure A1 Locations of RL data of WREL collected for 0.1-mile segments (excluding restriped marking locations)**



RL in 2020 • <100 mcd/m<sup>2</sup>/lux • 100-199 mcd/m<sup>2</sup>/lux • >199 mcd/m<sup>2</sup>/lux

**Figure A2 Locations of RL data of YCL collected for 0.1-mile segments (excluding restriped marking locations)**



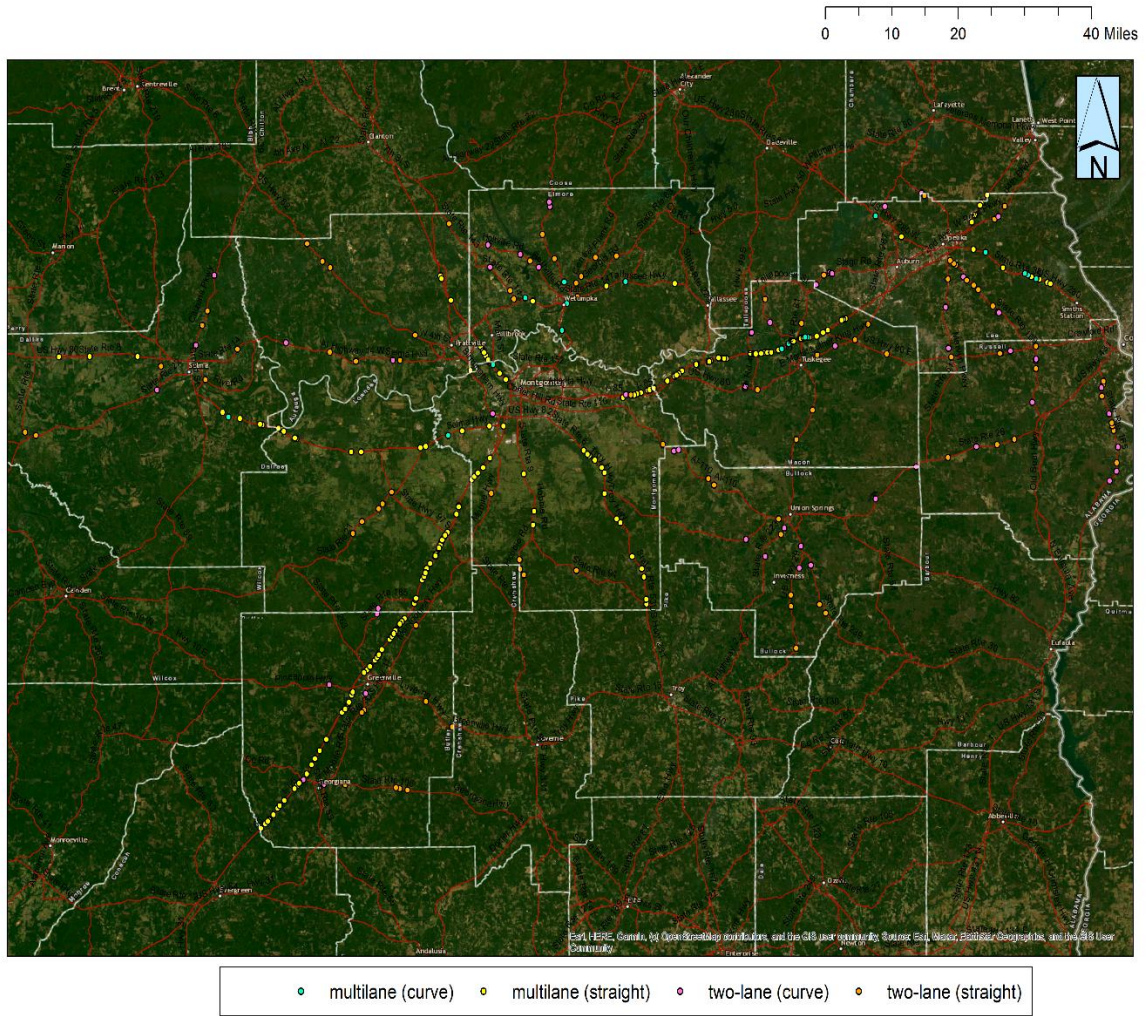


**Figure A3 Locations of single vehicle ROR crashes (March 2021 to November 2021)**



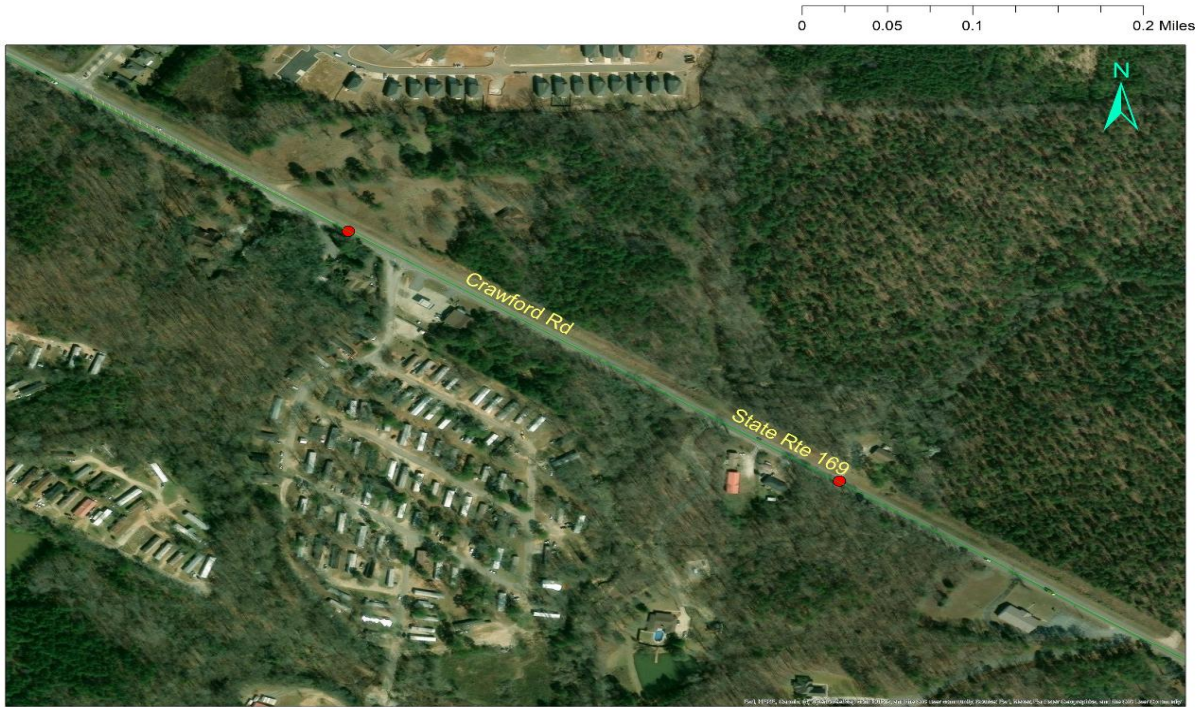


**Figure A4 A rural two-lane location with multiple single-vehicle ROR crashes occurring within a 0.5-mile segment with RL of WREL < 250 mcd/m<sup>2</sup>/lux**



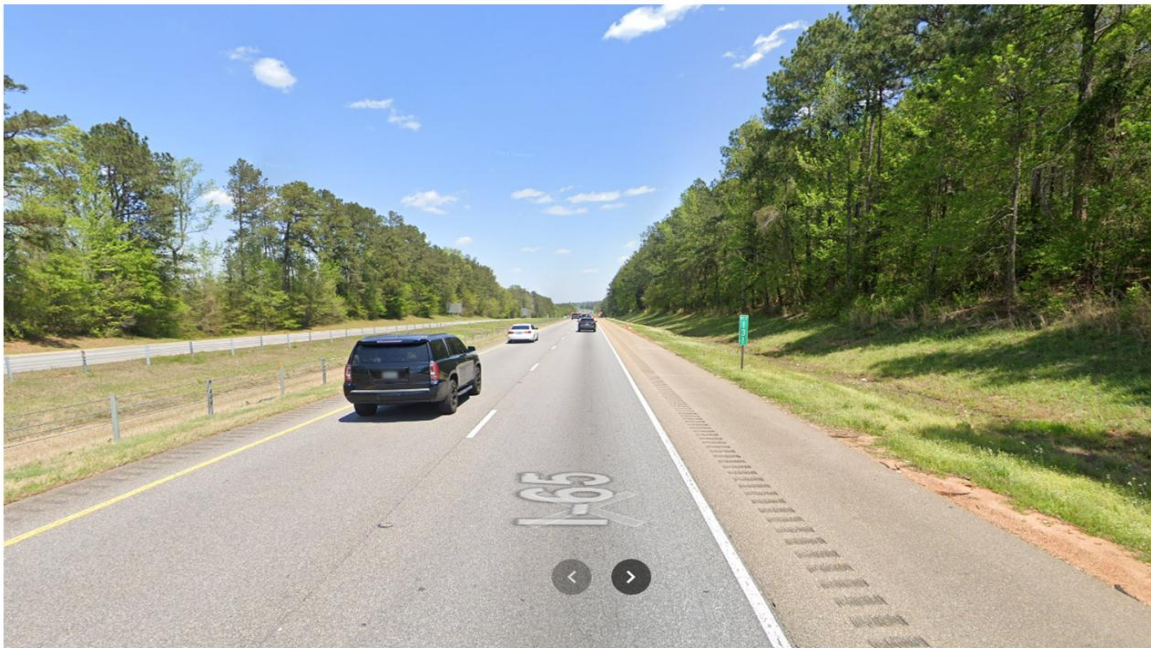


**Figure A5 A rural multilane location with multiple single-vehicle ROR crashes occurring within a 0.5-mile segment with RL of WREL < 250 mcd/m<sup>2</sup>/lux**